

# Initiating insensitive munitions by shaped charge jet impact

**AFA Bin Sultan**



**orcid.org 0000-0001-7331-8691**

Dissertation submitted in partial fulfilment of the requirements for the degree *Masters of Science in Mechanical Engineering* at the Potchefstroom Campus of the North West University

Supervisor: Prof WL den Heijer

Co-supervisor: Mr R Gouws

Examination: May 2018

Student number: 27360083

## **ACKNOWLEDGEMENTS**

I would like to sincerely thank Prof Willem Den Heijer and Mr Rudolf Gouws for their valuable feedback during the course of this work. I would also like to thank Dion Ellis, Louis Du Plessis, Fakhree Majit, Eugene Davids and Jackie Sibeko for their cooperative attitude in sharing their technical knowledge with me. I furthermore express my heartfelt gratitude to RDM and NWU for their assistance in funding this work. Finally, I would like to thank my wife for her patience and generosity with her time.

## ABSTRACT

When it comes to attacking munitions by means of a Shaped Charge Jet Impact (SCJI), various types of reactions are likely to occur, which range from a severe detonation to a simple burning type of reaction. These differences in responses are highly affected by the properties of energetic materials as well as the Shaped Charge (SC) calibre used. This paper aimed at investigating a series of different values of the jet threshold calculated by the jet tip velocities and diameters ( $V^2d$ ), which was obtained using a 38 mm conical SC. The main objective was to underline the critical values of  $V^2d$  responsible for initiating different types of reactions on 81 mm mortar bombs. Several values of the jet threshold were acquired by varying the conditioning steel plate. The jet tip velocities were measured by using two different experimental methods, by means of flash x-ray and by inserting velocity screens that accounted for computing the residual tip velocity after penetration. Explosive formulations used were 2,4,6-trinitrotoluene (TNT) as baseline and reference of conventional high explosives (HE), along with different explosive compositions based on 3-nitro-1,2,4-triazol-5-one (NTO) as insensitive high explosive (IHE) candidates.

In addition, the difference between the initiation behaviour of TNT and that of NTO/TNT-based was addressed by analysing the effects of jet tip velocity, tip diameter and reactions corresponding to the impact of each value of  $V^2d$ . This work focused on providing useful information towards understanding the effect of the jet energy, tip velocity and tip diameter to the response of munitions filled with various explosive formulations.

# TABLE OF CONTENTS

|   |             |
|---|-------------|
| <b>ACKNOWLEDGEMENTS .....</b>                             | <b>II</b>   |
| <b>ABSTRACT .....</b>                                     | <b>III</b>  |
| <b>LIST OF TABLES .....</b>                               | <b>VII</b>  |
| <b>LIST OF FIGURES .....</b>                              | <b>VIII</b> |
| <b>ABBREVIATION .....</b>                                 | <b>X</b>    |
| <b>NOMENCLATURE .....</b>                                 | <b>XI</b>   |
| <b>Chapter 1: Introduction .....</b>                      | <b>1</b>    |
| 1.1 Introduction .....                                    | 1           |
| 1.2 What is Insensitive Munitions? .....                  | 4           |
| 1.3 Technical Requirements of Insensitive Munitions ..... | 6           |
| 1.4 Shaped Charges .....                                  | 7           |
| 1.5 Problem Statement .....                               | 9           |
| 1.6 Research Objectives .....                             | 9           |
| 1.7 Research Scope and Limitation .....                   | 10          |
| 1.8 Dissertation Outline .....                            | 11          |
| 1.9 Summary .....   | 12          |
| <b>Chapter 2: Literature Review .....</b>                 | <b>13</b>   |
| 2.1 Introduction .....                                    | 13          |
| 2.2 Conventional High Explosives .....                    | 14          |

|  |           |
|--|-----------|
| 2.3 Insensitive High Explosives .....  | 16        |
| 2.4 Conceptual Considerations on Shock Sensitivity and Impact Ignition ..... | 18        |
| 2.5 Filling Techniques (melt-cast, cast-cured and pressed) .....             | 19        |
| 2.6 IM Testing (Methods & Classification) .....                              | 21        |
| 2.7 Relevant Results and Findings .....                                      | 26        |
| 2.8 Shaped Charge Jet.....   | 29        |
| 2.8.1 Jet Formation Process.....   | 30        |
| 2.8.2 Jet Breakup Time .....   | 31        |
| 2.9 Standoff Distance Effect and Penetration Models .....                    | 32        |
| 2.10 Summary .....   | 34        |
| <b>Chapter 3: Methodology.....</b>   | <b>36</b> |
| 3.1 Introduction.....  | 36        |
| 3.2 Characterisation Test of Shaped Charge Jet.....                          | 37        |
| 3.1.1 Test Set-up .....  | 38        |
| 3.3 Shaped Charge Jet Impact Test.....                                       | 41        |
| 3.3.1 Melt-cast Explosives Preparation .....                                 | 41        |
| 3.3.2 Firing Mechanism and Measuring Instruments .....                       | 41        |
| 3.3.2 Test Set-up.....   | 43        |
| 3.4 Summary .....  | 45        |
| <b>Chapter 4: Results.....</b>   | <b>46</b> |
| 4.1 Introduction.....  | 46        |
| 4.2 Optimum Standoff Distance.....   | 47        |

|  |           |
|--|-----------|
| 4.3 Characterisation and Evaluation of the SCJ Particles .....                     | 50        |
| 4.3.1 Breakup Time, Tip Velocity and Tip Diameter .....                            | 52        |
| 4.4 Reactions due to Impact of Shaped Charge Jets on 81 mm Mortar Projectiles..... | 55        |
| 4.3.1 Residual Velocities .....  | 59        |
| 4.5 Summary .....  | 61        |
| <b>Chapter 5: Discussion.....</b>  | <b>62</b> |
| 5.1 Introduction.....  | 62        |
| 5.2 Findings .....   | 62        |
| 5.3 Critical Evaluations of the main results.....                                  | 64        |
| 5.4 Results Verification.....  | 67        |
| 5.5 Summary .....  | 68        |
| <b>Chapter 6: Conclusion .....</b>   | <b>69</b> |
| 6.1 Introduction.....  | 69        |
| 6.2 Future Work.....   | 70        |
| <b>Bibliography.....</b>   | <b>71</b> |
| <b>Appendix A: Blast Over-pressure Measurements .....</b>                          | <b>1</b>  |

## LIST OF TABLES

|   |    |
|---|----|
| Table 1: A comparison of chemical properties and characteristics for conventional High Explosives (HE) [24].      | 15 |
| Table 2: A list of expected alternatives to conventional HE [28].   | 18 |
| Table 3: IM standard tests and their corresponding STANAG documents.  | 22 |
| Table 4: SCJI test on 81 mm mortar bombs filled with insensitive melt-cast explosive formulations [18].           | 27 |
| Table 5: SCJI test on 81 mm mortar bombs filled with insensitive melt-cast explosive formulations.                | 55 |
| Table 6: A summary of residual velocities and their corresponding <b>V2d</b> values measured by velocity screens. | 59 |
| Table 7: A comparison of SCJI test using 38 mm SC & 57 mm SC on 81 mm mortar bombs filled with NTO/TNT (50/50).   | 63 |
| Table 8: Blast overpressure measurements for detonated NTO/TNT (50/50).   | 64 |
| Table 9: Blast overpressure measurements for detonated NTO/TNT (20/80).   | 64 |

## LIST OF FIGURES

|   |    |
|---|----|
| Figure 1: A drawing of a 38 mm-conical SC.....  | 2  |
| Figure 2: A British battleship burned as a result of a sympathetic reaction [4]. ....   | 3  |
| Figure 3: List of IM relevant threats and accepted reactions [8]. ....  | 5  |
| Figure 4: Jet formation over time elapse.....   | 7  |
| Figure 5: Cross-section of an RPG-7 warhead. ....   | 8  |
| Figure 6: Different initiation methods used in shaped charges.....  | 8  |
| Figure 7: Chemical structure of TNT.....  | 14 |
| Figure 8: Chemical structure of NTO. ....   | 17 |
| Figure 9: Typical components of an explosive train. ....  | 19 |
| Figure 10: Melt-cast filling facility used by RDM [18].....   | 20 |
| Figure 11: Fast cook-off test set-up [18]. ....   | 23 |
| Figure 12: Sympathetic test set-up [18]. ....   | 24 |
| Figure 13: Varied SCC and their corresponding critical $V2d$ values [10].....   | 28 |
| Figure 14: Conical and trumpet SC liners [47]. ....   | 30 |
| Figure 15: from left to right: presence of cavity only vs cavity plus liner vs cavity plus liner plus<br>standoff distance [55]. ....     | 33 |
| Figure 16: Schematic view of the flash x-ray set-up [59].....   | 37 |
| Figure 17: A picture of the 38 mm SC used along with its attachments. ....  | 38 |
| Figure 18: Actual image of the test set-up. ....  | 40 |
| Figure 19: A different angle of the actual test set-up.....   | 40 |
| Figure 20: A schematic view (top-view) of major components for the SCJI test, showing the<br>direction of firing. ....                    | 42 |
| Figure 21: Blast-over pressure probes.....  | 43 |
| Figure 22: Schematic view of the SCJI set-up. ....  | 44 |
| Figure 23: SCJI test showing the 81 mm mortar projectile, steel conditioning plate, 38 mm SC<br>and the witness plate at the bottom. .... | 45 |
| Figure 24: Variable standoff distances and their resultant exit-holes on 10 mm steel conditioning<br>plates. ....                         | 47 |
| Figure 25: Optimum standoff distance effect on 20 mm steel plate.....   | 48 |
| Figure 26: Variable jet threshold ( $V2d$ ) measured by the flash x-ray analysis.....   | 49 |
| Figure 27: Radiographic image of the jet as it passes with no conditioning steel plate. ....  | 50 |
| Figure 28: Radiographic image of the jet after penetrating a 10 mm conditioning steel plate. ...  | 50 |
| Figure 29: Radiographic image of the jet after penetrating a 20 mm conditioning steel plate. ...  | 51 |
| Figure 30: Radiographic image of the jet after penetrating a 40 mm conditioning steel plate. ...  | 52 |
| Figure 31: Images of the jet captured at various time elapses with no conditioning steel plate. ...                                       | 53 |



|  |    |
|--|----|
| Figure 32: Total cumulative length of the jet particles as it stretched out. ....        | 53 |
| Figure 33: Type IV (deflagration) reaction observed on NTO/TNT (20/80).....              | 56 |
| Figure 34: Type III (explosion) observed on NTO/TNT (50/50) with 40 mm steel plate. .... | 56 |
| Figure 35: Type II (Partial detonation) observed on TNT. ....                            | 57 |
| Figure 36: Type I (detonation) observed on TNT. ....                                     | 57 |
| Figure 37: Type III (explosion) observed on NTO/TNT (50/50) with 60 mm steel plate. .... | 58 |
| Figure 38: Type VI (no reaction) observed on TNT with 75 mm steel plate.....             | 58 |
| Figure 39: Type III (explosion) observed on NTO/TNT (20/80) with 60 mm steel plate. .... | 59 |
| Figure 40: Variable jet threshold ( <b>V2d</b> ) measured by velocity screens.....       | 60 |
| Figure 41: A comparison of <b>V2d</b> measured by flash x-ray and velocity screens.....  | 66 |
| Figure 42: A comparison of: 38 mm SC vs 44 mm SC [10].....                               | 67 |

## **ABBREVIATION**

|               |                                    |
|---------------|------------------------------------|
| <b>AOP</b>    | Allied Ordnance Publication        |
| <b>AP</b>     | Armour piercing                    |
| <b>BI</b>     | Bullet impact                      |
| <b>BOP</b>    | Blast over-pressure probes         |
| <b>ERL</b>    | Explosives reaction level          |
| <b>EMP</b>    | Electromagnetic pulse              |
| <b>FCO</b>    | Fast cook-off                      |
| <b>FI</b>     | Fragment impact                    |
| <b>HE</b>     | High explosives                    |
| <b>HMX</b>    | Octogen                            |
| <b>HNS</b>    | Hexanitrostilbene                  |
| <b>HEAT</b>   | High explosive anti-tank           |
| <b>IHE</b>    | Insensitive high explosives        |
| <b>IM</b>     | Insensitive munitions              |
| <b>NATO</b>   | North Atlantic Treaty Organisation |
| <b>NTO</b>    | 3-nitro-1,2,4-triazol-5-one        |
| <b>PB</b>     | Polymer binder                     |
| <b>PBX</b>    | Polymer bonded explosive           |
| <b>PER</b>    | Pugh, Eichelberger and Rostoker    |
| <b>STANAG</b> | Standardization Agreement          |
| <b>RDX</b>    | Hexogen                            |
| <b>SC</b>     | Shaped charge                      |
| <b>SCC</b>    | Shaped charge calibre              |
| <b>SCJ</b>    | Shaped charge jet                  |
| <b>SCJI</b>   | Shaped charge jet impact           |
| <b>SCO</b>    | Slow cook-off                      |

|            |                          |
|------------|--------------------------|
| <b>SD</b>  | Sympathetic detonation   |
| <b>TNT</b> | 2,4,6-trinitrotoluene    |
| <b>USA</b> | United States of America |

## NOMENCLATURE

|               |   |
|---------------|---|
| $\alpha$      | Constant depending on the velocity gradient |
| $\beta$       | Constant representing the jet spreading     |
| $\psi$        | Constant depending on the velocity gradient |
| $\gamma$      | Ratio of specific heats                     |
| $\rho_J$      | Density of the jet                          |
| $\rho_T$      | Density of the barrier plate                |
| $d$           | Tip diameter                                |
| $P$           | Thickness of the barrier plate              |
| $P_o$         | Penetration at zero standoff                |
| $t_b$         | Breakup time                                |
| $S$           | Standoff distance                           |
| $U_D$         | Velocity of detonation                      |
| $V_{tip}$     | Tip velocity of the jet                     |
| $V_{res}$     | Residual velocity of the jet                |
| $V_{tip}^2 d$ | Threshold stimulus of the jet (jet energy)  |
| $V_{cut}$     | Slowest particle velocity of the jet        |
| $\sum l$      | Summation of broken-up jet elements         |

# Chapter 1: Introduction

## 1.1 Introduction

Explosives are classified as energetic materials that, when initiated, lead to chemical explosions. Energetic materials can be subdivided into several groups, such as pyrotechnics, propellants and explosives. Propellants are used to charge objects by means of producing gas, while pyrotechnics emit light and smoke as a result of exothermic reaction. On the other hand, explosives contain energy that is capable of being released very rapidly over a short period of time in a form of high temperature and pressure. This may result in very serious damage to the surroundings due to the resultant high blast pressure and shockwaves generated. Therefore, understanding what can cause these explosives to initiate is very important and plays a major part to provide a safe domain and work environment.

Explosives generally react and explode when subjected to external stimuli, such as heat, shock and mechanical impacts. When it comes to impacts, the fear of facing an attack by a shaped charge jet (SCJ) has always been considered to be a very critical threat to various types of military targets including munitions filled with explosives. This is due to the fact that impact from the SCJ can initiate explosives if it exceeds the minimum amount of energy needed to initiate the explosives. In addition to their extremely high-speed impact velocity, shaped charges are explosive devices that are simply assembled from a few components. Shaped charges consist of a cavity in one side separated by a desired geometrical liner and filled with explosives on the other side as depicted in Figure 1. In Chapter two, further details regarding the work mechanism of shaped charges are given and discussed.

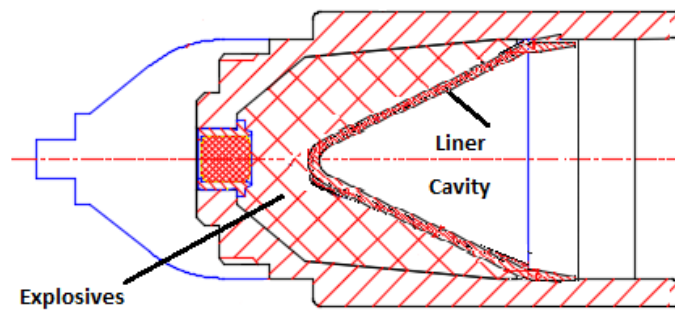


**Figure 1:** A drawing of a 38 mm-conical SC.

The exact date for the first appearance of explosives remained ambiguous. However, there is consensus among historians that gunpowder, which is the first chemical explosive discovered, originated in China more than a thousand year ago [1]. Gunpowder is a chemical mixture consists of potassium nitrate, sulphur, and charcoal. The Chinese used it to make fireworks rather than using it as a war instrument. As a result of this discovery, European nations, such as English and Germans, started to develop this chemical compound into more complicated mixtures that could be used for military purposes. In 1846, an Italian chemist named Ascanio Sobrero [2], invented nitro-glycerine, the first modern chemical explosive, which was based on treating glycerine with nitric and sulphuric acids. However, this new compound had several drawbacks when it came to its thermal stability. A thermal stable explosive does not react or detonate instantaneously due to a very quick change in temperature or any unexpected movements.

In 1862, Swedish scientist Alfred Nobel [3] proposed a solution to solve the issue of thermal instability found in nitro-glycerine. Nobel was inspired to seek a safer way of preparing and handling the nitro-glycerine. He found that when nitro-glycerine is mixed with inert materials, the resulting compound reduces the likelihoods of accidental explosions. In other words, it reduces the overall sensitivity of the explosive compound. Inert materials are those that do not undergo chemical reaction, used in explosives to reduce their sensitivity to external stimuli. This led to the invention of dynamite, a chemical explosive containing nitro-glycerine and absorbent substances. This attempt was considered the first initiative towards making explosives less sensitive.

The unexpected reactions of explosives have caused catastrophic accidents over the years. The unintended explosions events, whether they took place in munitions magazines or by means of enemies' actions, are examples of the explosives' sensitivity.

The sensitivity of any explosive is defined as the degree or measure of the ability of explosives to be initiated by external stimuli. An example of what the sensitivity of explosives may cause is illustrated in Figure 2, where a British battleship was lost in action due to fire caused by an unexploded enemy missile, which led to a sympathetic detonation [4]. The sympathetic-detonation initiated by a nearby explosion or fire, caused the ship to be destroyed. This illustrates how an important military resource, such as a battleship, can be vulnerable due to the lack of insensitivity of explosives carried on-board. Therefore, munitions experts focused on preventing such severe events from happening to stop unwanted collateral damages. One of the innovative solutions found was to reduce the sensitivity of high explosives.



**Figure 2:** A British battleship burned as a result of a sympathetic reaction [4].

Accidents, attacks and disasters caused by explosives encouraged modern explosives industries to shift towards using insensitive munitions (IM) that have a greater resistance against shock, heat and nearby detonating explosives. As time has progressed, it has become a commitment by the international military community to put regulations on the use, assessment and development of such IM in place. Several international organisations are committed to these policies, such as North Atlantic Treaty Organisation (NATO) and Allied Ordnance Publication (AOP), amongst others.

Insensitive munitions are safer to use, transport and store. This is due to their ability of withstanding heat, impact and friction. Although conventional high explosives (HE), such

as 2,4,6-trinitrotoluence (TNT), hexogen (RDX) and octogen (HMX) have shown relatively low sensitivity towards shock initiation, they are highly sensitive towards impact and friction [5]. Therefore, risks associated with the unintended initiation of sensitive munitions motivated many worldwide researchers to find an alternative way, or a replacement of the conventional HE with explosive formulations that exhibit better overall insensitive properties. The general desired outcomes of any IM is to use an insensitive high explosive (IHE) composition able to deliver high detonation velocity, density and detonation pressure. In other words, the desired solution aims at reducing the sensitivity aspect, and maintains/improves the superior strength as those found in conventional HE. The measure of the strength of any explosives depends on releasing a large amount of energy in a very short time. This requires, as mentioned above, high density and detonation velocity.


















There are internationally recognised standards and specifications used as references to measure and inspect the degree of sensitivity on various types of munitions. They are also used as an outline for the methodology of carrying-out evaluations that assist in distinguishing whether the explosive used to fill an ammunition is qualified and within the standards of IM or not. For instance, NATO uses several series of documents called “Standardization Agreement” (STANAG). STANAG 4439 [6] is the relevant document that defines and comprises number of policies used for introducing IM into service.

## **1.2 What is Insensitive Munitions?**

The executive board of the Chief of Naval Operations (CNO) of the United States of America (USA) provided a very comprehensive and concise definition of IM. It stated, “Insensitive Munitions are those that reliably fulfil their performance, readiness, and operational requirements on demand, but are designed to minimise the violence of a reaction and subsequent collateral damage when subjected to unplanned heat, shock, fragment or bullet impact, electromagnetic pulse (EMP), or other unplanned stimuli.” [7].

In practise, a very simple question such as which explosive filling is considered as a good IM candidate, or which explosive shows better IM characteristics than the other, are questions that cannot be answered accurately by theories. Rather, one needs to investigate the explosives by means of experiments to look for the overall sensitivity. Therefore, as per stated by STANAG 4439 [6], a whole set of tests with specific requirements have to be conducted in order to say whether this particular explosive filling

is qualified as an IM or not. A classification scale of IM relevant threats and their associated passing reactions are presented in Figure 3.

|   |                           |  |  |  |   |  |   |
|---|---------------------------|--|--|--|---|--|---|
| <p>IM classes of threats are relevant</p> <p>Standards are representative and one metric of munition response and technology maturity</p> <p>Reaction consequence Affects investment strategy for munition incremental improvements &amp; IM science &amp; technology</p> | Threats                   | FUEL FIRE<br>Such as a truck or an aircraft on a flight deck                       | NEARBY HEAT<br>Such as fire in adjacent magazine, store or vehicle.                | BULLETS<br>Such as small arms from terrorists or combat                            | FRAGMENTS<br>Such as from bombs, artillery, or IEDs                                 | SYMPATHETIC REACTION<br>Such as detonation of adjacent stores                        | SHAPED CHARGE JET<br>RPG, Bomblets, ATGMs: Combat or terrorists                     |
|   |                           |   |   |   |   |   |  |
|   |                           | Fast Cook-off<br>FCO   | Slow Cook-off<br>SCO   | Bullet Impact<br>BI  | Fragment Impact<br>FI   | Sympathetic Detonation<br>SD   | Shaped Charge Jet<br>SCJ  |
| Tests & Passing Reactions   | Tests & Passing Reactions |   |   |   |   |   |  |
|   |                           | Type V Burn  | Type V Burn  | Type V Burn  | Type V Burn   | Type III Explosion   | Type III Explosion  |
|   |                           |  |  |  |   |  |   |
| Reactions   | Reactions                 | Detonation/ Partial Detonation   | Explosion  | Deflagration/ Propulsion   | Burn  | No Sustained Reaction  |   |
|   |                           | Type I/II  | Type III   | Type IV  | Type V  | Type VI  |   |
|   |                           |  |  |  |  |  |   |

**Figure 3:** List of IM relevant threats and accepted reactions [8].

In fact, there is an ambiguity about the behaviour of IHE compared to conventional HE, especially when it comes to SCJ attacks [9]. As the jet velocity along with its diameter, differ in terms of the effect on explosives depending on the sensitivity of these energetic materials. IM tests are explained in further details in Chapter two. There exists many scientific contributions in literature that compare the sensitivity of explosives for known standard substances, such as the work done by W. Arnold and E. Rottenkolber ([9], [10], [11]) on plastic bonded explosives (PBX), and other explosive compositions. A brief description on PBXs is presented in Chapter two. However, since there exist a variety of manufacturing techniques and different ammunitions bodies depending on the country/manufacturer company of interest, IM tests need to be performed whenever a new explosive formulation is used for verification and qualification purposes.

The fact that energetic substances can be combined and mixed together led to the development of several insensitive explosive compositions. One of the most commonly used insensitive energetic substance is 3-nitro-1,2,4-triazol-5-one (NTO), a well matured explosive substance that proved to be effective on reducing the overall sensitivity when



mixed with TNT and its peers. The performances of IHE, as well as chemical properties, differ from energetic material to another as the case with conventional HE. In Chapter two, a discussion on the properties and factors affecting the performance and deliverables of IHE is presented.

### **1.3 Technical Requirements of Insensitive Munitions**

The standardisation agreement of NATO has suggested a number of six unique assessments to serve as a tool to investigate the reactions of explosives when subjected to thermal and mechanical impacts [6]. The main purpose of these assessments is to test whether the examined munition is meeting the technical requirements to be classified as IM or not. These unique tests, which form the basis of the technical requirements, cover thermal and mechanical inspections. They are grouped and categorised as follow:

- Fast cook-off (FCO)
- Slow cook-off (SCO)
- Bullet impact (BI)
- Fragment impact (FI)
- Sympathetic detonation (SD)
- Shaped charge jet impact (SCJI)

These tests simulate real life threats and incidents, such as fuel fire, nearby heat and impacts of various velocities. When it comes to kinetic impacts, high-velocity impact can have different consequences and responses on a target compared to slow-velocity impacts. This is simply due to the difference in kinetic energy carried-out by the object, which leads to diverse results in terms of perforation-depth and ability to ignite explosives [29]. Impact-induced reactions are difficult to predict numerically and theoretically. This is due to the involvement of many main variables/parameters, such as object diameter, threshold energy, material type of the target, etc. Therefore, empirical results are most likely used to the reference type of reactions took place during velocity-impact analysis. In addition, typical threats, hazards and reactions regarding the responses of munitions to IM tests have already been categorised officially by STANAG 4426, a documental policy used by NATO countries. A summary of all expected threats and their accepted resultant reactions in view of IM standards is presented in Figure 3.

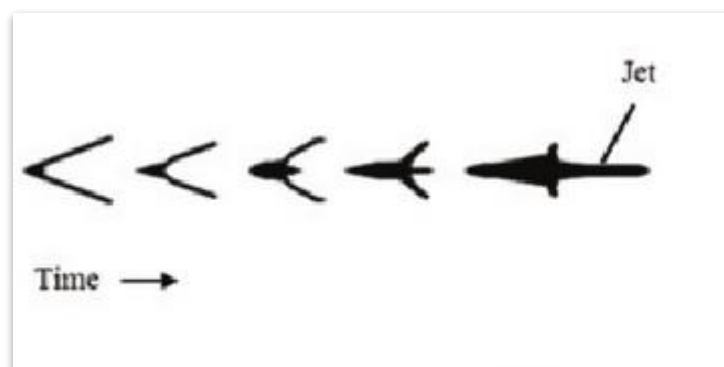
Impact threats are important due to the fact that it can ignite explosives upon impact with the least amount of energy needed. Therefore, it is serious safety concern in the military explosives sector. In addition, due to their significant effect, this research aims at

evaluating the responses of different explosives fillings used in 81 mm mortar projectiles when subjected to the impact of a SCJ. 81 mm mortar bombs were selected due to their wide operational usage in modern warfare. An overview of the principles of which the SCJ relies on is discussed in detail in Chapter two.

#### 1.4 Shaped Charges

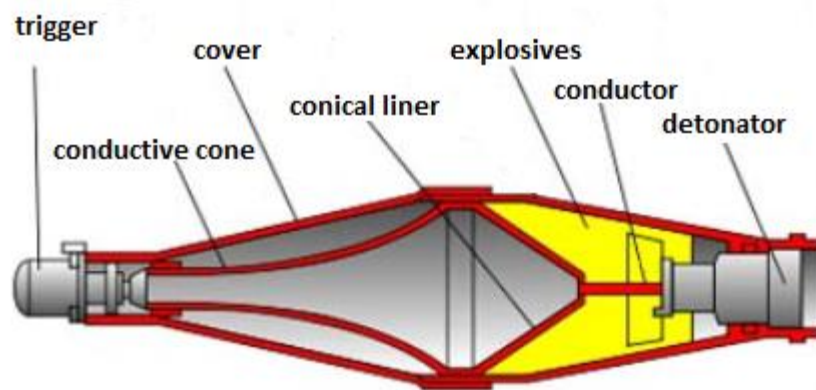
The introduction of the lined cavity charge technology by the Germans in 1943 had led to the invention of shaped charges (SC). It played a very significant role towards the advancement of the field of non-nuclear warhead in present time. The configuration of a typical SC has been well-defined in many sources. It is an explosive device that consists of an aerodynamic cover, air filled cavity separated by a liner on one side, and filled with explosives at the other side as depicted in Figure 1. A detonator and booster are placed on the back of the shaped charge to generate a detonation wave to sweep over the liner and collapse it.

Figure 4 presents a typical jet formation over time lapse. Another important parameter is the material type of which the metal liner is made of can be of various materials, such as lead, mild steel, copper, silver and gold. However, copper has proved to be an excellent choice due to its relative high density, ductility, high melting point, and cost effectiveness. In addition, the hollow cavity can also be of any desired shape, most commonly in a conical form. This is due to its ability to penetrate and forms a proper jet. However, each shape results in a specific level of performance in terms of target perforation and jet formation [12]. This incredible phenomenon is called the Munroe effect, dedicated after Charles E. Munroe who discovered it in 1888 [13]. Shaped charges have many applications and purposes depending on the tactical environment used in.



**Figure 4:** Jet formation over time elapse.

For instance, although shaped charges have a vast range of usages, they are primarily used as warheads for High Explosive Anti-Tank (HEAT) missiles, torpedoes and for some artillery propelled projectiles in military applications. One of the most widely used HEAT weapons is rocket-propelled grenade (RPG-7), due to its perforation-effectiveness, affordability and simplicity [14]. It is capable of penetrating approximately 250-700 mm of armour steel depending on the size of calibre used [15]. On the other hand, for non-military purposes, shaped charges are used for demolishing buildings, structures and has a wide range of applications in the mining industry [16].



**Figure 5:** Cross-section of an RPG-7 warhead.

There are two commonly used types of initiation systems in the design of a SC warhead. One is known as the axisymmetric initiation: used to ensure a symmetrical firing along the cone axis, especially, when using a symmetrical cone liner. The other method is called dual point initiation, which is based on initiating the liner from multiple-points: to add control that can result in forming a more desirable shape of the jet. Illustrations of different initiation mechanism are presented in Figure 6.

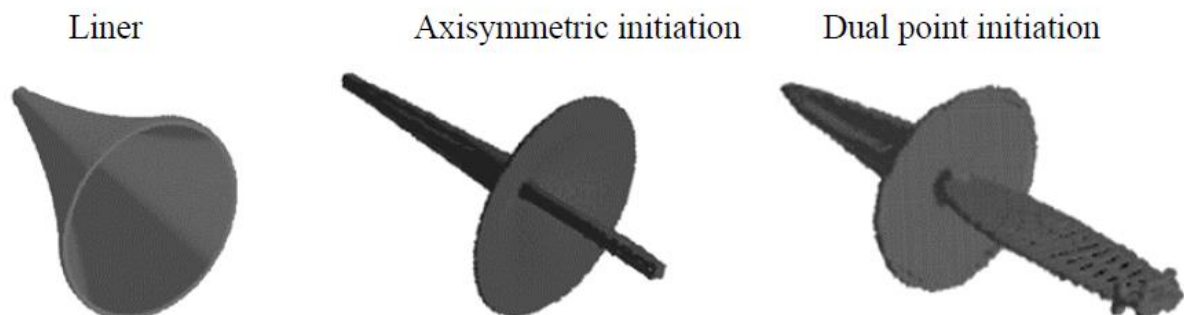


**Figure 6:** Different initiation methods used in shaped charges.

## 1.5 Problem Statement

The SCJ threat has become one of the most widely used attacks on various military targets and vehicles. This includes munitions carried on-board in battleships, or stored in a munitions magazine. In fact, shaped charges are found in many military applications, such as missiles, torpedoes, demolition charges, etc. This type of impact can prompt munitions on the other side of the barrier to react severely in a form of detonation causing damages to the surroundings. The criticality of shaped charges lies on delivering damages to targets with the least amount of energy needed, due to its high-speed jet that can reach up to 10000 m/s or even higher.

TNT is still being used as a main HE filling for mortar projectiles in many countries. Particularly in 81 mm mortar projectiles, which remained as an effective operational weapon that is used in abundance in modern warfare. 81 mm projectiles were used as main test items in this work. Therefore, the problem to be solved in this work is to determine the critical amount of SCJ threshold ( $V^2d$ ) needed to initiate 81 mm mortar projectiles filled with TNT and NTO/TNT-based explosives formulations. NTO/TNT-based explosives have proven their suitability for being potential candidates for IM. Results of TNT will be used as baseline for testing the selected IHE compositions based on NTO. In addition, the difference in responses observed on mortars filled with TNT will be investigated and compared to that observed on NTO-based compositions.

A secondary objective to be addressed is that a study done by Dr Arnold and his colleagues [10], stated that the threshold of a jet ( $V^2d$ ) cannot be treated as a constant value, and that the tip velocity ( $V_{tip}$ ) and diameter ( $d$ ) need to be analysed individually. Therefore, the problem to be solved is to show whether the results obtained in this work support the claim obtained in [10] or not.

## 1.6 Research Objectives

Based on the research problems noted above, the following primary objectives need to be achieved through this research:

- To determine explicitly by means of experiments the critical values of ( $V^2d$ ) responsible for initiating different types of reaction on 81 mm mortar projectiles filled with TNT, NTO/TNT (50/50) and NTO/TNT (20/80).

- To determine whether a low amount of NTO is sufficient to withstand a 38 mm SC attack.
- To identify the types of reactions, in accordance to STANAG 4439 [6], resulting from initiating the 81 mm mortar projectiles.

In order to meet the stated primary objectives of this research, the following secondary objectives need to be achieved:

- To characterise the 38 mm SCJ used in this work by means of flash x-ray analysis, by finding the leading particle velocity, tip diameter and jet breakup time;
- To generate different ( $V^2d$ ) values of the 38 mm SC by means of varying the thickness of the conditioning steel plate; and
- To verify whether the results obtained in this work correspond with the findings concluded by Dr Arnold and his colleagues with regard to disputing the constant rule of ( $V^2d$ ). This will be achieved by drawing a comparison with the results acquired by RDM [18] using 57 mm SC.

## 1.7 Research Scope and Limitation

The following are included in the scope of this research:

- 81 mm mortar projectiles filled with various explosives formulations, were used as test items for the SCJI test;
- melt-cast based explosives formulations were used to fill the 81 mm mortar bombs; TNT, NTO/TNT (50/50) and NTO/TNT (20/80); the parentheses describe the percentages of each explosive used to form the overall compositions; and
- 38 mm shaped charges with conical copper liner and uniform wall-thickness were used to attack the 81 mm mortar bombs. The cone used has an apex angle of 56.4°.

The following limitations apply to the research conducted:

- only SCJI test was taken into consideration to investigate the tested explosives compositions;
- only 38 mm SC were available for use, other calibres were restricted due to intellectual property rights; and

- melt-cast explosives were used due to their availability, cost and suitability as known matured explosives.

## 1.8 Dissertation Outline

**Chapter 1:** This chapter provides an introduction of the research and the various aspects pertaining to this research. It also provides background and state the research problem together with the various research objectives that need to be addressed through this research. The research scope/boundaries, as well as the research limitations are also defined in Chapter one.

**Chapter 2:** This chapter provides a concise literature review on types of explosives used in military industries. It focuses mainly on the necessity of using IHE in place of the typical conventional HE. It presents relevant results and contributions in the field of IM, and show drawbacks encountered in our modern time. In addition, the concept of SCJ is introduced in detail with restrictions to the scope of this research and a number of critical parameters affecting the performance/characteristics of the SCJ are explained. Furthermore, relevant results selected here will be used for the purpose of comparison and verification along with other available data. Lastly, the concept of reducing sensitivity by applying certain types of filling techniques on existing explosives compositions are also explained.

**Chapter 3:** The methodology used in this research is experimental based, in which results are going to be quantitatively analysed. All tests set-up involved in studying the characterisations and impacts of the SCJ are explained in detail. In addition, tests are conducted in accordance with STANAG documents and as per other approved scientific papers.

**Chapter 4:** Main results obtained from the conducted experiments in this research are stated in this section, such as jet characteristics by means of flash x-ray analysis and type of reactions resulted from initiating the 81 mm mortars. Tables, as well as illustrative graphs are provided in this chapter.

**Chapter 5:** This chapter provides a discussion of the main findings observed on the initiation of 81 mm mortar projectiles. This includes discussing the differences in behaviour between HE and IHE explosive formulations when subjected to SCJI. A critical evaluation of all results obtained on both tests, SCJI and flash x-ray analysis. Lastly,

results are verified by using two different methods and other relevant results from literature.

**Chapter 6:** A summary of all findings observed on the results obtained from tests, the author's remarks and recommended future studies are discussed in this chapter. The conclusion of whether objective were met or not are highlighted.

## **1.9 Summary**

The definition of energetic materials lie on the fact of releasing energy over a short period of time. They are widely used in military industries and have different applications depending on the type of energetic material used. The sensitive property of explosives and its impact on safety encouraged modern industries to find solutions that aim at making explosives less susceptible to external stimuli. The importance of shaped charges attacks rely on delivering severe damage to munitions and other relevant targets using the least amount of energy needed.

The main objectives of this work were to determine by means of experiments the critical values of the jet energy responsible for initiating different types of reaction on 81 mm mortar projectiles filled with various explosive formulations. The types of reactions resulting from initiating the 81 mm mortar projectiles were identified, in accordance to STANAG 4439 [6]. The significance of this research was to highlight the ambiguity in behaviour of different types of explosives by means of experiments when subjected to an attack by shaped charge jet. The following chapter consists of important concepts and theory related to explosives and shaped charges.

# Chapter 2: Literature Review

## 2.1 Introduction

The research objectives, problem statement, research outline and an overview of energetic materials and shaped charges were discussed in Chapter one. In Chapter two, several important concepts related to the properties and sensitivity of explosives used in modern military industries are discussed in detail. These include discussing common explosives formulations and compositions that are designed to be insensitive to external stimuli, such as heat, shock and various types of impacts.

A comparison between the properties of HE and that of IHE are also highlighted. In addition, a theoretical explanation in regards to shock sensitivity and impact ignition on explosives molecules is presented. A brief discussion on the IM test methods used by NATO and their associated reaction levels are further shown in this section.

In addition to the above-mentioned, several important theories related to jet formation, jet breakup time and the effects of standoff distance are discussed. Relevant experimental results obtained from literature and other sources are underlined for the purpose of comparing the results with the current work presented in this dissertation. This includes recent work conducted by Dr Arnold, Rottenkolber and Hartmann [10], titled “Challenging  $V^2d$ ”. This group of scientists were concerned about the statement stated by STANAG 4526 [17], which claims that the values of the jet threshold should be treated as constant, regardless the variation in SC calibre.

Relevant results obtained from a study conducted by Rheinmetall Denel Munitions (RDM) [18] on 81 mm mortar bombs using a 57 mm conical SC are depicted in this chapter. In the current study, a comparison was made in Chapter four to show the effect of different jet threshold values on initiating 81 mm mortar bombs filled with various explosive formulations. Munitions responses to impacts from different jet thresholds obtained from the 38 mm SC are compared to that acquired by the 57 mm SC.

Lastly, different mechanisms of explosives filling techniques, as well as their contribution on the overall insensitivity of explosives, are described in this chapter.



## 2.2 Conventional High Explosives

The most commonly used HE in military industries is Trinitrotoluene (TNT) due to the fact that it has a very low melting point, which allows for mixing it with other types of explosives, such as RDX and HMX, whilst in its molten state [19]. The melting point of TNT is achieved at approximately 80°C [20], while it is 205°C and 274°C for RDX and HMX respectively [21]. TNT possesses energy that is equal to 4686 J/g, which was measured accurately from a large sample of air blast experiments [22]. A typical amount of TNT used in 81 mm mortar bombs ranges from 392 to 680 gram. This amount of HE can cause the mortar bomb casing to scatter producing fragments that can travel at large distances. The term energy for explosives refers to the thermodynamic work produced by its detonation. The chemical structure of TNT is provided in Figure 7.

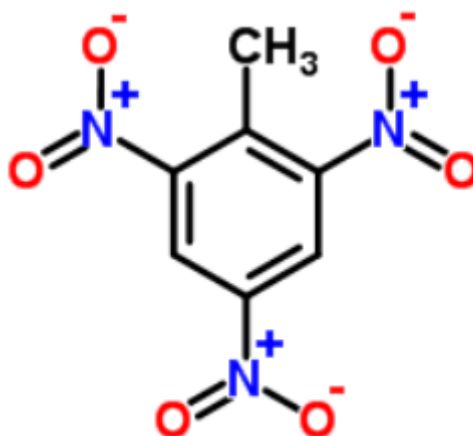


**Figure 7:** Chemical structure of TNT.

An important characteristic of TNT is the fact that its manufacturing process is completely safe and cost effective. TNT has been proven to possess relatively low sensitivity to impact when compared to RDX, HMX and other HE substances [23]. However, TNT has lower density and velocity of detonation than RDX and HMX as presented in Table 1. This provoked mixing TNT with higher energy explosives to increase the overall performance (i.e. high density and velocity of detonation) of the new formed composition, but on account of increasing the sensitivity.

**Table 1:** A comparison of chemical properties and characteristics for conventional High Explosives (HE) [24].

| <b>Explosive</b> | <b>Density<br/>(g/cm<sup>3</sup>)</b> | <b>Velocity of detonation<br/>(<math>U_D</math>)</b> | <b>Relative Effectiveness Factor<br/>(REF)</b> |
|------------------|---------------------------------------|--|--|
| TNT              | 1.60                                  | 6900 m/s   | 1.00   |
| HNS              | 1.70                                  | 7080 m/s   | 1.05   |
| Comp B           | 1.72                                  | 7840 m/s   | 1.33   |
| NG               | 1.52                                  | 8100 m/s   | 1.54   |
| RDX              | 1.78                                  | 8700 m/s   | 1.60   |
| PETN             | 1.71                                  | 8400 m/s   | 1.66   |
| HMX              | 1.86                                  | 9100 m/s   | 1.70   |

TNT is used in many military applications on a global scale; it became a standard measure reference for the strength of other explosives.

The relative effectiveness factor (REF) relates the power of explosives to that of TNT; Table 1 presents a list of REF for different explosives. Each type of explosive has unique properties that differentiate it from other energetic materials. For example, chemical properties like density, velocity of detonation ( $U_D$ ), and potential chemical energy vary from one energetic substance to another; Table 1 presents several energetic substances with different characteristics. Specific characteristics can consequently be obtained through a new explosive compound by mixing two or more energetic substances.

The 81 mm mortar shells used during this research have been filled with TNT to provide a baseline to measure the differences obtained in reactions and behaviours with respect to the other explosives compositions selected for this research. These explosive compositions are as follows with their mixture ratios shown:

- NTO/TNT (20/80); and
- NTO/TNT (50/50).

The mixture of NTO/TNT (50/50) is commonly known as “Ontalite”, which has been tested and proven as a suitable IM candidate for filling various types of munitions [18]. On the other hand, NTO/TNT (20/80) is a new composition that has not been tested before. As

NTO has higher density and velocity of detonation compared to TNT, it is also proved to be very insensitive explosive. Among other objectives of current work, one objective was aimed at investigating a low percentage of NTO in terms of SCJ attack and compare to that of NTO/TNT (50/50). Further details on the properties of NTO can be found in the next section.

### **2.3 Insensitive High Explosives**

TNT-based explosives have proven to be very effective in terms of performance and affordability when produced in large-scale. The performance of HE can be related to its velocity of detonation, density and detonation pressure. These parameters can give a preliminary indication on any explosive efficiency. However, their sensitivity to external stimuli drew a major drawback to safety aspect. Studies have shown that melt-cast TNT detonates when subjected to an impact by SCJ, and compositions contain TNT/HMX/RDX also failed to withstand high-velocity impacts delivered by either bullet or SCJ [9, 25].

Therefore, the essence of the search for explosives that are insensitive is to overcome the issue of safety found in working with conventional high explosives. This became a top priority in modern military industries. IHE are explosive compositions exhibiting good performance in terms of density and velocity of detonation, and meanwhile are well-tested for safety purposes against impact, shock, and heat. This desired safety mechanism is intended to develop munitions that can show reliable survivability and capability of withstanding accidents, enemy attacks and adjacent fires.

There are different types of energetic substances that when combined together lead to form IHE compositions. Each one has its own degree of thermal stability, velocity of detonation, degree of resistance to external stimuli, etc. In addition, the range of sensitivity for IHE differs in terms of their insensitivity performance. The insensitive performance of IHE lies mainly on passing all the IM tests [6], which account for the ability to resist thermal and mechanical threats. In other words, the more heat/impact a substance/composition can withstand, the better the IM performance. Details about the IM tests are further shown in Section 2.6. Although various IHE have different physical and chemical properties, the key of choosing a suitable IHE depends entirely on the purpose, desired objective, availability of the manufacturing/filling facilities and definitely the cost.

There is a number of different IHE depending on the method used for preparing them. Insensitive explosives have been classified into three main categories. These categories are:

- Melt-cast explosives;
- Cast-cured explosives; and
- Pressed explosives.

For relevance of this study, only melt-cast NTO/TNT-based explosives are used to fill the 81 mm mortar bodies. This was simply due to their availability, as well as their suitability for being good IM representative. NTO/TNT are commonly prepared by melt-cast process, which uses the fact that TNT has a very low melting point to allow mixing it with NTO to get its insensitive property. NTO is widely used as a key substance for reducing the overall sensitivity in an explosive composition [18, 26]. This is due to its high density and velocity of detonation, which are estimated empirically to be  $1.91 \text{ g/cm}^3$  and 8660 m/s respectively [27]. As NTO is classified as an extremely low sensitive explosive, it needs to be mixed with other sensitive HE, such as TNT, RDX, or HMX in order to ensure its initiation. In addition, studies have shown that it is less sensitive to impact, friction, heat and electrostatic sparks compared to TNT, HMX and RDX [21]. Figure 8 presents the chemical structure of NTO.

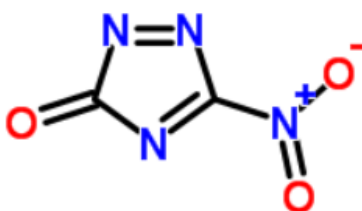


**Figure 8:** Chemical structure of NTO.

Since the development of IM aims at making explosives much safer and meanwhile exhibit better performance than that found in conventional HE, several compositions were evaluated and suggested as replacements for conventional HE in terms of velocity of detonation output as shown in Table 2.

**Table 2:** A list of expected alternatives to conventional HE [28].

| HE                  | Velocity of detonation ( $U_D$ ) | Alternative IHE       | Velocity of detonation ( $U_D$ ) |
|---------------------|----------------------------------|-----------------------|----------------------------------|
| TNT                 | 6900 m/s                         | NT0/TNT (50/50)       | 7630 m/s                         |
| HMX                 | 9100 m/s                         | NT0                   | 8600 m/s                         |
| Comp B<br>(TNT/RDX) | 7840 m/s                         | NT0/TNT/RDX(55/35/10) | 7930 m/s                         |

Comp B is an explosive formulation used primarily in large calibre projectiles specifically in artillery, such as 155 mm. It has proven to be an excellent candidate for increasing the lethality effects formed by the scattered fragments of the projectile casing. Lethality generally related to size and velocity of fragments. The addition of NT0 to TNT/RDX yielded an explosive formulation that can be potential candidate for both increasing lethality and decreasing sensitivity as for IM [28].

## 2.4 Conceptual Considerations on Shock Sensitivity and Impact Ignition

The mechanism of which shock and impact ignition relies on is that shock waves are responsible for triggering and releasing chemical energy in explosives molecules. This explains why detonators are used to initiate secondary explosives, such as TNT, HMX, NT0, etc. However, it needs to be accompanied with sufficient strength and duration in order for the exothermic reaction to take a place [29]. This eventually leads to a detonation wave that comprises the leading shock wave front along with the released chemical energy as a source of initiation. One can easily calculate the needed induction time to initiate the “thermal explosion” by using the basic equation of state of high pressure and temperature.

In case of a low velocity impact, which carries a small amount of pressure, two compressible waves are generated. One (elastic wave) propagates towards the explosives at a longitudinal-sound velocity and the latter (plastic wave) comes after it with a lower velocity [30]. As a result of impact ignition, heat is transferred to the explosives by means of friction, shear and other types of sources [31]. This eventually prompts what is called “Hot spots” that increases the possibility of an explosive to release its energy. These low velocity impacts can be investigated further quantitatively, and their results can be simulated with existing computational fluid models. The level of strength of the shock wave is proportional to the amount of pressure that it carries with. The higher the pressure

the stronger the shock compression becomes. However, there exists a way to avoid creating these growing hotspots, which are formed due to the existence of microscopic cavities on the surface of an explosive, this method relies on using the phenomena of “dead pressing”[32]. Therefore, the mission of initiating such high energetic material by a shock wave, or even a detonating wave will require much higher energy. Primary explosives were developed to be placed prior to the main charge to enable sufficient activation energy for initiating the main charge (secondary explosive). Primary and secondary explosives are expressions used to describe the components of a typical explosives train; Figure 9 presents an illustration of such explosives train.

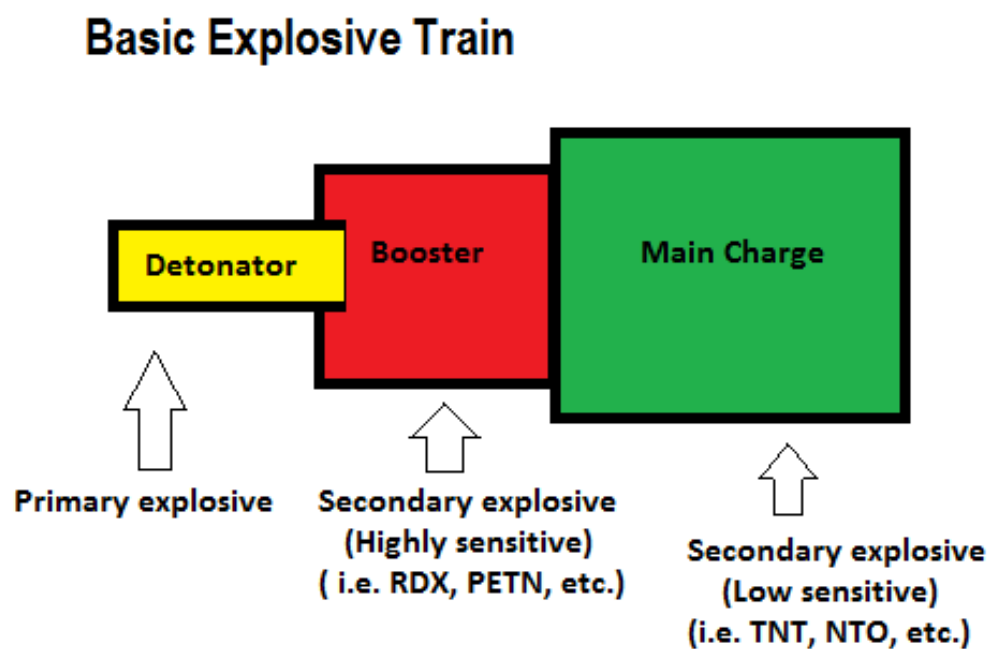


**Figure 9:** Typical components of an explosive train.

## 2.5 Filling Techniques (melt-cast, cast-cured and pressed)

Ammunitions are usually filled via using one of these three main processing technologies:

- Melt-cast process;
- Cast-cured process; or
- Pressed process.

These processing mechanisms are known as melt-cast, pressed and cast-cured. Melt-cast technique relies on the property of low melting point that TNT has, which allows it to be mixed with different types of explosives [33]. Various types of explosives are allowed

to be mixed with melted TNT under high temperature ranges from 100°C-120°C. Once the mixture is properly stirred, it is poured into ammunitions under constant temperature and then left to cool and solidify.

For instance, NTO/TNT-based explosives are generally prepared by means of melt-cast process. The addition of NTO to TNT results in a composition that is insensitive and powerful in terms of detonation and pressure released. A melt-cast process is used for several military applications since it is a well-established and matured technique. NTO-based explosive compositions are widely used in 81 mm mortars due to its frequent operational usage in battlefield, and hence low-cost IM filling is preferred [28]. Figure 10 presents a melt-cast filling facility used to fill the 81 mm mortar bodies with TNT.

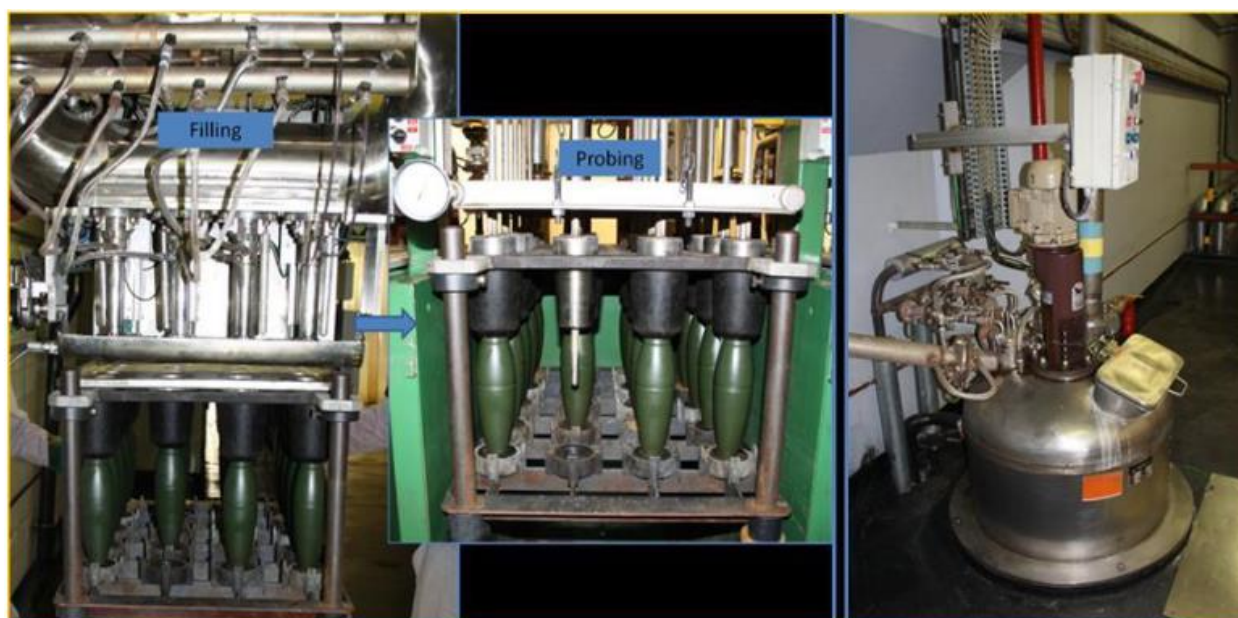


**Figure 10:** Melt-cast filling facility used by RDM [18].

Figure 10 shows a typical melt-cast process. Mortar bodies were preheated to approximately 70°C prior to filling to ensure no thermal shock is encountered. This is to avoid a sudden reduction in temperature which eventually may lead to presence of voids and air bubbles inside the mortar bombs. Mortar bodies were then filled with melted TNT at around 120°C to ensure that TNT is completely melted. Finally, a probing process was used to regulate the cooling process until proper solidification of TNT was achieved.

Cast-cured process generally involves melting explosives combined with some polymers and left for heat treatment (i.e. curing). The key advantage that it has is the ability of containing a high portion of high sensitive explosives (i.e. RDX) bounded with polymers

to produce a composition that is less vulnerable to external stimuli. It is very complicated and time consuming compared to a melt-cast and pressed techniques. Therefore, it is not as cost effective as that of melt-cast technique. A pressed technique generally focuses on pressing the explosive mixture to gain higher density in small volume.

For instance, PBXs, which are prepared by either pressing or cast-cured techniques, are considered as a viable alternative for TNT based melt-cast explosives due to the following advantages [34]:

- Pressing capability to achieve higher density;
- Mechanical strength; and
- Thermal stability.

In fact, what really determines the choice of filling is the acquisition of technology, cost and a capability of using that particular technique. However, each technique implies a certain level of limitations and contributions toward reducing the overall insensitivity of ammunitions [36].

Large calibre projectiles, such as 155 mm used for heavy artillery, are mainly intended to cause damages by means of fragments. This is done by using explosives formulations that have high velocity of detonation and detonation pressure. As a result, fragments can travel over long distances at very high velocities. Therefore, the selection of the type and amount of energetic materials are crucial in determining the characteristics of the final explosive compositions.

## **2.6 IM Testing (Methods & Classification)**

The insensitive property of ammunitions is based on the response of IM tests presented in Table 3 according to STANAG 4439 [6]. STANAG 4439 is a document that handles the policies and assessments of the IM tests. Each IM test is described in detail in a separate document and presented in Table 3.



**Table 3:** IM standard tests and their corresponding STANAG documents.

| Test                    | Method/Relevant STANAG document |
|-------------------------|---------------------------------|
| Fast Cook-off           | STANAG 4240 [37]                |
| Slow Cook-off           | STANAG 4382 [38]                |
| Bullet Impact           | STANAG 4241 [39]                |
| Fragment Impact         | STANAG 4496 [40]                |
| Sympathetic Detonation  | STANAG 4396 [41]                |
| Shape Charge Jet Impact | STANAG 4528 [42]                |

Fast and slow cook-off tests are used to simulate scenarios where sources of fast and slow heating reactions are taking a place. For instance, fuel fire in a vehicle transporting munitions (fast cook-off), or a fire adjacent to a magazine (slow cook-off). This test is done by placing the test item (ammunition) inside an oven where fuel (i.e. kerosene) is placed a distance underneath it as shown in Figure 11. Critical temperatures responsible for detonating the ammunition are measured by thermo-couple.

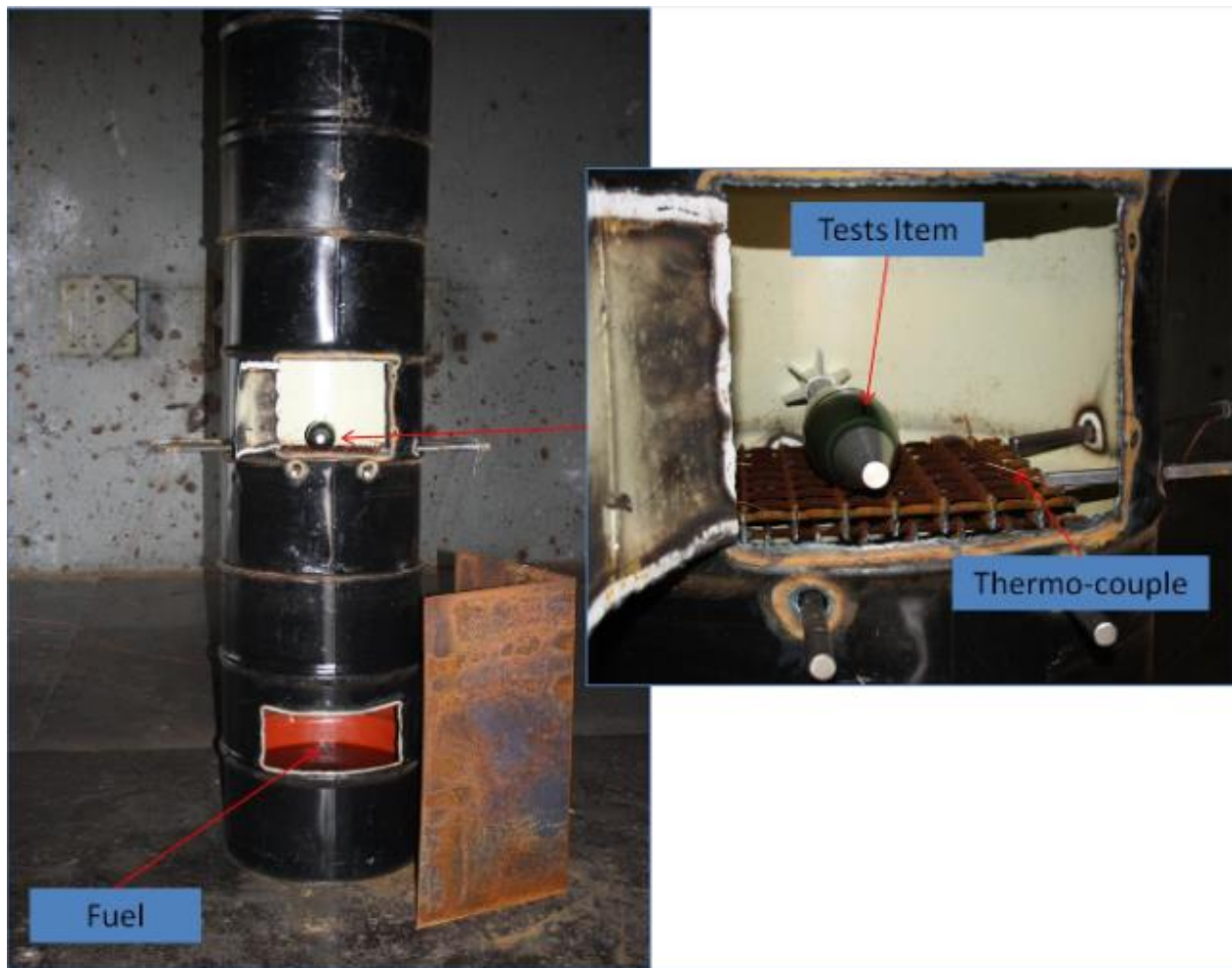


**Figure 11:** Fast cook-off test set-up [18].

Bullet and fragment impact tests are used to simulate a scenario where munitions are hit with small arms attack and fragments from detonated munitions respectively. This is simulated by using a 12.7 mm armour piercing (AP) round at an impact velocity of roughly 900 m/s for bullet impact, while fragments are shot by using a 40 mm gun at a velocity of impact equal to ~1900 m/s.

The sympathetic detonation test aims to determine what would happen to the ammunition when adjacent munitions detonated. This is to simulate a scenario where a number of munitions are transported or stored together. This is done as shown in Figure 12.

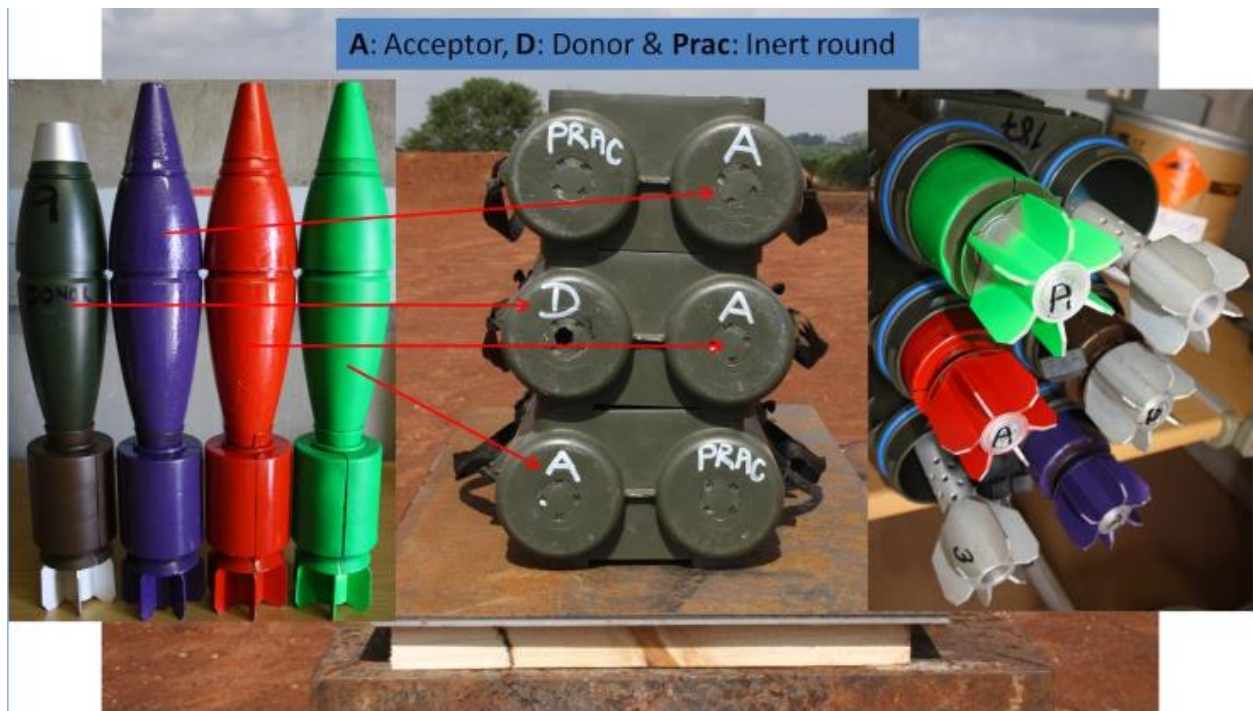


**Figure 12:** Sympathetic test set-up [18].

The sixth and final test is called the SCJI test. SCJI test simulate a scenario where munitions are hit with bomblet, rocket, etc. This test is relevant to the work presented in this dissertation and is concerned about the response of ammunition when under attack from a shaped charge. The velocity of impact in this case can reach up to 9 km/s depending on the SC calibre used. The 38 mm SC used in current research produced a jet with a maximum velocity equal to 7.38 km/s.

In order for the explosive to be qualified as an IM, its IM signature has to comply with the passing criteria defined by STANAG 4439 [6]. The term IM signature is defined as the summary of results obtained from testing an item against all six of the above-mentioned IM tests. The passing criteria consist of acceptable reaction levels for each IM test performed on a specific item filled with explosive. Figure 3 presented in Chapter one presents the acceptable reactions level for each IM test.

There are approximately five different reactions types, which are explained in detail in the following paragraphs. These types of reactions were used to classify the response of the mortar bombs used in this work.

a) Type I reaction

Type I is classified as a full detonation reaction. This implies that all energetic material contained in the ammunition are fully reacted to detonation. The ammunition body will be shattered into small fragments causing severe damages to the surrounding. The blast over-pressure measurements will show measurements that are similar to a detonated ammunition in battlefield.

b) Type II reaction

Type II is classified as a partial detonation reaction. This is due the presence of an undetonated portion of the energetic material contained in the ammunition. The damages caused by this reaction are not as severe as in type I; however, small and large fragments are observed and can cause strong damages to the surroundings. The blast over-pressure measurements are lower than that observed in type I.

c) Type III reaction

Type III is classified as an explosion reaction. The energetic material in this case is ignited and burnt leading to a violent pressure release. The ammunition body will be broken into large fragments causing relative damages to the surrounding. However, blast over-pressure measurements are lower than that for type I and type II reactions.

d) Type IV reaction

Type IV is classified as a deflagration reaction. The energetic material in this case is ignited and burnt in a propulsive manner. The energetic material contained in the ammunition will not be subjected to a violent pressure release since pressure can be easily escaped through the small gaps around the fuse. The ammunition body may be fractured, however, presence of fragments will not be observed while only unburned energetic material will be propelled causing no damages to the surroundings.

.

e) Type V reaction

Type V is classified as a burning reaction. The energetic material in this case is ignited and burnt in a non-propulsive manner. This means the rate of burning is relatively low

compared to the deflagration reaction observed in Type IV. The ammunition body may split into two pieces in a non-violent manner. The ammunition fuse may be propelled to a long distance, however, it will not cause a damage to the surroundings.

f) Type VI reaction

Type VI simply means no reaction took place at all.

## 2.7 Relevant Results and Findings

Scientists from RDM [18] conducted IM investigation on 81 mm mortar bombs filled with various explosive fillings. Although the study covered all IM tests, only the results from the SCJI test are discussed due to their relevance to the scope of the current research.

The above-mentioned study was performed using 57 mm conical SC with varied  $V^2d$  values. A variation of  $V^2d$  values was obtained by using a conditioning steel plate. A number of explosive formulations were tested, including NTO/TNT (50/50), GUNTOL and RXHT-80.

GUNTOL is a melt-cast composition containing TNT/FOX12, where FOX12 is a new energetic material proved to be very insensitive and a good IM candidate [43].

RXHT-80 is a cast-cured PBX composition consisting of RDX/binders. Plastic binders are inert materials used as desensitizers to lower the sensitivity of an explosive formulation by acting as a bounding agent to explosive molecules. Results of the SCJI test obtained from this investigation are summarised in Table 4.

**Table 4:** SCJI test on 81 mm mortar bombs filled with insensitive melt-cast explosive formulations [18].

| Explosive Formulation | SCJI Test # | Conditioning Plate (mm) | $V^2d$ ( $\frac{mm^3}{\mu s^2}$ ) | Reaction Type |
|-----------------------|-------------|-------------------------|-----------------------------------|---------------|
| RXHT-80               | 1           | 50                      | 100                               | II            |
|                       | 2           | 60                      | 88                                | IV            |
|                       | 3           | 75                      | 75                                | V             |
|                       | 4           | 125                     | 50                                | V             |
| NTO/TNT (50/50)       | 5           | 25                      | 145                               | II            |
|                       | 6           | 35                      | 121                               | III           |
|                       | 7           | 50                      | 100                               | IV            |
|                       | 8           | 75                      | 75                                | IV            |
| GUNTOL                | 9           | 0                       | 662                               | II            |
|                       | 10          | 25                      | 145                               | II            |
|                       | 11          | 50                      | 100                               | III           |
|                       | 12          | 75                      | 75                                | IV            |

The investigation conducted by RDM [18] used a 57 mm SC, while the current work presented in this dissertation used a 38 mm SC. The advantage of using a higher SC calibre is that it increases the scope of testing by allowing higher values of  $V^2d$ . A high SC calibre implies higher jet diameter, which has detrimental effects on munitions. On the contrary, a small SC calibre is used for the current research, which allowed using low  $V^2d$  values. This is suitable for finding critical values responsible for initiating conventional sensitive HE, such as TNT. The critical value of  $V^2d$  responsible for initiating TNT was obtained by experimental means and is presented in Chapter four.

A recent study conducted by Arnold, Rottenkolber and Hartmann [10], stated that the  $V^2d$  rule presented by STANAG 4526 [17] is not applicable when SC calibre is varied. The study concluded that detonation was achieved using various SC calibres and different jet stimulus values. In particular, detonation was initiated by 44 mm SC using low values of  $V^2d$ , compared to higher values of  $V^2d$  generated by 75 mm and 115 mm SC calibres. Therefore, the above-mentioned scientists proposed an adjustment to the current edition

of STANAG 4526 [17] due to the inconsistency of  $V^2d$  rule stated by STANAG 4526. Figure 13 presents the results of  $V^2d$  values obtained by [10].

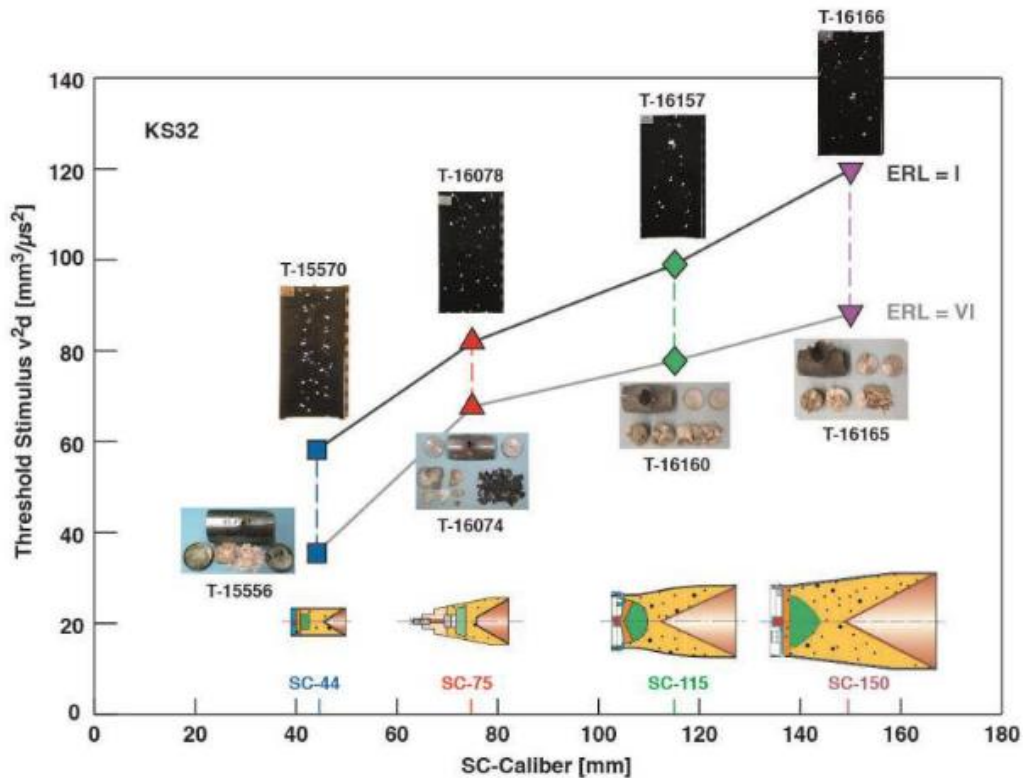


**Figure 13:** Varied SCC and their corresponding critical  $V^2d$  values [10].

Figure 13 clearly indicates that low value of  $V^2d$  created by 44 mm SC is required to induce a detonation of the test item compared to higher values of  $V^2d$  created by 75 mm, 115 mm and 150 mm. These tests were performed on standard cylindrical casing filled with HMX/PB (85/15), where PB refers to polymer binder (i.e. Polybutene).

The current work conducted in this study has a secondary objective of investigating the possibility of a small SC calibre to deliver severe reaction responses on 81 mm mortar bombs with small values of  $V^2d$ . This was done to show whether there is agreement with what was stated and concluded by Dr Arnold and his colleagues [10] or not. A direct comparison between the results obtained from current work presented here and results found by [10] will not be applicable due to different usage of explosives fillings and test items. However, from a conceptual point of view, the effect of varied  $V^2d$  values from varied SCC are compared.

## 2.8 Shaped Charge Jet

There are several different phases during the process of SCJ formation:

- Jet formation;
- Jet breakup; and
- Jet-target interaction.

Upon the formation of a shaped charge jet, the liner material undergoes a high dynamic pressure due to the detonation of the high explosive. As the liner material collapses, due to a mechanical tensile distortion, it becomes subjected to high temperatures ranging from ~ 400-700 C [44]. The jet then starts to form and move at a very high speed of up to 9 km/s or higher in some instances.

The jet generated from the collapsing of the liner components carries an energy that has the ability of perforating various thicknesses of steel. The factors that determine the amount of the jet threshold depends on the SC calibre, standoff distance used, the material of which the liner is made of and type of explosive used to fill the SC. In addition, the geometrical shaped of the liner contributes immensely to the efficiency of the formed jet [46]. The energy of which the SCJ forms is referred to as the “threshold stimulus”.

The jet threshold stimulus is the product of the jet tip velocity squared with its particle diameter ( $V^2d$ ). As the jet stretches out, it is very important to maintain its length before “particulating”, a technical term refers to the state when the jet starts to become divided into particles, in order to deliver the highest amount of penetration. Therefore, many researchers have centred their focus on increasing the jet ductility [45].

There are several important ways and techniques involved in developing and manufacturing SC liners, such procedures known as cold, hot and warm forging. Each of which has its own advantages and disadvantages on the overall characteristics of the jet. However, this is beyond the scope of the work presented in this dissertation.

The SC liner may have different geometrical shapes, such as conical, trumpet, etc. depending on the SC applications. For instance, a linear-cutting SC usually comes with an inverted “V” shape liner to allow for cutting ability, while the one aims at maximising penetration depth is most likely to have a conical liner shape. Conical and trumpet liners shapes are presented in Figure 14. In this dissertation, a copper conical liner is used for the 38 mm SC.



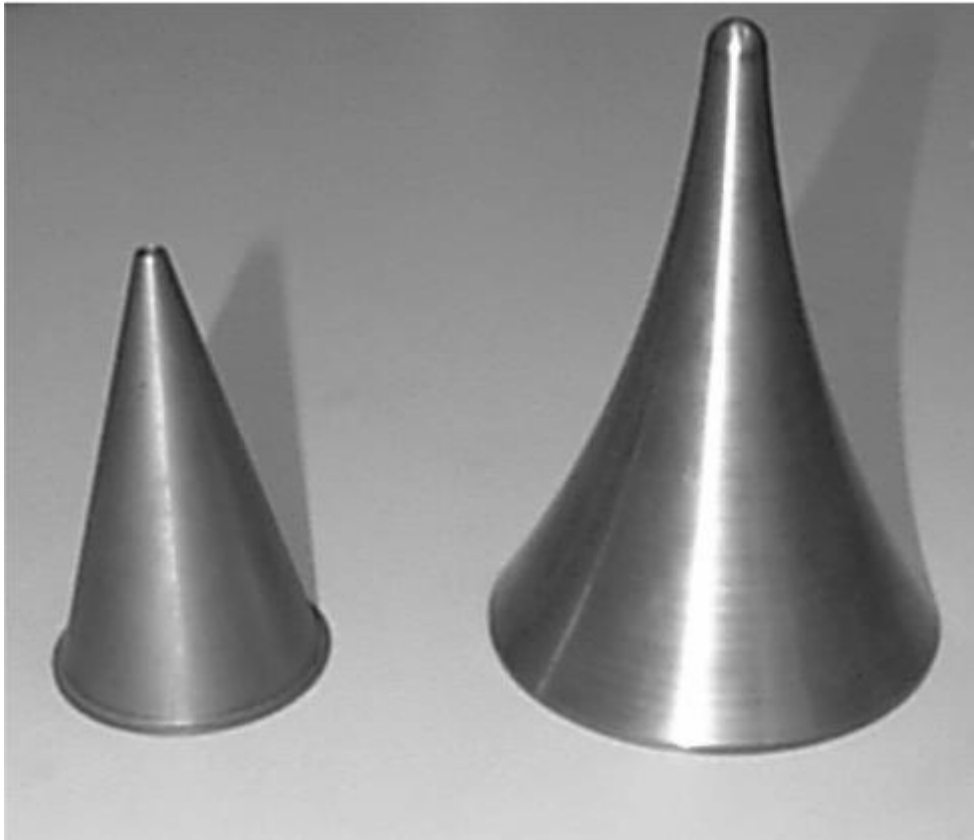


**Figure 14:** Conical and trumpet SC liners [47].

### 2.8.1 Jet Formation Process

There are number of theories and models that aimed to describe the jet formation of conical shaped charges. It started in 1948 with the Birkhoff theory [48], which assumed a constant collapse velocity of the conical liner. This was done by means of assuming a steady-state collapse model, which assumed that the liner components are accelerated to their final velocity over a constant length equal to the slant height of the cone. This theory failed to explain why the velocity gradients observed in the jet particles exist. As the jet stretches out over-time, it allows the jet to become more effective in terms of penetration. This obstacle was overcome by Pugh, Eichelberger and Rostoker (PER) theory in 1952 [49], by accounting for a velocity gradient of the liner elements. The PER theory eventually led to more accurate and realistic results when compared to Birkhoff theory. One drawback of this theory is that it does not include the effect of viscosity during the jet formation process. Lastly, the Visco-Plastic model developed by Godunov [50] was able to modify the steady-state theory made by Birkhoff to account for the strain-rate effect.

- Birkhoff Theory [48]

- A steady-state model, assumes that liner collapse velocity is constant.
- Cons: failed to explain why there exist a velocity gradients in the jet particles.
- PER Theory [49]
  - An unsteady-state model, assumes that the jet velocity is variable, meaning that the tip is faster than the tail.
  - Pros: accounts for the variation in velocity of the jet particles.
- Visco-plastic model and jet coherency [50]
  - It concerns more with the jet coherency, emphasising on having radial jet velocity is not permitted. Otherwise, the jet will tend to deviate from travelling in a straight line.
  - It emphasis also on the importance of flow velocity to be subsonic for the jet to form coherently.

### 2.8.2 Jet Breakup Time

There are many empirical formulas developed by several scientists to calculate the jet breakup time, such as Hirsch [51] and Pfeffer [52]. However, their applicability was considered limited due to the unaccountability of jet stretching rate and its strength [53]. As the SCJ stretches, a velocity gradient is observed amongst its particles. This lead to a very noticeable decrease in the jet penetration efficiency. This explains why the jet has to be continuous prior to impact in order to deliver optimum perforation depth. The importance of understanding the jet breakup time allowed scientists to enhance the design of a SC.

According to Held [54], the empirical breakup time of a SCJ can be obtained from flash x-ray analysis as:

$$\bar{t}_b = \frac{\sum l}{V_{tip} - V_{cut}}$$

$\sum l$  is the cumulative jet length after it particulates.  $V_{tip}$  and  $V_{cut}$ , are the jet velocities from tip to tail respectively.

The jet breakup time can be calculated and determined using several methods, each of which yields different results. However, one accurate way of calculating it is by dividing the cumulative jet length by the change in jet velocity, which is the difference from the fastest jet particle (tip) to the slowest jet particle (tail). It is important to know that the jet breakup time is based on a number of assumptions [55]. One is assuming that the jet is stretching out at a constant rate from a point of zero until it reaches a maximum. This process has a time reference from which the jet starts to originate.

The second assumption is that the jet breaks up simultaneously from tip to tail during the time when the jet has reached its maximum length. Moreover, one important information that the jet breakup time provides is the total jet length available for penetration. However, in many cases, the relation between the jet velocity and the accumulated jet length is nonlinear. A study showed by Held [54], he stated that the cumulative jet length can be expressed with more accuracy using a piecewise linear function in terms of the jet velocity. As a result, each velocity of the jet particle is associated with a specific breakup time. The empirical breakup time formula mentioned-above was used in present work to calculate the jet breakup time to draw a comparison with the experimental value obtained here.

## **2.9 Standoff Distance Effect and Penetration Models**

Standoff distance is defined as the distance from the edge of the liner to the target. In case of using a conditioning steel plate to vary the jet threshold, the standoff distance in this case will be the distance from the edge of the liner to the conditioning steel plate. Along with the liner material and explosive filling used, standoff distance plays a major factor in determining the optimum penetration depth that can be attained by the SCJ. In addition, choosing the optimum standoff distance allows the jet to properly form, which leads to better performance in terms of higher residual velocity, continuity of the jet particles and therefore better penetration. The tip velocity after penetrating an object is called residual velocity. An illustration of the significance of standoff distance is depicted in Figure 15.

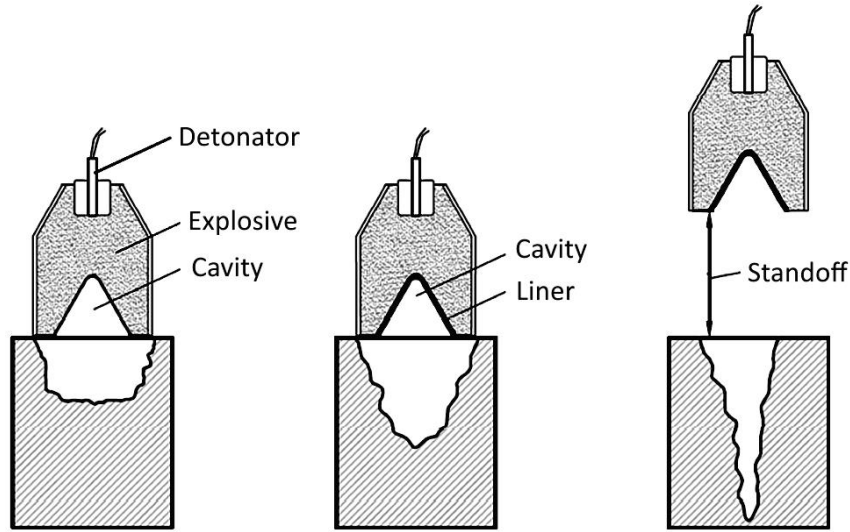


**Figure 15:** from left to right: presence of cavity only vs cavity plus liner vs cavity plus liner plus standoff distance [55].

As shown in Figure 15, the role of standoff distance in increasing the penetration capability of SC is clearly significant. In this study, a number of shots were initiated first to determine the optimum/suitable value of standoff distance needed to be used for the SCJI test.

One of the earliest penetration models is called the Birkhoff model [47], which assumes a steady-state liner collapse model, and account for the standoff distance effect on penetration. The following equation is applicable for continuous jet:

$$P = \frac{P_o(1 + \alpha S)}{1 + \beta S}$$

P is the total penetration. S is the standoff distance,  $P_o$  is penetration at zero standoff,  $\alpha$  and  $\beta$  are constants depend on the jet velocity slope and jet spreading.

In case of the jet is not continuous, the equation becomes:

$$P = P_o \frac{\sqrt{2}(1 + \psi S)^{0.5}}{1 + \beta S}$$

Where  $\psi$  is a constant depend on the jet velocity slope.

Therefore, more accurate and realistic theoretical model was constructed to account for jet penetration and to find the residual velocity of the jet is called the extended hydrodynamic penetration model [56-58]:

$$V_{res} = V_o \left[ \frac{S}{P + S} \right]^\gamma ; \gamma = \left( \frac{\rho_T}{\rho_j} \right)^{0.5}$$

$$V_{res} = V_o \left[ \frac{S}{P + S} \right]^\gamma$$

Where  $V_o$  is the jet impact velocity;  $V_{res}$  is the jet velocity after penetrating the target,  $S$  is the standoff distance and  $P$  is the penetration depth. This formula accounts for the variability of the jet velocity and it assumes that the jet breakup time occurs simultaneously. The standoff distance in this case depends on the virtual origin of the SC. The virtual origin is a technical term refers to the point where the SCJ starts to formulate. This virtual origin point may lie within the liner cone close to the apex or outside the cone in some instances. However, once flash x-ray analysis is used, it will be effectively sufficient to find relevant SCJ parameters, such as the residual tip velocity, without the need of calculating the value of the virtual origin.

## 2.10 Summary

In summary, the degree of resistance of conventional HE is different from that of IHE when subjected to SCJI. The amount of jet threshold needed to initiate a particular ammunition depends on the type of explosive used to fill that ammunition. The detonation waves from a primary explosive (i.e. booster) in a typical explosive train are responsible for initiating the chemical energy stored in the explosive molecules (i.e. main charge). Melt-cast, cast-cured and pressed are all techniques and methods used to fill explosives in ammunitions. The most suitable filling technique depends on the availability of such technology and the purpose for what it will be used for. There are number of IM tests used to qualify ammunitions to whether the explosive filling used is insensitive to external stimuli, such as heat, shock and impact or not.

Results from literature in regards to the SCJI test was given in Chapter two for drawing a comparison with the results obtained in this dissertation. The threshold of the SCJ depends on the jet tip velocity and diameter, the higher the SC calibre the higher the jet threshold. The SC liner may come with different geometrical liners, such as cone and

trumpeted shapes, each of which yields its unique penetration capability. The penetration capability of a SC depends on several factors, such as standoff distance and liner material. The following chapter describes the tests set-up used to perform the SCJI and jet characterisation analysis.

# Chapter 3: Methodology

## 3.1 Introduction

In compiling this chapter, several experiments were conducted in order to determine and investigate:

- the velocity of the jet tip, diameter of the leading tip, jet breakup time (right on the point when the jet started to particulate), and the optimum standoff distance (from the edge of the conical liner to barrier plate); and
- the classifications of reactions resulting from the impact of SCJ on 81 mm mortar shells filled with various explosives fillings.

The overall experimental approach consisted of two main tests. The first test aimed at characterising the SCJ, which is a pre-requisite step to use its obtained inputs for the impact test. Inputs such as, tip velocity, tip diameter, jet breakup time and optimum standoff distance.

The second test was the SCJI on mortar shells, where reactions due to SCJ impacts are classified and analysed. The mortar bodies used in this test are made of cast iron with density equal to  $6.85 \left( \frac{g}{cm^3} \right)$ . The mortar bodies are filled with various explosive formulations, which were TNT, (NTO/TNT (20/80) and NTO/TNT (50/50)). They are all melt-cast compositions based on NTO, and TNT is used as a reference and a baseline for comparison purposes. The preparation procedure of these melt-cast explosives is discussed in Section 3.3.1.

The energy formed by the SCJ is expressed in terms of tip velocity multiplied by its diameter (  $V_{tip}^2 D$  ). This term is referred to as the “threshold stimulus”, which is expressed in units of  $\frac{mm^3}{\mu s^2}$  . The jet is impacted on the mortar bombs with various values of threshold stimulus; this is achieved by using a conditioning steel plate with variable thicknesses prior to the point of impact. The conditioning steel plates serve as steel barriers to reduce the jet threshold values as the jet penetrates the plate.

### 3.2 Characterisation Test of Shaped Charge Jet

The most commonly used method to characterise the SCJ is by means of using flash x-ray analysis. This diagnostic tool was developed and applied by S.G. Tatake and D.K. Kharat [59]. It is a very powerful technique used to evaluate the overall performance of the jet. The main significant purpose of this method is to give a solid indication for the maximum penetration depth that may be attained by the jet.

This method is very effective as it enables a full observation of the jet particles, tip velocity and tip diameter. The method consists of using multiple x-ray units that allow a capture of images of the SCJ at pre-determined time intervals. Consequently, radiographs of the jet then stored in a film cassette for analysing and determining the tip velocity, tip diameter, breakup time and velocity of each particle. The images obtained on the radiograph flash x-ray had a magnification factor of 1.37. The magnification factor in this case was acceptable as large factor implies inaccuracy of the test set-up. The magnification factor is due to the distance from object to the x-ray tube. A schematic view of the flash x-ray set-up is depicted in Figure 16.

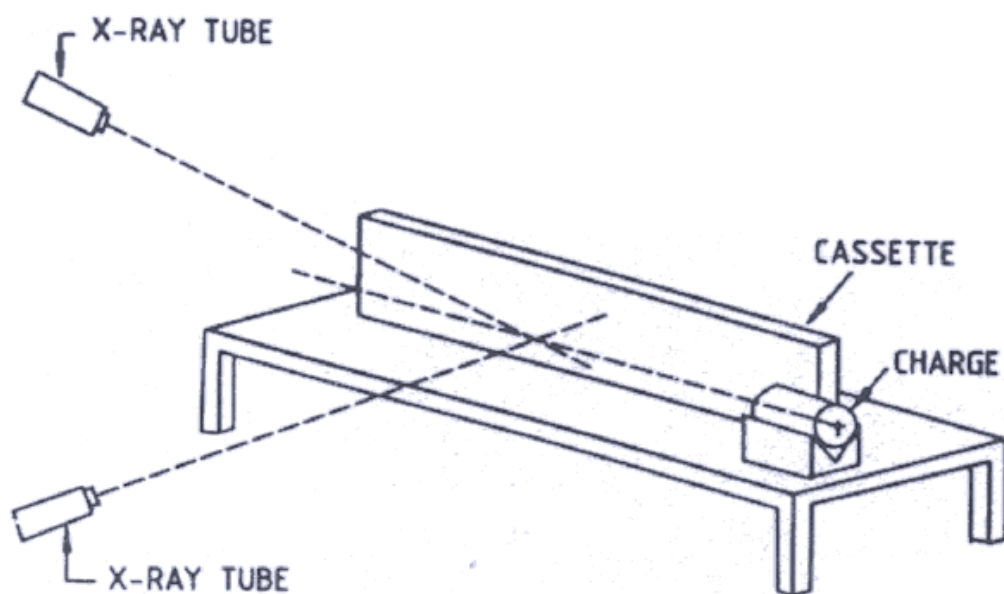


**Figure 16:** Schematic view of the flash x-ray set-up [59].

The length of the film cassette used in this experiment was 1.2 m, due to limitations in the length of the film cassette, capturing the entire jet with its all particles in a single x-ray shot was not possible. This is due to the fact that the x-ray film needs to be protected from the explosive blast and cannot be exposed. The total jet breakup time was calculated



by dividing the cumulative jet length over the change in the jet velocities, such that the difference between the tip and the slowest particle were considered.

### 3.1.1 Test Set-up

The shaped charge used in this test was a 38 mm calibre with a copper conical liner filled with composition CH6. The cone had an apex angle of  $56^\circ$  with uniform wall-thickness ( $1 \pm 0.5 \text{ mm}$ ). CH6 is a pressed composition based on RDX/graphite, more information on its chemical properties can be found in literature [24]. A CH6 booster pellet was attached through a wood holder allowing an M2A3 electric detonator to be placed on the back of the booster; the electric detonator was used as a single point initiation source to ensure a symmetrical firing of the jet. Figure 17 presents a picture of the 38 mm shaped charge used.

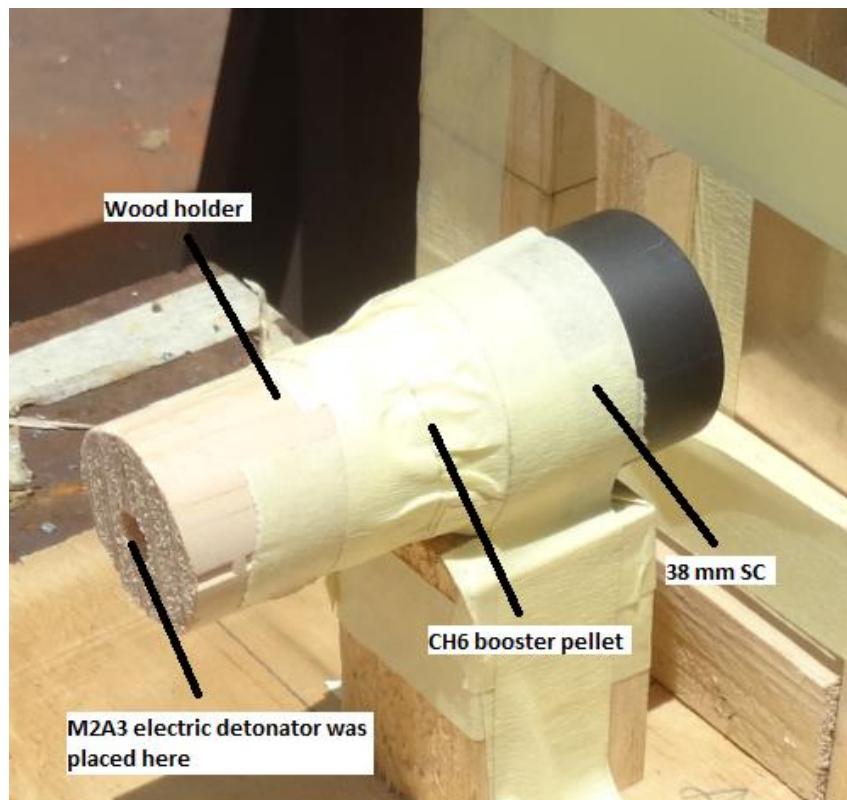


**Figure 17:** A picture of the 38 mm SC used along with its attachments.

Test requirements:

- A flash x-ray system with two x-ray tubes placed symmetrically in a vertical plane as presented in Figure 16.

- The SC needs to be positioned in alignment with the point of intersection of the x-ray beams as shown in Figure 16.
- A film cassette to record the images of the captured jet, placed along the line where events took place as presented in Figure 16.

Since the shaped charges used in this work were able to generate jets that can travel with velocities up to 7.3 km/s, capturing images of these jets required very short time interval in matters of microseconds. Firstly, two shots were taken to determine the proper time interval needed to capture the jet on the cassette film. Secondly, eight shots were tested for the purpose of determining the approximate optimum standoff distance. A 10 mm conditioning steel plate was used as a reference to vary the length of standoff distances. Standoff distances were initially chosen to be 15 mm, 40 mm, 60 mm and 80 mm. The purpose of these increments in distances was to seek a value that gives the optimum value of residual tip velocity ( $V_{res}$ ) and thereafter optimum  $V_{tip}^2 D$  value.

After the optimum standoff distance was found, another set of eight shots took place to determine the ( $V_{tip}^2 D$ ) measurements of the 38 mm SC after penetrating various steel conditioning thicknesses. The thickness of the steel conditioning plate was varied as follow: 10 mm, 20 mm, 40 mm, 60 mm and 75 mm.

To yield accurate measuring results, a light box was used in all instances for analysing the radiograph images to ensure clear images for accurate measurements. The jet diameters were measured using a vernier and a magnifying glass.



**Figure 18:** Actual image of the test set-up.



**Figure 19:** A different angle of the actual test set-up.

### **3.3 Shaped Charge Jet Impact Test**

The SCJI test was performed after the SCJ was characterised. As the tip velocity, tip diameter, breakup time and optimised standoff distance were very important parameters, which needed to be measured before commencing this test. These important parameters are used as input values for the SCJI test.

#### **3.3.1 Melt-cast Explosives Preparation**

The mortar bombs used in this test were filled with various explosives fillings. TNT, NTO/TNT (50/50) and NTO/TNT (20/80) were specifically used, such that five bombs were filled of each explosive filling. TNT and NTO/TNT (50/50) was prepared using the melt-cast facility at RDM. Figure 10, in Section 2.5 of Chapter two, presents a picture of the major components used by the facility.

First, the mortar bombs were pre-heated to 70°C to avoid any thermal shock due to high filling temperature. Then, NTO/TNT (50/50) were poured into the 81 mm mortar bombs at a temperature of about 90°C using a 15 mm filling nozzle, this is due to high viscosity of the mixture. After this was done, probing was used to regulate the cooling process at constant temperature and to ensure that no air bubbles and voids are present in the filling. Finally, the mortar bombs were left for 24 hours to properly solidify. The TNT preparation took the same procedure as explained above, except that it was done with 8 mm filling nozzle.

The NTO/TNT (20/80) was prepared manually at the laboratory. It was prepared by diluting TNT into an existing melted NTO/TNT (50/50) mixture contained in a vessel, until the (20/80) ratio was acquired. After this was done, the whole mixture was poured into the 81 mm mortar bomb using a 15 mm filling nozzle and thereafter held at a constant temperature of 70°C.

#### **3.3.2 Firing Mechanism and Measuring Instruments**

A view of all major test items as well as the exact arrangement of the SCJI test set-up can be viewed schematically in Figure 20. In addition, the length of standoff distance, the space left between the velocity screens and the firing mechanism are shown in Figure 20.

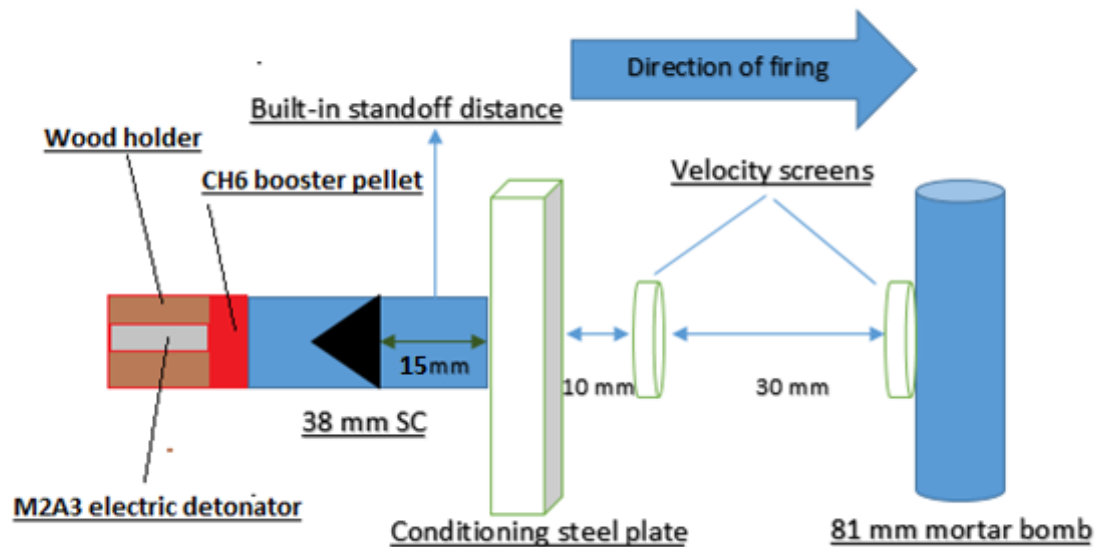


**Figure 20:** A schematic view (top-view) of major components for the SCJI test, showing the direction of firing.

The firing mechanism used to initiate the SC was through a wired electric firing device connected to the electric detonator. The electric firing device is simply used to trigger the electric detonator (M2A3) allowing it to initiate the booster pellet and thereafter the main charge filled into the SC. The conical liner then collapses to form a jet that can easily penetrate the conditioning steel plate, passing through the two velocity screens to the 81 mm mortar bomb. The velocity screens were attached by wires connected to an oscilloscope. The oscilloscope captures the pulses triggered by the jet as it passes through the velocity screens. The velocity screens are simply used as velocity sensors to record the time it took for the jet to impact the 81 mm mortar bomb. Then the residual velocity, which responsible for attacking the mortar bomb, can be easily calculated by the difference in distance over difference in time.

The following instrumentation were used to determine the type of reaction:

- Air blast over-pressure (BOP) probes was configured as shown in Figure 21.
- Photography of all events (reactions) took place.
- Fragments recovery to indicate the type of reaction occurred.
- Velocity screens were used to calculate the residual tip velocity after penetrating the conditioning steel plates.

- Oscilloscope was used to capture the time pulses triggered by the jet as it passed the velocity screens. This was used to calculate the residual velocity attacking the test item (an 81 mm mortar bomb).

The following observations and actions were made after completing the tests:

- The reaction type observed on the test item.
- Photographs of the witness plates and photographs of residue and fragments.
- high speed video of the reaction occurred.

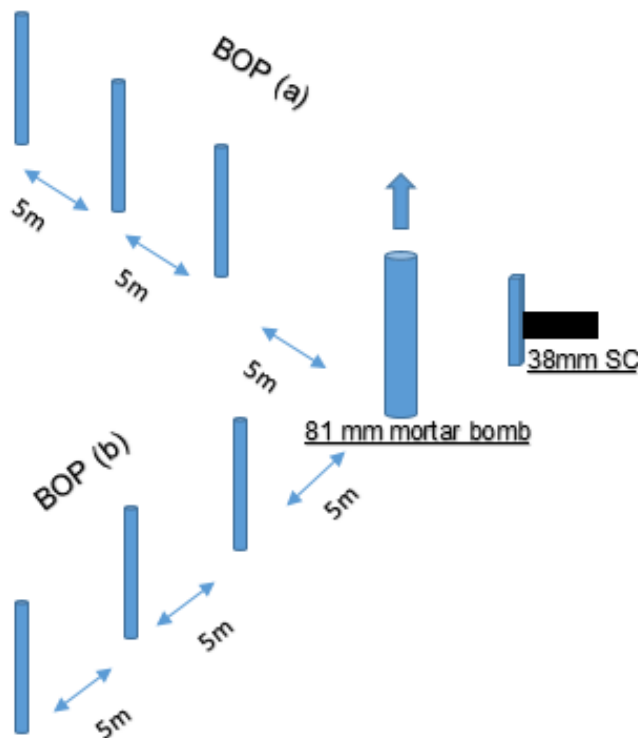


**Figure 21:** Blast-over pressure probes.

### 3.3.2 Test Set-up

This test set-up was done in accordance with STANAG 4526 [17]. The secondary charges, such as propellant and exploders were removed from the 81 mm mortar bombs used in this test. The reason for this is to prevent any possibility of contamination to the test range that can lead to pollution of the environment. To avoid any unplanned influences on the blast over-pressure measurements obtained during the tests.

Inputs needed from the characterisation tests:

- Velocity of leading tip at 0 mm, 10 mm, 20 mm, 40 mm and 60 mm conditioning steel plate.
- Diameter of leading tip at 0 mm, 10 mm, 20 mm, 40 mm and 60 mm conditioning steel plate.
- Breakup time (from detonation to “jet-particulation”).
- Optimum standoff from shaped charge cone to conditioning steel plate.
- Penetration capability.

Requirements were performed in accordance with on STANAG 4526 [17]:

- The test configuration was set up as shown schematically in Figure 22.
- Five mortar bombs was used for each explosive formulation.
- A 38 mm conical shaped charge was used for the test.
- Witness plates as shown in Figure 23.
- Velocity screens to account for the jet residual velocity.
- Conditioning steel plates were used for varying the values of  $V^2d$ .

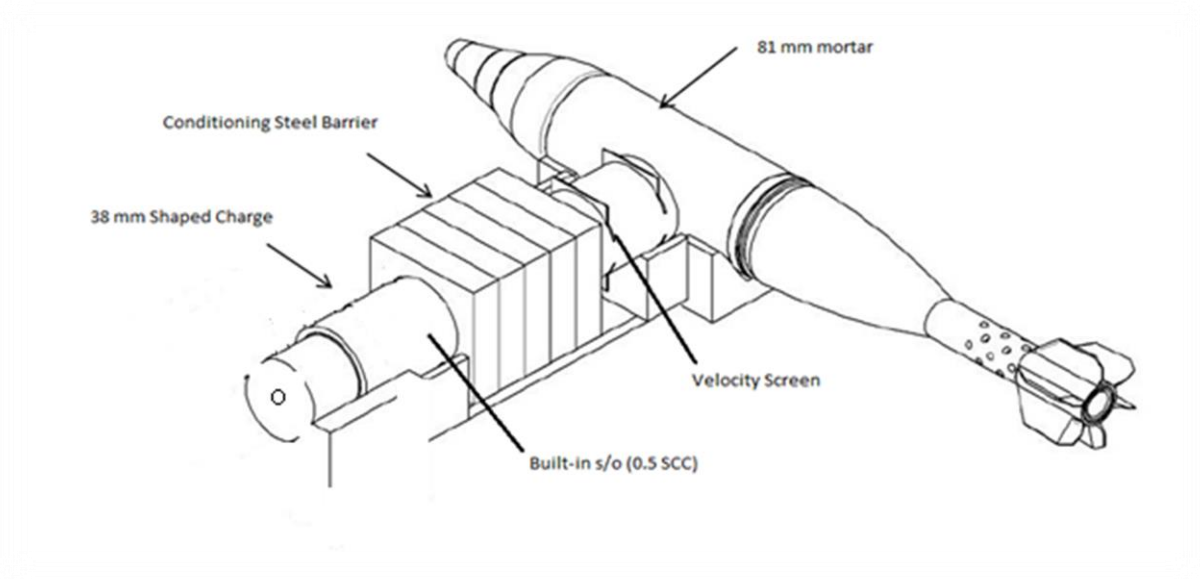


**Figure 22:** Schematic view of the SCJI set-up.





**Figure 23:** SCJI test showing the 81 mm mortar projectile, steel conditioning plate, 38 mm SC and the witness plate at the bottom.

### 3.4 Summary

To review the overall information stated in this chapter, two experiments were performed using 38 mm shaped charge and 81 mm mortar bombs. The SCJ characterisation test set-up aimed to obtain jet tip velocity, tip diameter and jet breakup time by means of flash x-ray analysis. The SCJI test set-up aimed to obtain reaction levels from 81 mm mortar bombs. The tests set-up were arranged and built according to STANAG 4526 [17] and as per other approved scientific papers [59]. The 81 mm mortar bombs were filled using various explosives fillings; TNT, NTO/TNT (50/50) and NTO/TNT (20/80). The technique used to fill the 81 mm mortar bombs was via melt-cast process. Detailed procedure of performing these tests was stated in this chapter as well as explanation about the measuring instruments. The firing mechanism used to initiate the 38 mm SC was by means of using M2A3 electric detonator. The following chapter presents the results obtained from performing the above-mentioned tests.



# Chapter 4: Results

## 4.1 Introduction

In this chapter, the results for the SCJ characterisation tests as well as the SCJI tests on 81 mm mortar bombs are presented. The types of reactions of the examined explosive formulations used in the tested 81 mm mortar bombs are classified and interpreted in accordance to STANAG 4439 [6].

The optimum standoff distance was obtained by firing a number of shots with variable distances with respect to the 10 mm conditioning steel plate. The reason for choosing 10 mm thickness was to ensure that any undesired variations in velocity at the tip is removed. Among the different standoff distances, the one that showed higher residual tip velocity and jet threshold was selected. The jet breakup time was calculated to detect at what time the jet starts to particulate. This is very critical and as stated by STANAG 4526 [17], the jet has to impact the tested item while it is still continuous.

After the optimum standoff distance had been acquired, several radiographic images were obtained from the flash x-ray analysis. Each of these images captured the jet while moving continuously against no barrier, 10 mm barrier, 20 mm barrier, 40 mm barrier and 60 mm barrier. Conditioning steel plates used were mild steel plates with density equal to  $\sim 7.40 \left( \frac{g}{cm^3} \right)$ . Figure 27 to Figure 30 depict visual illustrations of these conditions as it is required that the jet to be continuous at each time it penetrates the plate.

The jet characteristics were important to use as inputs for the SCJI test, as the tip velocity along with its diameter determined the jet threshold responsible for initiating the 81 mm mortar projectiles.

## 4.2 Optimum Standoff Distance

The optimum standoff distance was selected by measuring the optimum residual velocity acquired from varying the standoff distances. The size of the hole left on the conditioning steel plate was also put into consideration due to the fact that it gave an indication of the amount of energy carried out by the jet. The bigger the size of the hole on the conditioning steel plate, the higher the amount of jet threshold generated. This is shown in Figure 24.



**Figure 24:** Variable standoff distances and their resultant exit-holes on 10 mm steel conditioning plates.

The standoff distances depicted in Figure 24 were measured from the SC cone to the conditioning steel plate. The result of each shot was analysed on radiographic images. The optimum standoff distance was measured to be 15 mm as shown below in Figure 25.

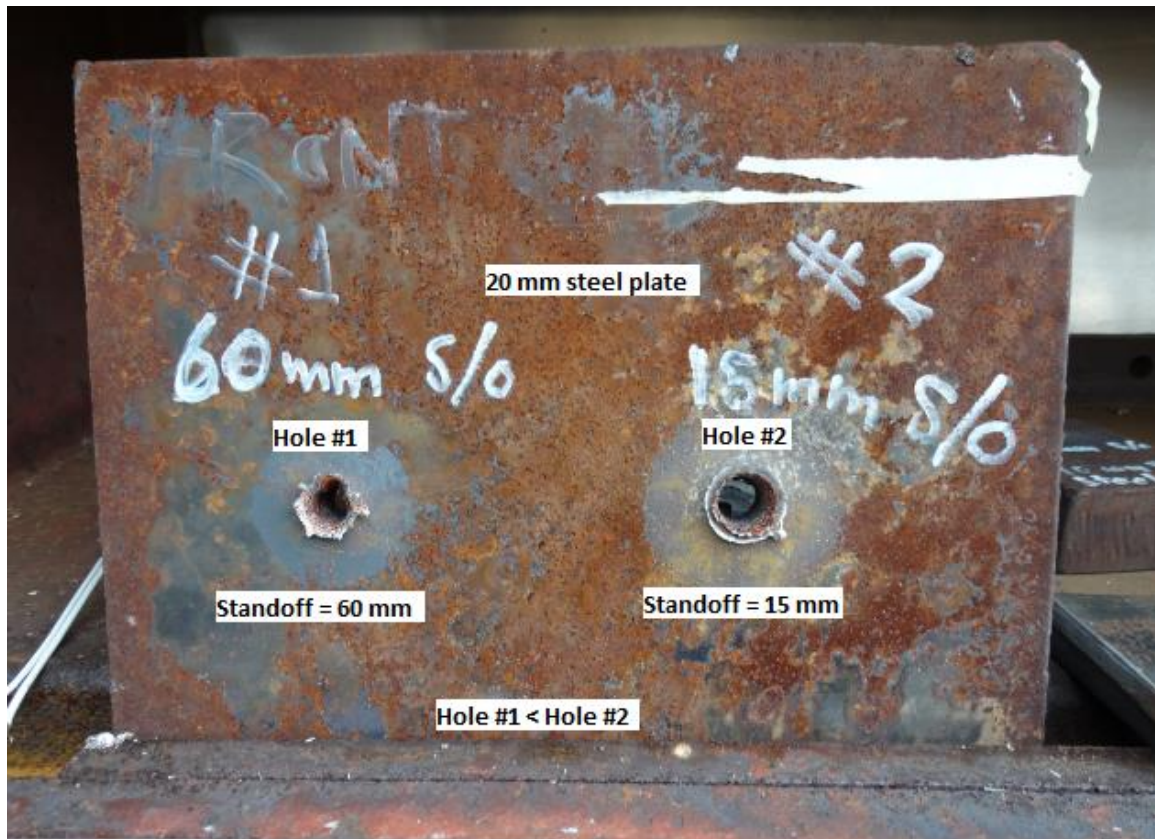


**Figure 25:** Optimum standoff distance effect on 20 mm steel plate.

It is clearly shown that the higher the selected standoff, the smaller the diameter of the hole became. A very important observation is that a large portion of the copper liner got wasted on the plate as the standoff distance increased. The optimum standoff distance was selected to be 15 mm, which is approximately equal to 0.4 SCC. This allowed the jet to properly penetrate with no noticeable waste of copper on the penetrated condition steel plates as depicted in Figure 25.

After determining the optimum standoff distance, which was measured to be 15 mm, various  $V^2d$  values were plotted against variable steel plate thicknesses. This is presented in Figure 26.

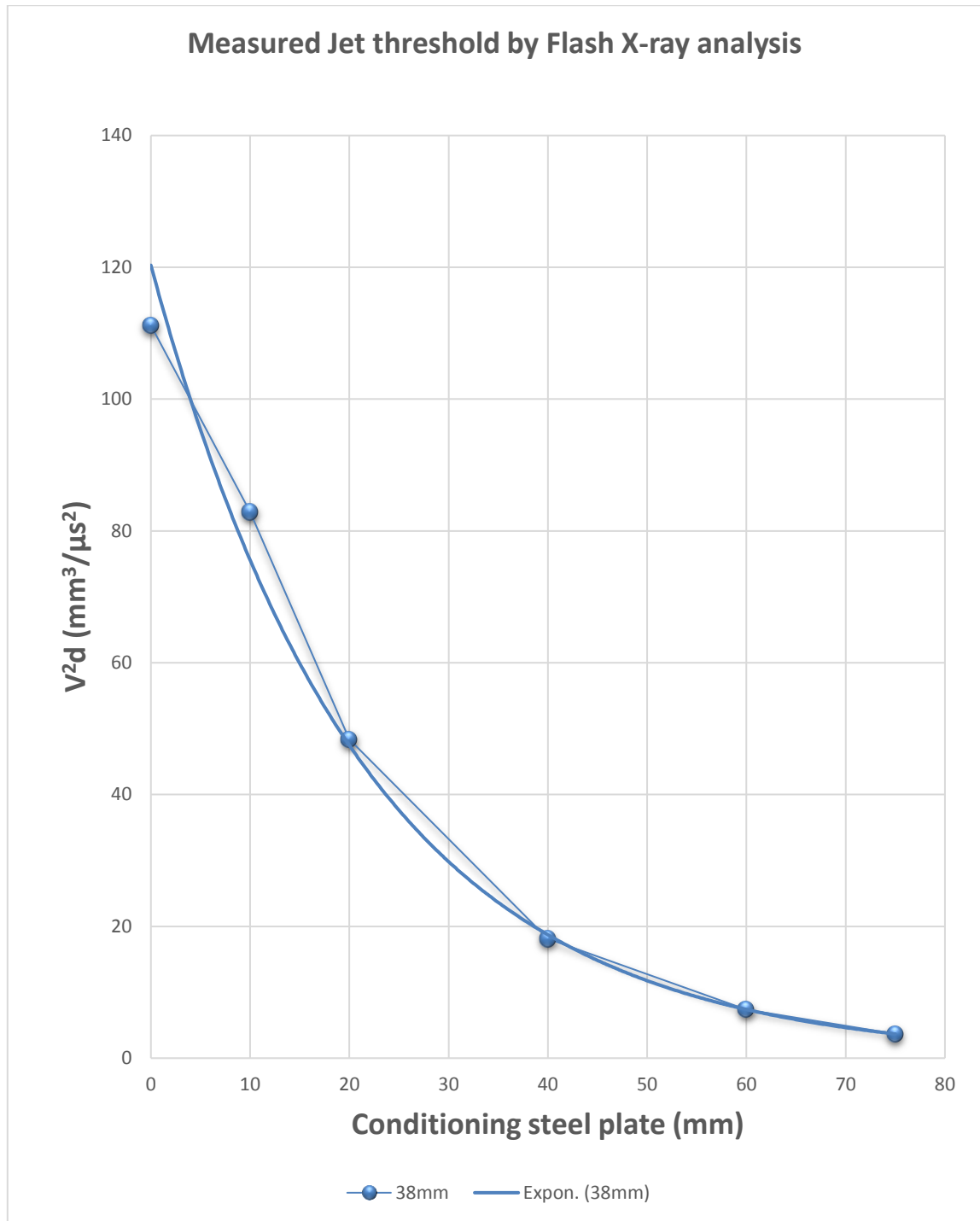


**Figure 26:** Variable jet threshold ( $V^2d$ ) measured by the flash x-ray analysis.

Numerous work done in literature showing that the reduction in  $V^2d$  values can be best represented by an exponential decay function [9, 10, 11 and 18]. Figure 26 above shows agreement with the theories by indicating an exponential drop behaviour of  $V^2d$  values obtained from the 38 mm SC used in this work. Further verifications with other work found in literature are discussed in Chapter five.

### 4.3 Characterisation and Evaluation of the SCJ Particles

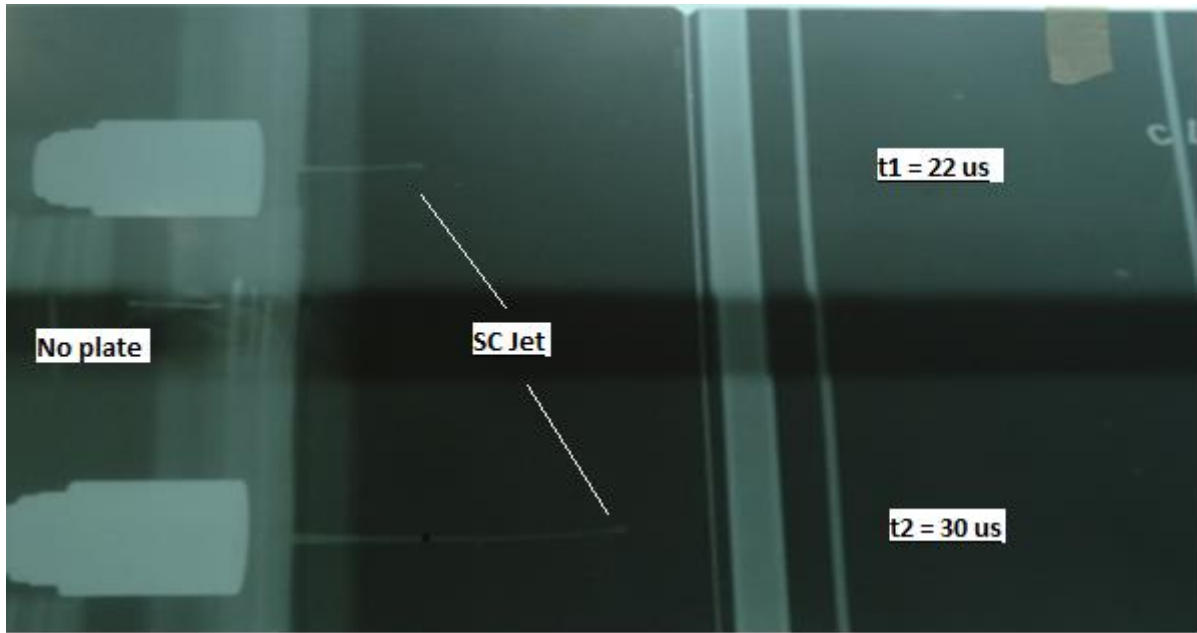


**Figure 27:** Radiographic image of the jet as it passes with no conditioning steel plate.

The tip diameter was measured using a vernier and magnifying glass as 2 mm. The tip velocity was simply calculated by taking the difference in length between the two jets divided by their difference in time as shown in Figure 27. The tip velocity was then

calculated as  $\frac{\Delta L}{\Delta t} = \frac{59 \text{ mm}}{8 \mu s} = 7.38 \frac{\text{mm}}{\mu s}$ .

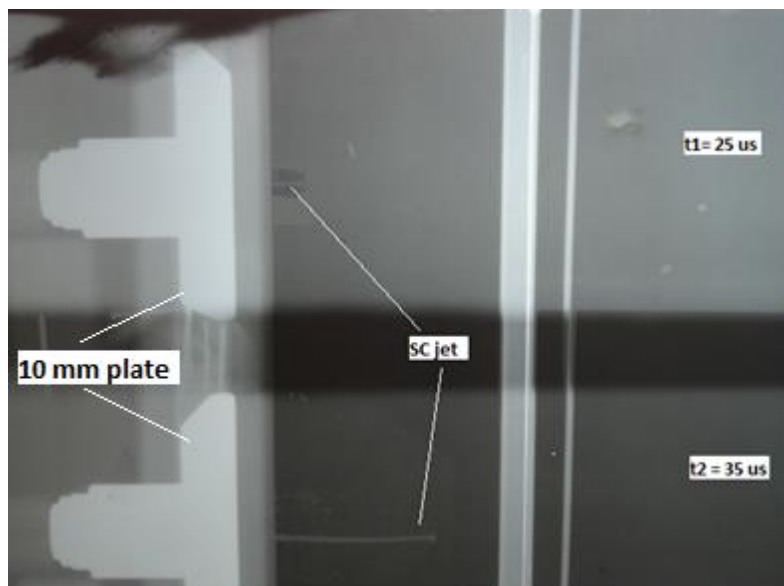


**Figure 28:** Radiographic image of the jet after penetrating a 10 mm conditioning steel plate.

A 10 mm conditioning steel plate was used here to reduce the jet threshold. This radiographic image allows for the calculation of the jet residual velocity after penetrating a 10 mm thickness plate. The tip velocity then was calculated as:

$$\frac{\Delta L}{\Delta t} = \frac{64.5 \text{ mm}}{10 \mu s} = 6.45 \frac{\text{mm}}{\mu s}.$$

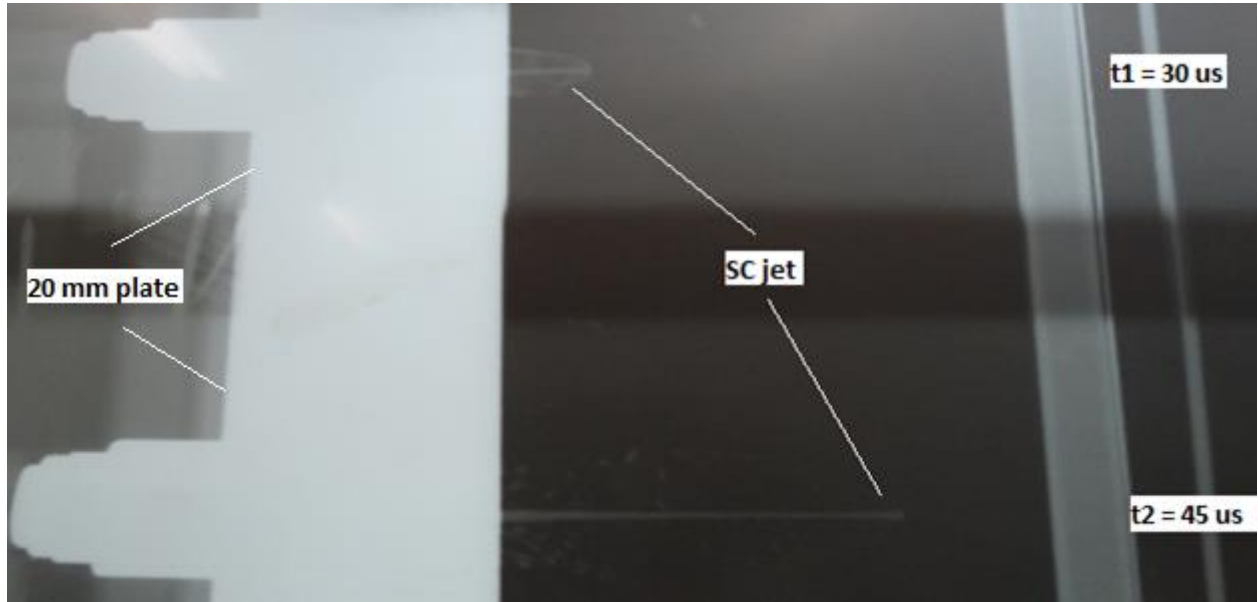


**Figure 29:** Radiographic image of the jet after penetrating a 20 mm conditioning steel plate.

The residual velocity after penetrating a 20 mm conditioning steel plate was calculated.

The tip velocity then was calculated as  $\frac{\Delta L}{\Delta t} = \frac{72 \text{ mm}}{15 \mu s} = 4.80 \frac{\text{mm}}{\mu s}.$

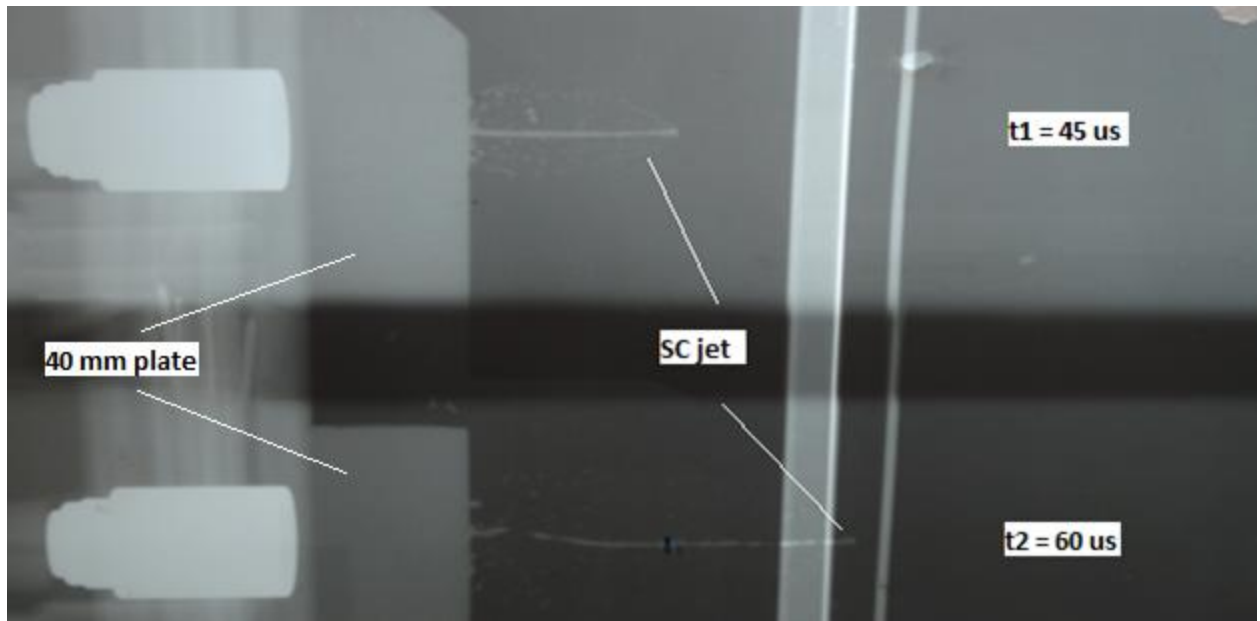


**Figure 30:** Radiographic image of the jet after penetrating a 40 mm conditioning steel plate.

The residual velocity after penetrating a 40 mm conditioning steel plate was calculated.

The tip velocity then was calculated as  $\frac{\Delta L}{\Delta t} = \frac{44 \text{ mm}}{15 \mu s} = 2.93 \frac{\text{mm}}{\mu s}$ .

#### 4.3.1 Breakup Time, Tip Velocity and Tip Diameter

The jet was allowed to stretch out for several time intervals:  $40 \mu s$ ,  $60 \mu s$ ,  $80 \mu s$ ,  $100 \mu s$  and  $120 \mu s$ . This was to get a preliminary indication of the time interval when the jet would start to particulate. The behaviour of the jet particles as they move over length and time was visualised.

It is clearly seen in Figure 31 that the jet breakup took place within the time interval of  $(40 \mu s < t_b < 80 \mu s)$ . In order to calculate the jet breakup time, the approximate total cumulative length of the jet particles was measured as presented by Figure 32. Then, the empirical equation suggested by Held [54] was applied to draw a comparison with the approximated empirical value of breakup time obtained in this study. To see whether it lies into the time interval determined for the breakup time or not.



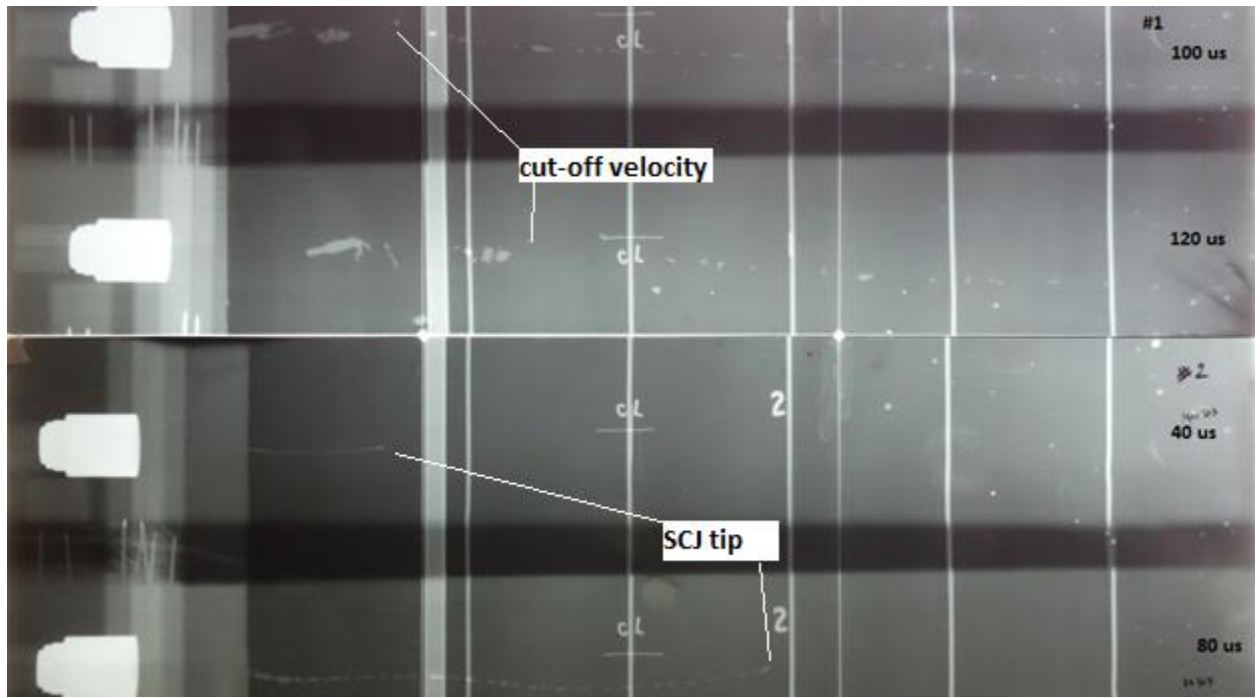


**Figure 31:** Images of the jet captured at various time elapses with no conditioning steel plate.

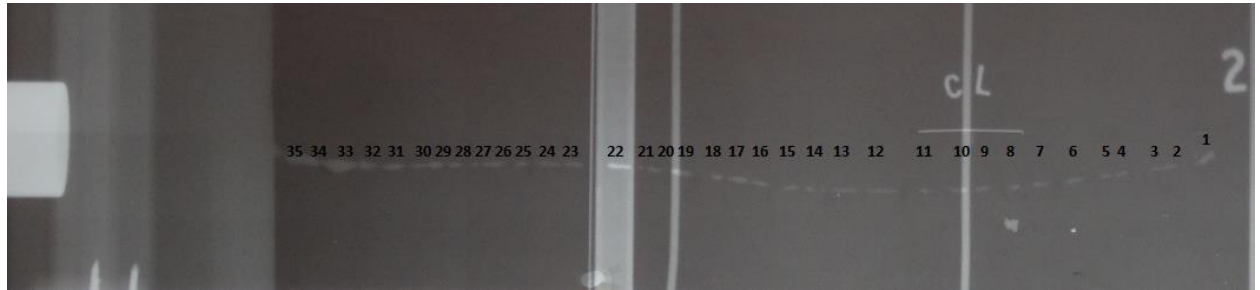


**Figure 32:** Total cumulative length of the jet particles as it stretched out.

The total cumulative length of the jet particles was calculated to be 151 mm. The maximum and minimum particle velocity were measured as 7380 m/s and 4750 m/s respectively. Therefore, the average breakup time was calculated using Held [54] equation, which accounts for the total length of the jet particles divided by the difference between the fastest and slowest particle. The equation used as follow:

$$\bar{t}_b = \frac{\sum l}{V_{j,o} - V_{j,cut}}$$

$$\bar{t}_b = \frac{151 \text{ mm}}{7.38 \frac{\text{mm}}{\mu\text{s}} - 4.75 \frac{\text{mm}}{\mu\text{s}}}$$

$$\bar{t}_b = 46.92 \mu\text{s}$$



The jet breakup time was crucial in this work to determine the maximum allowed length for placing the test item as the jet must impact on the mortar projectiles while it is still continuous. The maximum attained length before the jet starts to particulate was determined to be approximately 105 mm through the radiographic images. This distance was put into consideration when SCJI test was set-up.

This was put into consideration when conditioning steel plates were varied. Evidence for capturing the residual jet after penetrating 0 mm, 10 mm, 20 mm and 40 mm were presented in Figure 27 to Figure 30. The calculated value for the breakup time correlated with the time interval found empirically as shown in Figure 31.

$$\bar{t}_b = 46.92 \mu s \in (40 \mu s < t_b < 80 \mu s)$$

The jet breakup time increases as the thickness of the conditioning steel plate increased. This was due to the reduction observed in the jet velocities as they perforated the conditioning steel plates. Breakup time of the jets during each penetration of the conditioning steel plates was not calculated since evidence for the continuity of the jets was observed on the radiographic images.

#### 4.4 Reactions due to Impact of Shaped Charge Jets on 81 mm Mortar Projectiles

All reactions resulted from the 81 mm projectiles and their corresponding  $V^2d$  values are summarised in Table 5.

**Table 5:** SCJI test on 81 mm mortar bombs filled with insensitive melt-cast explosive formulations.

| Formulation     | Shot # | Conditioning Plate (mm) | $V_{tip}(\frac{mm}{\mu s})$ | $V^2d(\frac{mm^3}{\mu s^2})$ | Reaction Type   |
|-----------------|--------|-------------------------|-----------------------------|------------------------------|-----------------|
| TNT             | 1      | 0                       | 7.4                         | 111.0                        | I (Figure 37)   |
|                 | 2      | 10                      | 6.4                         | 82.9                         | II              |
|                 | 3      | 20                      | 4.8                         | 48.4                         | III             |
|                 | 4      | 40                      | 2.9                         | 18.1                         | II              |
|                 | 5      | 60                      | 1.8                         | 7.4                          | III             |
|                 | 6      | 75                      | 1.3                         | 3.7                          | VI (Figure 39)  |
| NTO/TNT (50/50) | 1      | 0                       | 7.4                         | 111.0                        | IV              |
|                 | 2      | 10                      | 6.4                         | 82.9                         | IV              |
|                 | 3      | 20                      | 4.8                         | 48.4                         | IV              |
|                 | 4      | 40                      | 2.9                         | 18.1                         | III (Figure 35) |
|                 | 5      | 60                      | 1.8                         | 7.4                          | III (Figure 38) |
| NTO/TNT (20/80) | 1      | 0                       | 7.4                         | 111.0                        | IV (Figure 34)  |
|                 | 2      | 10                      | 6.4                         | 82.9                         | IV              |
|                 | 3      | 20                      | 4.8                         | 48.4                         | III             |
|                 | 4      | 40                      | 2.9                         | 18.1                         | IV              |
|                 | 5      | 60                      | 1.8                         | 7.4                          | III (Figure 40) |



**Figure 33:** Type IV (deflagration) reaction observed on NTO/TNT (20/80).

The mortar bomb was ruptured and no fragments were identified. No violent pressure release was recorded, only some unreacted explosives were propelled to the surrounding. The internal body showed evidence of ignited and burned explosives.



**Figure 34:** Type III (explosion) observed on NTO/TNT (50/50) with 40 mm steel plate.

Large fragments were propelled at distance > 15 m indicating a possibility of causing damage to the surrounding. A moderate pressure release was recorded by blast over-pressure measurements. This was determined as a type III reaction (explosion).



**Figure 35:** Type II (Partial detonation) observed on TNT.

Only a small portion of the explosives did not detonate. Presence of large and small fragments were identified. The violent pressure release was slightly lower than that obtained for a full detonation measurement.



**Figure 36:** Type I (detonation) observed on TNT.

A full detonation was observed with TNT filling. The mortar body was scattered into small fragments leaving hits evidence on the witness plate as indicated in Figure 37. The blast over-pressure measurements recorded a violent release of pressure. The blast over-pressure measurements matched with that obtained from a detonated TNT reference shot. All reference shots along with all blast over-pressure measurements are attached in Appendix A.





**Figure 37:** Type III (explosion) observed on NTO/TNT (50/50) with 60 mm steel plate.

This case was similar to that found in Figure 34. Large fragments were produced and propelled at distance > 15 m. The blast over-pressure measurements were slightly lower than that found in Figure 34. This case was identified as a type III reaction (explosion) due to presence of large fragments recovered at far distances.



**Figure 38:** Type VI (no reaction) observed on TNT with 75 mm steel plate.

This case was identified as Type VI (no reaction). The SCJ experienced a major loss in strength after it penetrated a 75 mm steel thickness. This caused a reduction in the jet penetration capability on the test item and the same applied to its velocity of impact. The jet residual velocity measured was 1.3 km/s, which contributed to a very small  $V^2d$  value.



**Figure 39:** Type III (explosion) observed on NTO/TNT (20/80) with 60 mm steel plate.

#### 4.3.1 Residual Velocities

During the SCJI test, two velocity screens were used to measure the time needed for the jet to impact the 81 mm mortar bomb. This allowed calculation of the residual jet velocity. The velocity screens were placed right after the conditioning steel plate, separated by a 30 mm distance. Their averages, as well as their corresponding  $V^2d$  are presented in Table 6. In addition, variable  $V^2d$  values were plotted against variable conditioning steel plates in Figure 41.

**Table 6:** A summary of residual velocities and their corresponding  $V^2d$  values measured by velocity screens.

| Shot # | $V_{res}$<br>(m/s) | $V_{res}$<br>(m/s) | $V_{res}$<br>(m/s) | $\bar{V}_{res}$<br>(m/s) | $\bar{V}_{res}$<br>( $\frac{mm}{\mu s}$ ) | Steel<br>plate<br>(mm) | Tip diameter<br>(mm) | $V^2d$<br>( $\frac{mm^3}{\mu s^2}$ ) |
|--------|--------------------|--------------------|--------------------|--------------------------|---|------------------------|----------------------|--------------------------------------|
| 1-3    | 7484.7             | 7032.4             | 7355.8             | 7290.9                   | 7.29                                      | 0                      | 2                    | 106.3                                |
| 4-6    | 6597.9             | 6875.0             | 6273.8             | 6582.2                   | 6.58                                      | 10                     | 2                    | 86.6                                 |
| 7-9    | 4246.6             | 4342.1             | 4561.4             | 4383.4                   | 4.38                                      | 20                     | 2.1                  | 40.3                                 |
| 10-12  | 2608.7             | 2752.3             | 2702.7             | 2687.9                   | 2.68                                      | 40                     | 2.1                  | 15.1                                 |
| 13-15  | 1833.3             | 1848.1             | 1843.6             | 1841.7                   | 1.84                                      | 60                     | 2.2                  | 7.5                                  |
| 16-18  | 1245.3             | 1235.5             | 1266.8             | 1249.2                   | 1.24                                      | 75                     | 2.2                  | 3.4                                  |

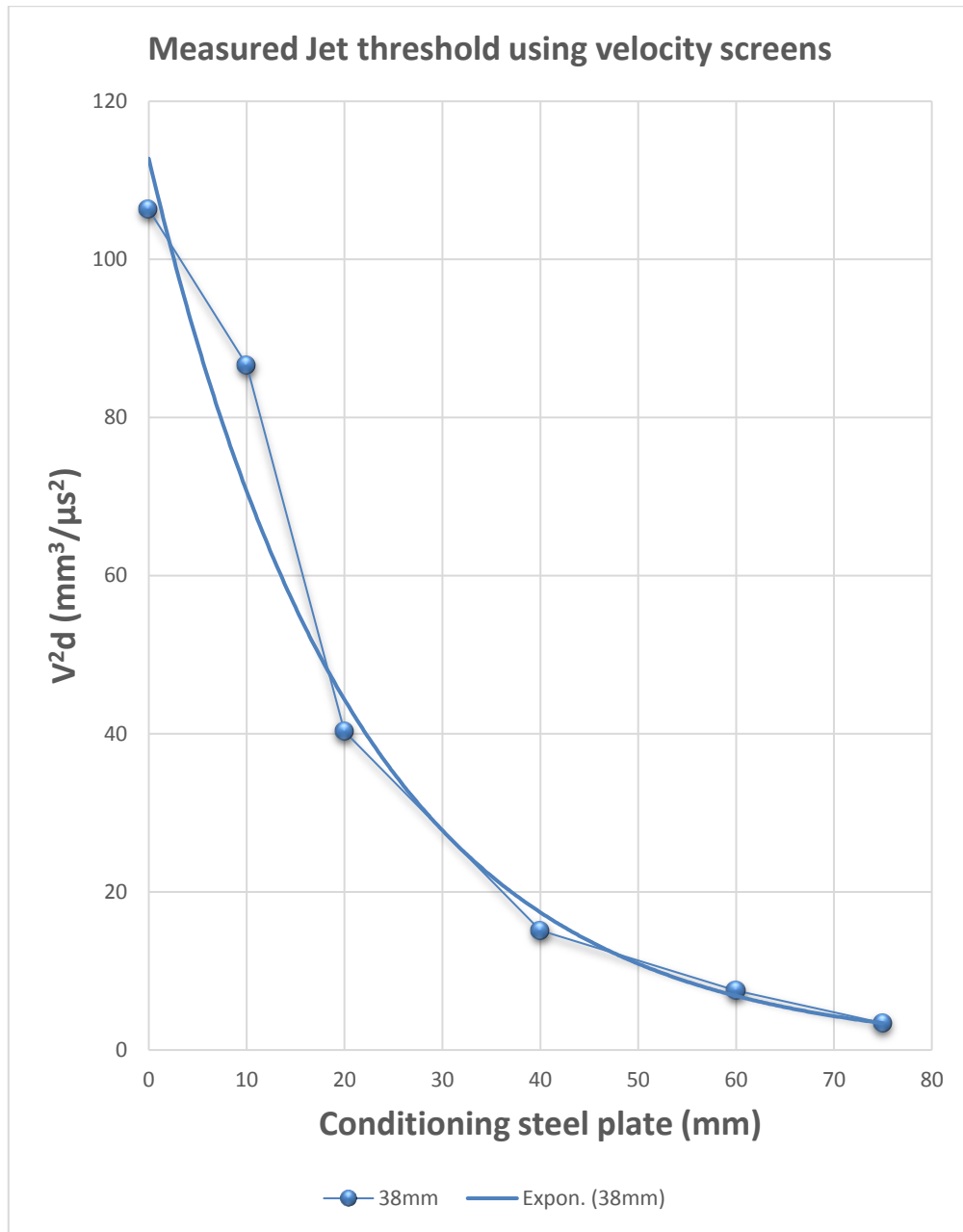


**Figure 40:** Variable jet threshold ( $V^2d$ ) measured by velocity screens.

Figure 41 shows the calculated values of  $V^2d$  using velocity screens indicating a decay exponential fit. This in return agrees with what have been found in literature. A comparison between the jet threshold values calculated using the two methods mentioned above is presented and discussed in Chapter five for verification purposes.

## 4.5 Summary

In summary, the characterisation of the SCJ and its impact on 81 mm mortar bombs, filled with various explosive fillings, were presented. The results were based on using a 38 mm conical SC. Several SCJ shots were conducted for the purpose of finding the optimum standoff distance. The calculated residual tip velocities using flash x-ray analysis and velocity screens were depicted. Various  $V^2d$  values were measured by altering the thickness of a conditioning steel plate placed prior to the point of impact. The SCJ breakup time-interval obtained during the study was in agreement with the empirical formula suggested by Held [54]. The reaction responses observed on the 81 mm mortar bombs were classified and analysed according to STANAG 4439 [6]. The following chapter presents discussions on the findings observed during this study, along with critical evaluations of the main results.



# Chapter 5: Discussion

## 5.1 Introduction

The results of all conducted tests were discussed earlier in Chapter four. In this chapter, all findings observed and concluded from conducting these tests are highlighted. Critical evaluations on the responses of the 81 mm mortar bombs due to SCJI tests are discussed in detail. A plot showing a comparison between the two methods used in calculating  $V^2d$  values is depicted in this chapter for verification purposes.

## 5.2 Findings

The reaction responses observed on 81 mm mortar bombs filled with TNT, showed predicted behaviour when attacked by SCJ. This means the higher the  $V^2d$  value, the severer the reaction becomes. However, with TNT as reference, NTO/TNT-based explosives whether they were (50/50) or (20/80) compositions, showed a very interesting and diverse behaviour. Results showed that they tended to withstand SCJ attacks at high jet velocity (i.e.  $\sim 7.4 \frac{mm}{\mu s}$ ), with jet diameter ranges from 2-2.2 mm. On the contrary, when velocity became slower (i.e.  $\sim 1.8-2.9 \frac{mm}{\mu s}$ ), reaction responses tended to become more violent as oppose to TNT. These results may lead to formulate a relationship on the behaviour of NTO/TNT-based explosive formulations when it comes to attacks by SCJ.

As published by Dr Arnold [10], the reaction responses of several IHE, when attacked by different SC calibres, were studied. The results of his studies showed a disagreement with the constant-rule of  $V^2d$  as per stated by STANAG 4526 [17]. He concluded that a detonation occurred with small values of  $V^2d$ , using a small SC calibre (44 mm), compared to higher values of  $V^2d$  using higher SC calibres, such as 75, 115 and 150 mm. This could mean that the severity of small SC, under certain conditions, on the initiation of munitions is higher than that with large SC calibres.

The results found in this study were compared to those obtained by RDM [18]. According to their SCJI test, they had determined the critical values of  $V^2d$  responsible for initiating NTO/TNT (50/50) by means of using a 57 mm conical SC as presented in Table 5. A comparison was made between current work presented here and work done by RDM, which is depicted in Table 7 below.

**Table 7:** A comparison of SCJI test using 38 mm SC & 57 mm SC on 81 mm mortar bombs filled with NTO/TNT (50/50).

| Formulation        | $\bar{V}_{res}$<br>( $\frac{mm}{\mu s}$ ) | $d_{tip}$<br>(mm) | $V^2d$<br>( $\frac{mm^3}{\mu s^2}$ )<br>38 mm<br>SC | Reaction<br>Type | $\bar{V}_{res}$<br>( $\frac{mm}{\mu s}$ ) | $d_{tip}$<br>(mm) | $V^2d$<br>( $\frac{mm^3}{\mu s^2}$ )<br>57 mm<br>SC | Reaction<br>Type |
|--------------------|---|-------------------|---|------------------|---|-------------------|---|------------------|
| NTO/TNT<br>(50/50) | 7.29                                      | 2                 | 106.3   | IV               | 7.3                                       | 2.5               | 145   | II               |
| NTO/TNT<br>(50/50) | 6.58                                      | 2                 | 86.6  | IV               | 6.7                                       | 2.5               | 121   | III              |
| NTO/TNT<br>(50/50) | 4.38                                      | 2.1               | 40.3  | IV               | 6.1                                       | 2.6               | 100   | IV               |
| NTO/TNT<br>(50/50) | 2.68                                      | 2.1               | 15.1  | III              | 5.3                                       | 2.6               | 75  | IV               |
| NTO/TNT<br>(50/50) | 1.84                                      | 2.2               | 7.5   | III              | NO<br>Record                              | NO<br>Record      | NO<br>Record  | NO<br>Record     |

It is clearly shown that severe reactions in form of explosions were achieved by very low values of  $V^2d$  when 38 mm SC was used. This was applicable when NTO/TNT (50/50) & (20/80) were used as main explosive fillings for the 81 mm mortar bombs. On the contrary, higher values of  $V^2d$  were required to achieve explosions by using a 57 mm SC. Therefore, these results indicate that, as jet velocity reduced and diameter slightly increased, NTO/TNT-based explosives were susceptible to explosion. The advantage of using the 38 mm SC allowed testing small residual jet velocities, with small tip diameters ranging from 2 to 2.2 mm. On the other hand, with the 57 mm SC, explosion and detonation were possible as the jet velocity increased with jet diameters ranging from 2.5 to 2.6 mm. This finding may show that jet diameter are more detrimental on munition than its velocity.

Therefore, results obtained in this study clearly agree that  $V^2d$  cannot be treated as constant for variable SC calibres, particularly when using SCJI tests on NTO/TNT-based explosives. Focus should rather be placed on considering a relationship between  $V_{tip}$  and  $d_{tip}$  to obtain a convincing answer on the initiation behaviour of IM when subjected to an attack by a SCJ.

Another finding observed in this work was that each explosive composition used in this work was detonated by convention using an M2A3 electric detonator and a CH6 booster pellet. This was done to get reference detonation measurements of blast over-pressure. The blast over-pressure obtained for detonating NTO/TNT (20/80) was higher than that of NTO/TNT (50/50). These results were quite surprising due to the fact that NTO has higher density and velocity of detonation compared to TNT. This experimental finding may lead to formulate a hypothesis accounting for the existence of a limit for mixing TNT and NTO together. In other words, a boundary might exist where only a certain amount of NTO is allowed to be mixed with TNT to yield optimum performance desired in terms of pressure release in NTO/TNT explosive formulations. However, future investigations are required to verify whether such boundary exists or not. Blast over-pressure measurements are depicted in Table 8-9.

**Table 8:** Blast overpressure measurements for detonated NTO/TNT (50/50).

|                                | <b>Probe 1</b> | <b>Probe 2</b> | <b>Probe 3</b> | <b>Probe 4</b> | <b>Probe 5</b> | <b>Probe 6</b> |
|--------------------------------|----------------|----------------|----------------|----------------|----------------|----------------|
| <b>Measured Pressure (kPa)</b> | 8.821          | 4.931          | 3.929          | 5.181          | 4.64           | 2.651          |
| <b>True Pressure (kPa)</b>     | 9.311          | 4.191          | 2.762          | 5.292          | 3.081          | 2.109          |
| <b>Arrival Time (ms)</b>       | 18.87          | 33.201         | 47.172         | 20.051         | 33.11          | 48.179         |

**Table 9:** Blast overpressure measurements for detonated NTO/TNT (20/80).

|                                | <b>Probe 1</b> | <b>Probe 2</b> | <b>Probe 3</b> | <b>Probe 4</b> | <b>Probe 5</b> | <b>Probe 6</b> |
|--------------------------------|----------------|----------------|----------------|----------------|----------------|----------------|
| <b>Measured Pressure (kPa)</b> | 16.953         | 10.478         | 8.167          | 15.009         | 13.416         | 6.667          |
| <b>True Pressure (kPa)</b>     | 17.59          | 10.681         | 7.491          | 15.412         | 13.627         | 6.912          |
| <b>Arrival Time (ms)</b>       | 20.033         | 33.83          | 47.856         | 22.01          | 33.734         | 48.27          |

### 5.3 Critical Evaluations of the main results

During the jet characterisation test, standoff distances were varied to seek the optimum value. A 10 mm conditioning steel plate was used as a reference to measure the optimum jet residual velocity with respect to selected standoff distance. As standoff distance was increased from 15 mm to 80 mm, the amount of copper liner that was wasted on the conditioning steel plate increased. This implied a loss in the jet strength, as it penetrated the conditioning steel plate, due to unsuitable selection of standoff distance. In addition,

the hole left in the conditioning steel plate started to decrease as standoff distance increases. This implied that the jet threshold was decreasing. However, approximately 0.4 SCC (15 mm) was determined to be the optimum standoff distance due to obtaining a higher jet threshold compared to 40 mm, 60 mm and 80 mm.

Two different methods were used to measure the residual tip velocity. Firstly by means of flash x-ray analysis which took place during the jet characterisation test. The second by means of using velocity screens placed prior to the point of impact on the test item (81 mm mortar bomb). Results showed that both methods gave reasonable values in terms of values obtained for jet threshold. The observed exponential decay behaviour for the jet threshold values obtained in the current study agreed with what have been found in literature. An illustration of such verification is depicted in Section 5.4. Several repeated shots were performed to calculate the residual velocity using velocity screens and average value was considered. The jet threshold values ( $V^2d$ ) were calculated using both methods. A comparison of the two methods used showing the jet threshold values versus variable conditioning steel plate is depicted in Figure 42.

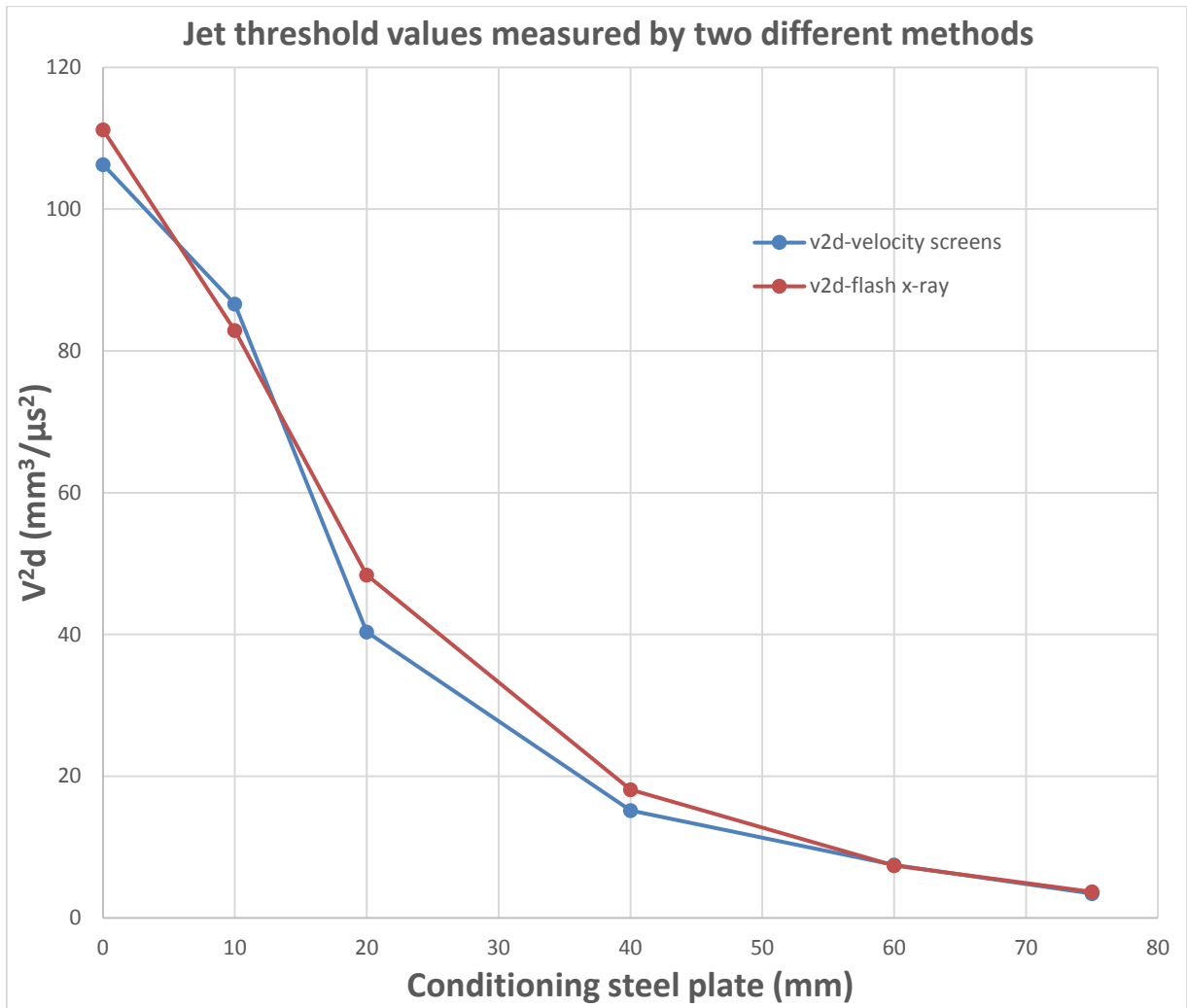


**Figure 41:** A comparison of  $V^2d$  measured by flash x-ray and velocity screens.

During the SCJI test, several explosive formulations were tested. TNT was more likely to detonate with high jets velocity compared to slow jets velocity. The higher the  $V^2d$ , the more violent the reaction obtained was. All critical  $V^2d$  values responsible for initiating different types of reactions on the 81 mm mortar bomb filled with TNT were acquired in Table 5. On the other hand, NTO/TNT-based compositions were more likely to react violently in form of explosions with slower jet tip velocities and increasing tip diameter. This was achieved by low jet threshold values. Although high jet threshold values produced by the 57 mm SC, which was obtained from literature [18], managed to explode NTO/TNT (50/50) filling, explosions were also susceptible to low jet threshold values from the 38 mm SC. This implied that the jet  $V_{tip}$  and  $d_{tip}$  need to be analysed individually instead of only relying on the values of the jet threshold.

## 5.4 Results Verification

The higher the SCC, the higher the jet threshold. All  $V^2d$  values measured in this work had a maximum of  $106.3 \frac{\text{mm}^3}{\mu\text{s}^2}$ . In addition, the best fit that described the decrease in  $V^2d$  found using flash x-ray analysis and velocity screens is a simple exponential decay function. The results obtained in this work were clearly in agreement with what was stated above. This exponential drop is commonly observed on a number of different conical SC calibres found in literature. Figure 43 depicts a comparison of jet threshold values between 38 mm SC and 44 mm SC [10].

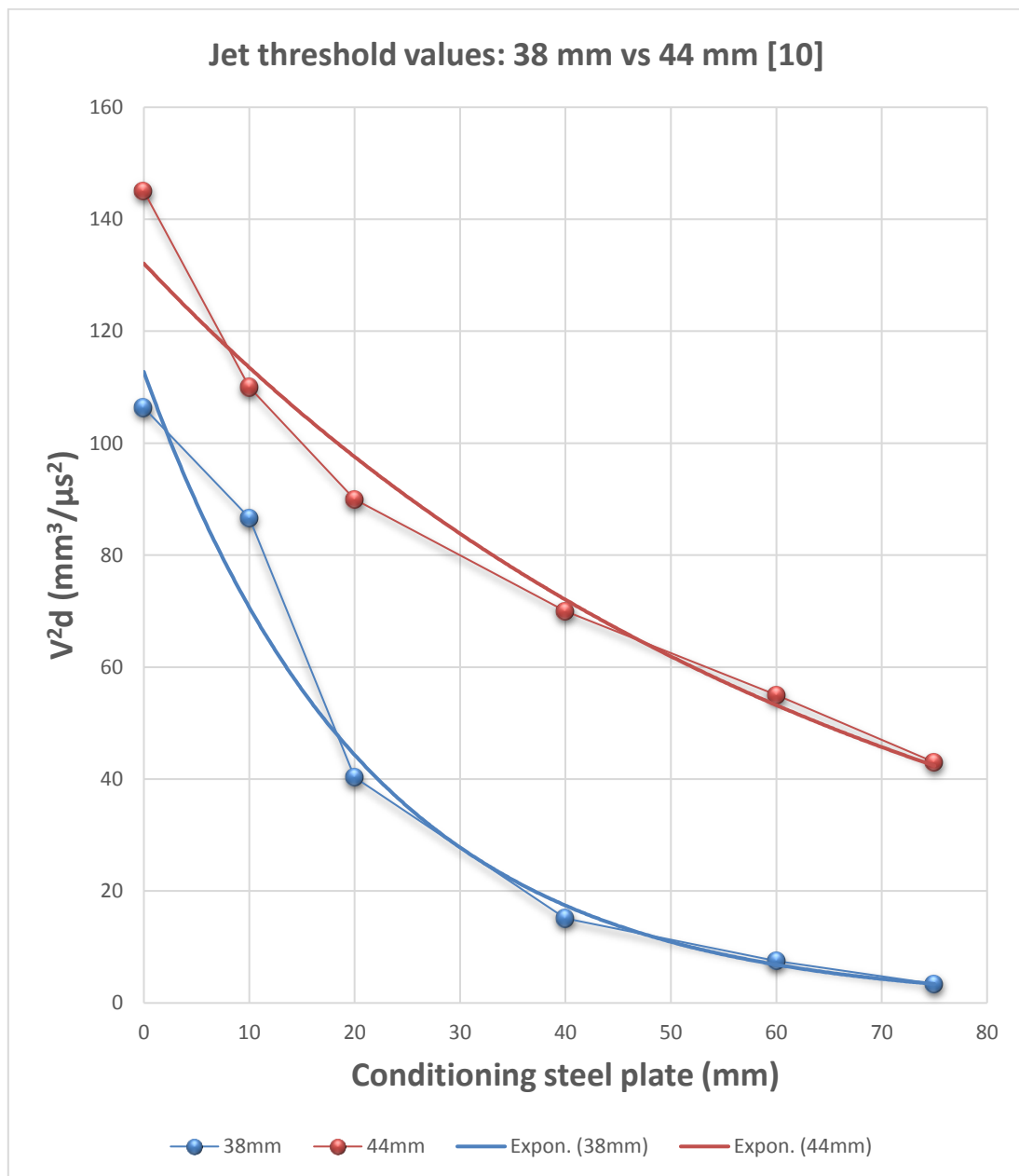


**Figure 42:** A comparison of: 38 mm SC vs 44 mm SC [10].

## 5.5 Summary

In summary, findings observed during this study was presented and discussed. The response behaviour of TNT when subjected to SCJ impacts was clearly different compared to NTO/TNT explosive compositions. The SCJ threshold ( $V^2d$ ) values did not give a full explanation of the resultant reactions on the 81 mm mortar bombs. One rather needs to investigate the jet velocity along with its diameter to obtain a better understanding for the induced reaction type. Furthermore, the type of explosives used in filling the 81 mm mortar bombs played a critical role in determining the reaction outcome in response to the SCJ attacks. The following chapter presents the conclusion of main objectives met as well as possible future work derived during this study.

# Chapter 6: Conclusion

## 6.1 Introduction

In this chapter, the primary objectives that have been achieved through this research are:

- Critical values of ( $V^2d$ ) are obtained for initiating different types of reactions on 81 mm mortar projectiles filled with TNT, NTO/TNT (50/50) and NTO/TNT (20/80); and
- A low percentage (20%) of NTO was added to TNT to form a new explosive formulation that displayed a preliminary indication to resist impacts from 38 mm SCJ impacts; and
- The types of reactions resulted from initiating the 81 mm mortar bombs have been identified in accordance to STANAG 4439 [6].

The secondary objectives that had to be conducted first in order to meet the primary objectives are:

- The 38 mm SCJ used in current study are characterised by means of flash x-ray analysis to measure the leading particle velocity, tip diameter and jet breakup time; and
- The ( $V^2d$ ) values after penetrating various thicknesses of the conditioning steel plate are obtained experimentally by means of flash x-ray and by using velocity screens prior to the point of impact; and
- The  $V^2d$  values obtained in this work are compared to previous work conducted by RDM [18], which used higher SC calibre (57 mm) to verify the statement concluded by Dr Arnold and his colleagues [10] with regards to disputing the constant rule of ( $V^2d$ ).

Two main tests are conducted to meet the above-mentioned objectives. One is aimed to characterise the SCJ by finding its tip velocity and diameter. The other is aimed to record the reactions types observed on the 81 mm mortar bombs due to SCJI. The jet threshold values ( $V^2d$ ) of the 38 mm SCJ have been verified using flash x-ray analysis and velocity screens. Only slight difference in  $V^2d$  values have been noticed from using both methods. The critical values of  $V^2d$  responsible for triggering different types of reactions on the 81 mm mortars bombs have been determined experimentally. Mortars bombs filled with TNT



have shown different initiation behaviour from NTO/TNT (50/50) and NTO/TNT (20/80). The reactions types have been determined in response to 38 mm SCJ attacks and identified in accordance with STANAG 4439 [6]. The critical values of  $V^2d$  attacked on TNT have managed to cause detonation, partial detonation, explosion and no reaction. The initiation behaviour of NTO/TNT fillings, NTO/TNT (50/50) and NTO/TNT (20/80), in response to SCJI are similar. NTO/TNT melt-cast compositions have managed to withstand high velocity SCJI, while low values managed to cause explosion.

As per work done by Dr Arnold and his colleagues, which showed that there is a disagreement with the “( $v^2d$  – rule)” stated by STANAG 4256 [17], results obtained in this study show agreement with this statement. Particularly on the severity of jets impacts produced by small SC calibres on munitions. Low jet velocities obtained from 38 mm SC have caused more violent reactions, on the 81 mm mortar bombs, than high velocity jets. The jet tip velocity along with its diameter gave a clearer indication on explaining the resultant reactions on mortar bombs instead of  $v^2d$  values.

## 6.2 Future Work

NTO/TNT melt-cast explosives have proven to be potential filling candidates for IM. Very interesting blast over-pressure measurements were recorded on NTO/TNT (20/80). It showed a pressure release equal to almost double the amount found from NTO/TNT (50/50) at 5 m, 10 m and 15 m distances away with respect to the point of detonation. However, more tests are required to confirm the validity of such results of pressure. If this result is confirmed, this might lead to a relationship that may govern the amount needed of NTO to be mixed with TNT to yield optimum performance in terms of blast over-pressure released. This can also reduce the overall cost of using a larger amount of NTO as a main filling ingredient in insensitive munitions.

One way of investigating hypothesis is by manipulating the amount of NTO mixed with TNT, to seek a mixture that can provide optimum performance. Another significance of pursuing a confirmation of this hypothesis is the fact that a high blast over-pressure value may be suitable for fragments-lethality applications applied on military projectiles.

# Bibliography

- [1] G.I. Brown, *The Big Bang: A History of Explosives*. Stroud, Gloucestershire: Sutton Pub Ltd, 1998, p. 85.
- [2] D. Lance and I. McNeil, *Biographical dictionary of the history of technology*. 1996, p. 655-656.
- [3] H. de Mosenthal, *The Inventor of Dynamite in Nineteenth Century*. 1898, p. 567–581.
- [4] “The History of Insensitive Munitions,” History of Insensitive Munitions. [Online]. Available: <http://www.insensitivemunitions.org/>. [Accessed: 13-Nov-2017].
- [5] O. Johnson, "HMX as a Military Explosive", U.S. Naval Ordnance Laboratory, White Oak, Maryland, 1956.
- [6] STANAG 4439, Edition 3, “Policy For Introduction And Assessment Of Insensitive Munitions”, March 2010.
- [7] CNO Executive Board (CEB) on Insensitive Munitions briefing book dated 29 March 1984.
- [8] AOP-39, Edition 3, “Guidance On The Assessment And Development Of Insensitive Munitions”, March 2010.
- [9] W. Arnold and E. Rottenkolber, "High Explosive Initiation Behavior by Shaped Charge Jet Impacts", *Procedia Engineering*, vol. 58, pp. 184-193, 2013.
- [10] W. Arnold, E. Rottenkolber and T. Hartmann, “Challenging v<sup>2</sup>d”, *Proceeding of the Insensitive Munitions & Energetics Materials Technology Symposium*, Rome, Italy, May 18-21, 2015.
- [11] W. Arnold, E. Rottenkolber and T. Hartmann, “Shaped Charge Jet Initiation Phenomena of Plastic Bonded High Explosives”, *Proceeding of the Insensitive Munitions & Energetics Materials Technology Symposium*, Las Vegas, NV, May 14-17, 2012.

- [12] J. Milinazzo, "Energy Transfer of a Shaped Charge", Sandia National Laboratories, Albuquerque, NM, 2016.
- [13] C. Munroe, "Wave-like effects produced by the detonation of guncotton", *American Journal of Science*, vol. 36, pp. 48–50. 1888.
- [14] B. Woebkenberg, J. DeVine, R. Rush, B. Starnes and H. Stinger, "Nonconventional Uses of the Rocket-Propelled Grenade and Its Consequences", *Military Medicine*, vol. 172, no. 6, pp. 622-624, 2007.
- [15] J. Pike, "RPG-7", [Globalsecurity.org](https://www.globalsecurity.org/military/world/russia/rpg-7.htm), 2018. [Online]. Available: <https://www.globalsecurity.org/military/world/russia/rpg-7.htm>. [Accessed: 15-May 2018].
- [16] C. Joachim, "Rapid runway cutting with shaped charges", *Proceeding of International Symposium on the Interaction of Non-nuclear Munitions with Structures*, Colorado Springs, CO, May 9-13, 1983.
- [17] STANAG 4526, Edition 2, "Shaped Charge Jet Munitions Test Procedure", December 2004.
- [18] J. Sibeko\*, C. du Toit and D. van Zyl, "IM and Fragmentation Assessment of 81 mm Mortar Bombs Filled with Insensitive Melt-Cast Explosive Formulations", *Proceeding of the 2010 Insensitive Munitions and Energetic Materials Technology Symposium*, Munich, Germany, October 11-14, 2010.
- [19] D. Dattelbaum, R. Chellappa, P. Bowden, J. Coe and M. Margevicius, "Chemical stability of molten 2,4,6-trinitrotoluene at high pressure", *Applied Physics Letters*, vol. 104, no. 2, p. 021911, 2014.
- [20] J. Rosen, D. Sickman, and W. Morris, "The melting behaviour of TNT", U.S. Naval Ordnance Laboratory, White Oak, Maryland, 1956.
- [21] K. Kishore, "Comparative Studies on the Decomposition Behaviour of Secondary Explosives RDX and HMX", *Indian Institute of Science*, Bangalore, 1977.
- [22] P. Cooper, *Explosives Engineering*. New York: John Wiley, 2010, p. 406.

- [23] O.H. Johnson, "HMX as a Military Explosive", U.S. Naval Ordnance Laboratory, White Oak, Maryland, 1956.
- [24] R. Weinheimer, "Properties of Selected High Explosives", *Proceeding of the 27<sup>th</sup> International Pyrotechnics Seminar*, Grand Junction, CO, July 16 – 21, 2000.
- [25] S. Singh\*, L. Jelinek, P. Samuels, A. DiStasio and L. Zunino, "IMX-104 CHARACTERIZATION FOR DoD QUALIFICATION", *Proceeding of the 2010 Insensitive Munitions and Energetic Materials Technology Symposium*, Munich, Germany, October 11-14, 2010.
- [26] M. Cliff and M. Smith, "Assessment of a Melt-Castable NTO/TNT Formulation", DSTO Aeronautical and Maritime Research Laboratory, Melbourne, Australia, 2000.
- [27] W. Xiong, "A simple method for calculating detonation parameters of explosives", *Journal of Energetic Materials*, vol. 3, no. 4, pp. 263-277, 1985.
- [28] C. SPYCKERELLE, C. SONGY and G. ECK, "IM Melt Cast Compositions based on NTO", *Proceeding of the 2010 Insensitive Munitions and Energetic Materials Technology Symposium*, Munich, Germany, October 11-14, 2010.
- [29] C. Tarver, "what is a shock wave to an explosive molecule?", *Proceeding of the 12<sup>th</sup> American Physical Society Topical Conference*, Atlanta, GA, June 24-29, 2001.
- [30] C. Tarver, P. Urtiew, S. Chidester and L. Green, "Shock Compression and Initiation of LX-10", *Propellants, Explosives, Pyrotechnics*, vol. 18, pp. 117-127, 1993.
- [31] J. Field, "Hot spot ignition mechanisms for explosives", *Accounts of Chemical Research*, vol. 25, no. 11, pp. 489-496, 1992.
- [32] A. Campbell and J. Travis, "The Shock Desensitization of PBX-9404 and Composition B-3", *Proceeding of the Eighth Symposium (International) on Detonation*, Albuquerque, NM, July 15-19, 1985.
- [33] S. Weckert and C. Anderson, "A Preliminary Comparison between TNT and PE4 Landmines", DSTO Weapons Systems Division, Melbourne, Australia, 2006.

- [34] A. Singh, M. Kumar, P. Soni, M. Singh and A. Srivastava, "Mechanical and Explosive Properties of Plastic Bonded Explosives Based on Mixture of HMX and TATB", *Defence Science Journal*, vol. 63, no. 6, pp. 622-629, 2013.
- [35] J. Lee and C. Hsu, "Thermal properties and shelf life of HMX–HTPB based plastic-bonded explosives", *Thermochimica Acta*, vol. 392-393, pp. 153-156, 2002.
- [36] A. WILSON, "Improved melt cast explosives", *Proceeding of the 2006 Insensitive Munitions and Energetic Materials Technology Symposium*, Bristol, UK, April 24-28, 2006.
- [37] STANAG 4240, Edition 2, "Liquid Fuel / External Fire, Munition Test Procedures," April 2003.
- [38] STANAG 4382, Edition 2, "Slow Heating, Munition Test Procedures," April 2003.
- [39] STANAG 4241, Edition 2, "Bullet Impact, Munition Test Procedures," April 2003.
- [40] STANAG 4496, Edition 1, "Fragment Impact, Munitions Test Procedure", 2006.
- [41] STANAG 4396, Edition 2, "Sympathetic Reaction, Munition Test Procedures," April 2003.
- [42] STANAG 4526, Edition 1, "Shaped Charge Jet Impact, Munition Test Procedures," October 2002.
- [43] S. Helen, E. Genevieve, C. Philippe, C. Songy and B. Nouguez, "Recent developments in the formulation of high explosives", *Proceeding of the Insensitive Munitions & Energetics Materials Technology Symposium*, Rome, Italy, May 18-21, 2015.
- [44] W. von Holle and J. Trimble, "Shaped-charge temperature measurement", *Proceeding of the 6th Symposium on Detonation*, Coronado, CA, August 24–26, 1976.
- [45] E. Baker, G. Voorhis, R. Campbell and C. Choi, "Development of Molybdenum Shaped Charge Liners Producing High Ductility Jets", *Proceeding of the 14<sup>th</sup> International Symposium on Ballistics*, Quebec, Canada, 26-29 September, 1993.
- [46] T. Elshenawy, "Criteria of design improvement of shaped charges used as oil well perforators", Ph.D, University of Manchester, 2012.

- [47] E. Baker, "Jet break-up Characterization of Molybdenum Shaped Charge Liners ", U.S. Army, Armament Research Development and Engineering Centre, Picatinny Arsenal, NJ, 2003.
- [48] G. Birkhoff, D. MacDougall, E. Pugh and G. Taylor, "Explosives with lined cavities", *Journal of Applied Physics*, vol. 19, no. 6, pp. 563-582, 1948.
- [49] E. Pugh, R. Eichelberger and N. Rostoker, "Theory of Jet Formation by Charges with Lined Conical Cavities", *Journal of Applied Physics*, vol. 23, no. 5, pp. 532-536, 1952.
- [50] S. Godunov, A. Deribas and V. Mali, "Influence of material viscosity on the jet formation process during collisions of metal plates", *Combustion, Explosion and Shock Waves*, vol. 11, no. 1, pp. 1-13, 1975.
- [51] E. Hirsch, "A Formula for the shaped charge jet breakup-time", *Propellants, Explosives, Pyrotechnics*, vol. 4, no. 5, pp. 89-94, 1979.
- [52] G. Pfeffer, "Determination par simulations numtriques de L'etat et des lois de fragmentation des jets de charges Creusses", *Proceeding of the 5th International Symposium on Ballistics*, Toulouse, France, April 16-18, 1980.
- [53] B. Haugstad, "On the breakup of shaped charge jets", *Propellants, Explosives, Pyrotechnics*, vol. 8, no. 4, pp. 119-120, 1983.
- [54] M. Held, "Determination of the Material Quality of Copper Shaped Charge Liners", *Propellants, Explosives, Pyrotechnics*, vol. 10, no. 5, pp. 125-128, 1985.
- [55] W.P. Walters and J.A. Zukas, *Fundamental of Shaped Charges*, John Wiley & Sons, 1989, p.138-140.
- [56] F. Allison and R. Vitali, "A New Method of Computing Penetration Variables for Shaped Charge Jet", U.S. Ballistic Research Laboratory, Maryland, 1963.
- [57] W. Schwartz, "Modified SDM Model for the Calculation of shaped charge hole profiles", *Propellants, Explosives, Pyrotechnics*, vol. 19, no. 4, pp. 192-201, 1994.
- [58] J. Simon, R. Dipersio, A. Merendino, "Penetration of Shaped-charge Jets into Metallic Targets", U.S. Ballistic Research Laboratory, Maryland, 1965.

[59] S. Tatake and D. Kharat, "Flash X Ray: A Diagnostic Tool for Shaped Charge Studies", *Defence Science Journal*, vol. 42, no. 4, pp. 259-264, 1992.

## **Appendix A: Blast Over-pressure Measurements**



# Test: SCJI Test 1

Date & Time : 13/12/2017 @12h10

Item : 81 mm mortar bomb

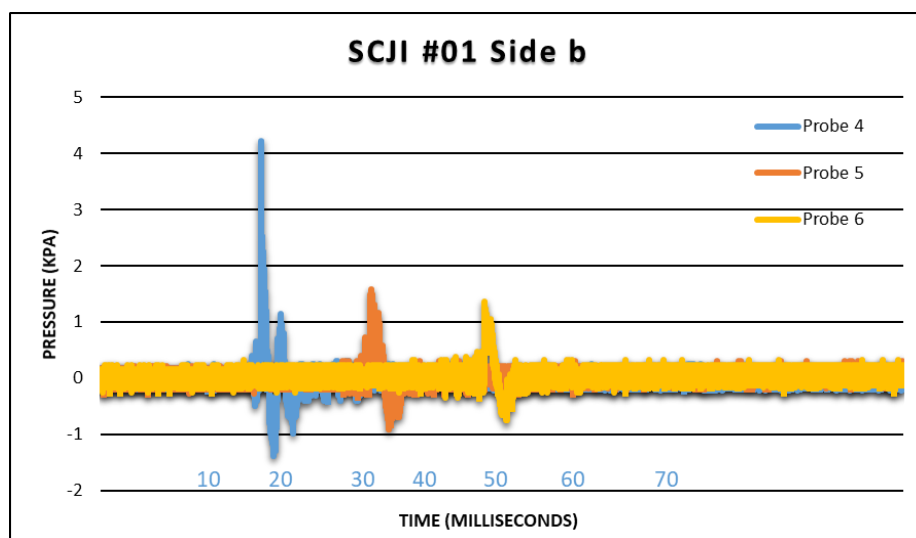
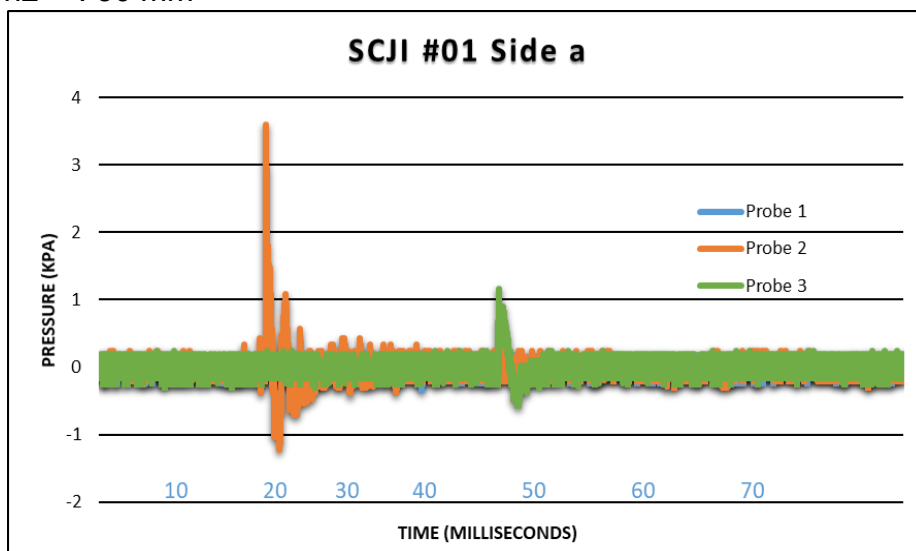
Explosive filling : 20/80 NTO/TNT

Barrier Thickness : 40 mm conditioning plate (steel)

SCJ Velocity : 2608.69 m/s

Screen1-Screen2 : 30 mm

**BOP:**

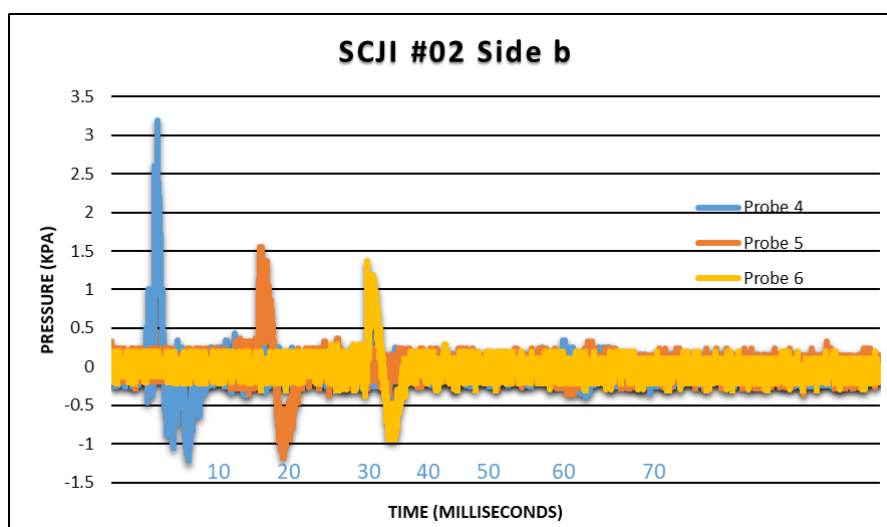
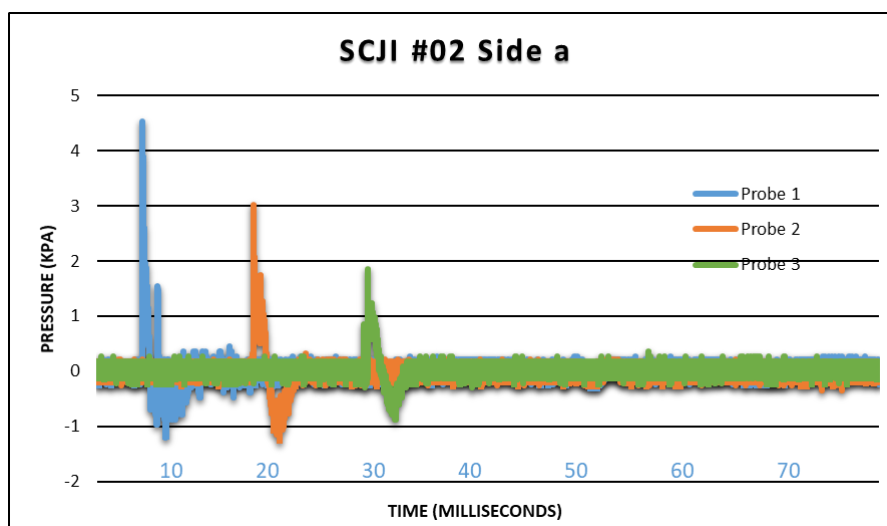


|                         | Probe 1 | Probe 2 | Probe 3 | Probe 4 | Probe 5 | Probe 6 |
|-------------------------|---------|---------|---------|---------|---------|---------|
| Measured Pressure (kPa) | -       | 3.888   | 0.927   | 4.272   | 2.808   | 2.387   |
| True Pressure (kPa)     | -       | 3.604   | 1.168   | 4.219   | 1.577   | 1.360   |
| Arrival Time (ms)       | -       | 20.742  | 49.770  | 20.002  | 33.800  | 47.920  |

## Test: SCJI Test 2

Date & Time : 13/12/2017 @ 14h00  
Item : 81mm mortar bomb  
Explosive filling : 50/50 NTO/TNT  
Barrier Thickness : 40 mm conditioning plate (steel)  
SCJ Velocity : 2752.29 m/s  
Screen1-Screen2 : 30 mm

### BOP:



|                         | Probe 1 | Probe 2 | Probe 3 | Probe 4 | Probe 5 | Probe 6 |
|-------------------------|---------|---------|---------|---------|---------|---------|
| Measured Pressure (kPa) | 4.640   | 3.034   | 1.766   | 3.293   | 1.675   | 1.036   |
| True Pressure (kPa)     | 4.534   | 3.019   | 1.859   | 3.187   | 1.546   | 1.370   |
| Arrival Time (ms)       | 5.810   | 20.008  | 34.660  | 5.972   | 19.348  | 33.372  |

### Test: SCJI Test 3

Date & Time : 13/12/2017 @ 15h00

Item : 81mm mortar bomb

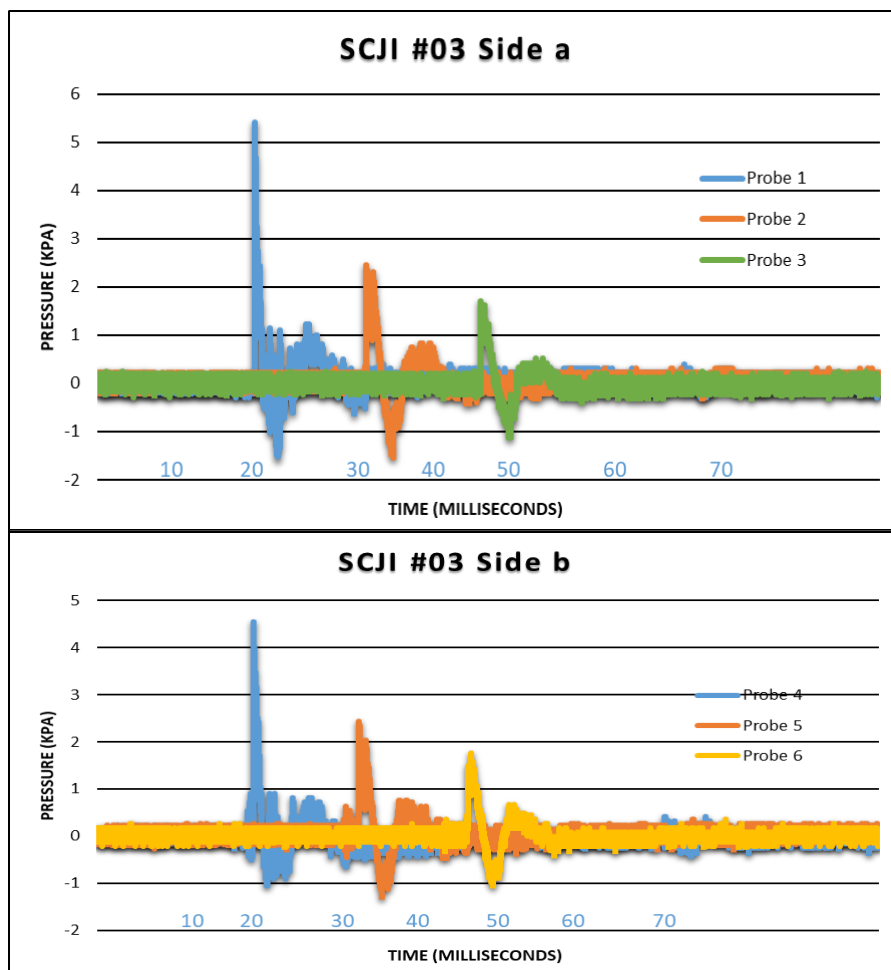
Explosive filling : TNT

Barrier Thickness : 40 mm conditioning plate (steel)

SCJ Velocity : 2702.70 m/s

Screen1-Screen2 : 30 mm

#### **BOP:**



|                         | Probe 1 | Probe 2 | Probe 3 | Probe 4 | Probe 5 | Probe 6 |
|-------------------------|---------|---------|---------|---------|---------|---------|
| Measured Pressure (kPa) | 6.156   | 3.888   | 1.943   | 4.539   | 2.762   | 2.882   |
| True Pressure (kPa)     | 5.412   | 2.447   | 1.702   | 4.552   | 2.444   | 1.755   |
| Arrival Time (ms)       | 20.166  | 34.388  | 49.080  | 20.008  | 33.572  | 47.950  |

Test: SCJI Test 04

Date & Time : 30/1/2018 @ 10:45  
Item : 81mm mortar bomb  
Explosive filling : 20/80 NTO/TNT  
Barrier Thickness : 60 mm conditioning plate (steel)  
SCJ Velocity : 1833.33 m/s  
Screen1-Screen2 : 30 mm

**BOP:** No Blast Results Captured

## Test: SCJI Test 05

Date & Time : 30/1/2018 @ 12:55

Item : 81mm mortar bomb

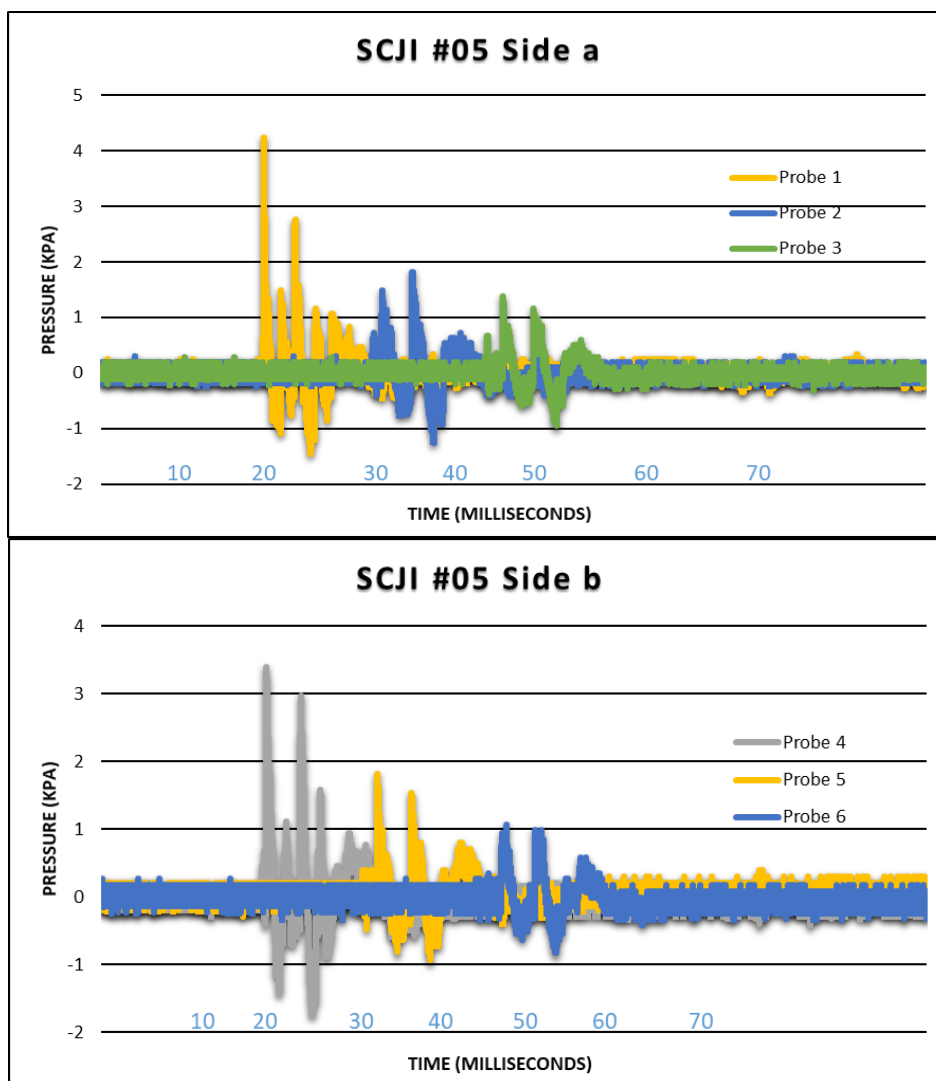
Explosive filling : 50/50 NTO/TNT

Barrier Thickness : 60 mm conditioning plate (steel)

SCJ Velocity : 1848.1 m/s

Screen1-Screen2 : 30 mm

### BOP:



|                         | Probe 1 | Probe 2 | Probe 3 | Probe 4 | Probe 5 | Probe 6 |
|-------------------------|---------|---------|---------|---------|---------|---------|
| Measured Pressure (kPa) | 3.951   | 1.896   | 2.11    | 3.922   | 2.526   | 0.18    |
| True Pressure (kPa)     | 4.242   | 1.816   | 1.385   | 3.459   | 1.816   | 1.072   |
| Arrival Time (ms)       | 19.84   | 37.82   | 48.85   | 20.016  | 33.438  | 49.108  |

# Test: SCJI Test 06

Date & Time : 30/1/2018 @ 13:35

Item : 81mm mortar bomb

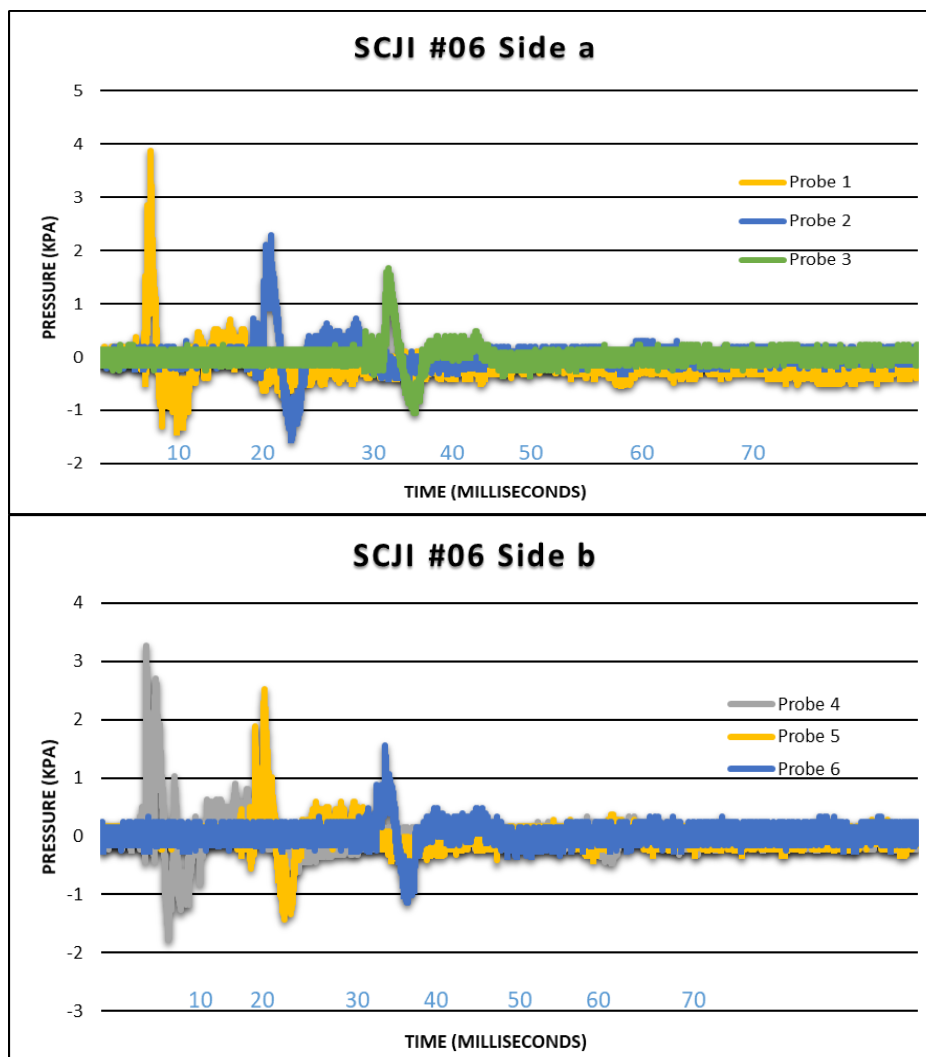
Explosive filling : TNT

Barrier Thickness : 60 mm conditioning plate (steel)

SCJ Velocity : 1843.57 m/s

Screen1-Screen2 : 30 mm

## BOP:



|                         | Probe 1 | Probe 2 | Probe 3 | Probe 4 | Probe 5 | Probe 6 |
|-------------------------|---------|---------|---------|---------|---------|---------|
| Measured Pressure (kPa) | 3.951   | 3.129   | 2.207   | 2.633   | 1.791   | 1.261   |
| True Pressure (kPa)     | 3.874   | 2.294   | 1.684   | 3.267   | 2.523   | 1.557   |
| Arrival Time (ms)       | 6.1     | 20.82   | 35.41   | 5.556   | 20.018  | 34.762  |

# Test: SCJI Test 07

Date & Time : 31/1/2018 @ 09:40

Item : 81mm mortar bomb

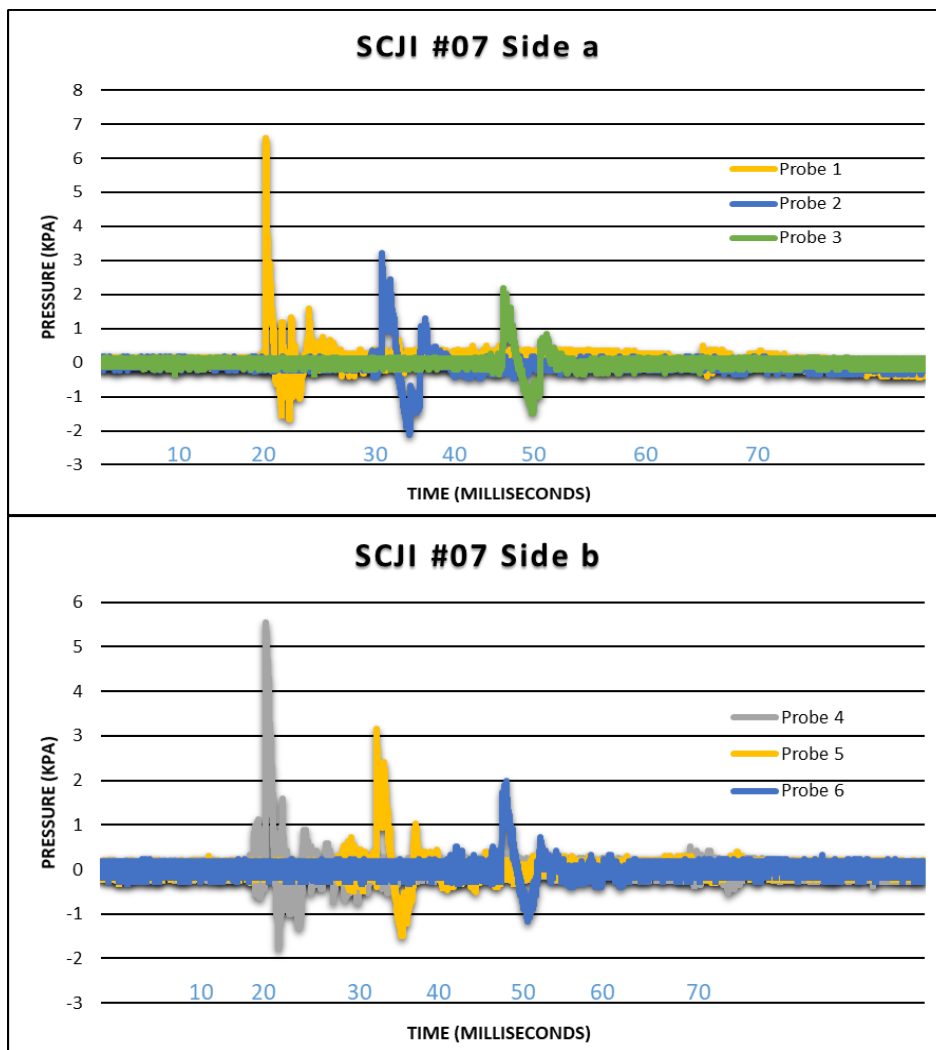
Explosive filling : 20/80 NTO/TNT

Barrier Thickness : 20 mm conditioning plate (steel)

SCJ Velocity : 4342.11 m/s

Screen1-Screen2 : 30 mm

**BOP:**

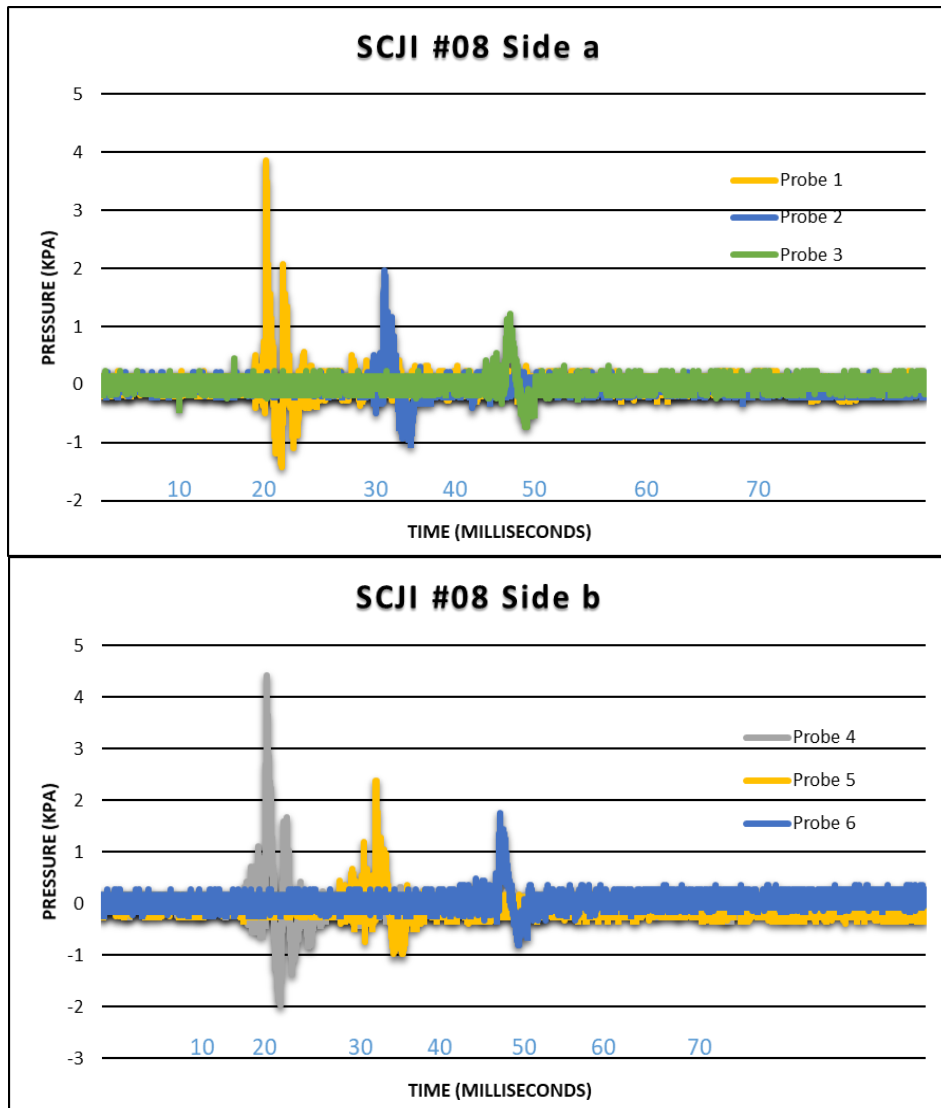


|                         | Probe 1 | Probe 2 | Probe 3 | Probe 4 | Probe 5 | Probe 6 |
|-------------------------|---------|---------|---------|---------|---------|---------|
| Measured Pressure (kPa) | 6.34    | 3.413   | 3.178   | 5.656   | 3.124   | 2.792   |
| True Pressure (kPa)     | 6.605   | 3.215   | 2.204   | 5.561   | 3.151   | 1.993   |
| Arrival Time (ms)       | 20.044  | 34.156  | 48.846  | 20.071  | 35.53   | 49.271  |

# Test: SCJI Test 08

Date & Time : 31/1/2018 @ 11:45  
Item : 81mm mortar bomb  
Explosive filling : 50/50 NTO/TNT  
Barrier Thickness : 20 mm conditioning plate (steel)  
SCJ Velocity : 4246.58 m/s  
Screen1-Screen2 : 30 mm

**BOP:**



|                         | Probe 1 | Probe 2 | Probe 3 | Probe 4 | Probe 5 | Probe 6 |
|-------------------------|---------|---------|---------|---------|---------|---------|
| Measured Pressure (kPa) | 4.226   | 2.465   | 2.251   | 4.706   | 2.205   | 0.09    |
| True Pressure (kPa)     | 3.864   | 1.97    | 1.211   | 4.426   | 2.376   | 1.754   |
| Arrival Time (ms)       | 20.026  | 34.362  | 49.642  | 20.002  | 48.362  | 48.362  |



# Test: SCJI Test 09

Date & Time : 31/1/2018 @ 12h24

Item : 81mm mortar bomb

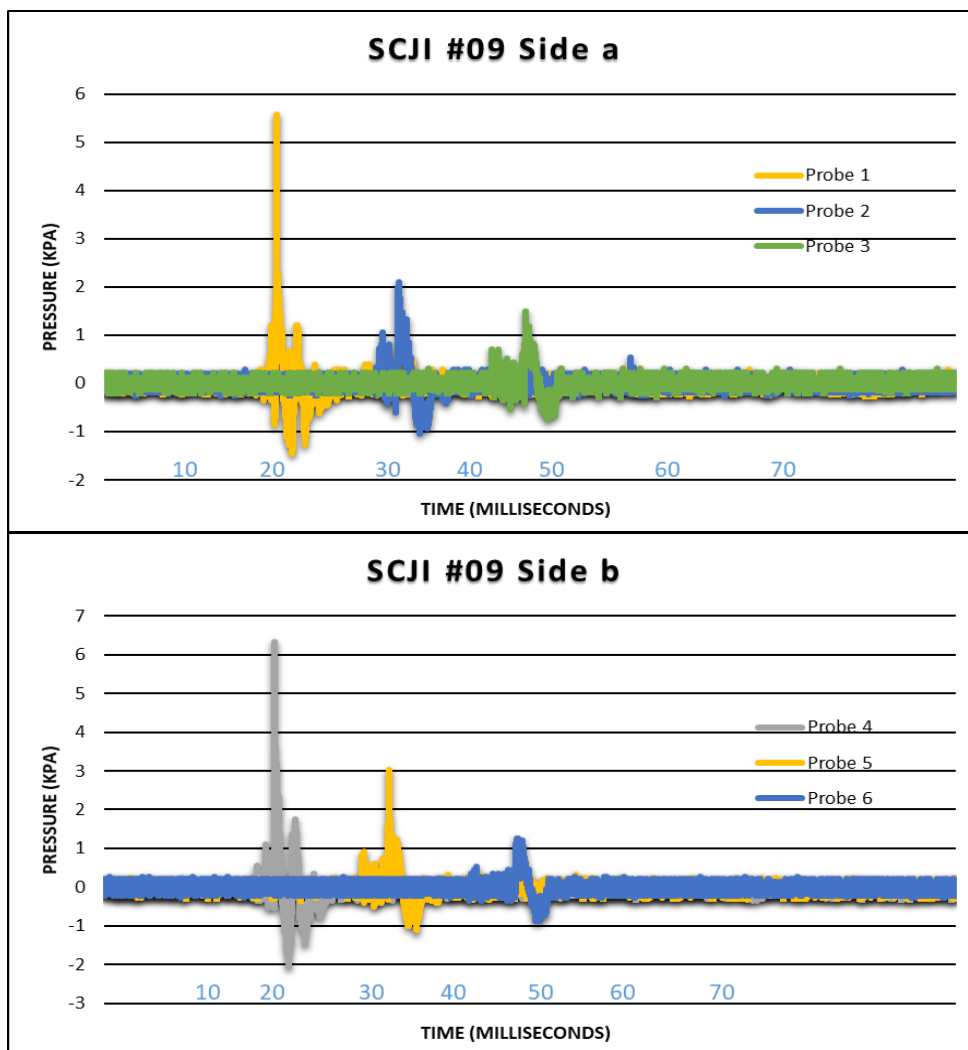
Explosive filling : 50/50 NTO/TNT

Barrier Thickness : 10 mm conditioning plate (steel)

SCJ Velocity : 6597.94 m/s

Screen1-Screen2 : 30 mm

## **BOP:**



|                         | Probe 1 | Probe 2 | Probe 3 | Probe 4 | Probe 5 | Probe 6 |
|-------------------------|---------|---------|---------|---------|---------|---------|
| Measured Pressure (kPa) | 4.549   | 1.659   | 2.428   | 5.267   | 2.846   | 1.576   |
| True Pressure (kPa)     | 5.578   | 2.092   | 1.496   | 6.336   | 3.033   | 1.253   |
| Arrival Time (ms)       | 20.231  | 34.84   | 49.562  | 20.002  | 33.484  | 48.501  |

# Test: SCJI Test 10

Date & Time : 31/1/2018 @ 14h10

Item : 81mm mortar bomb

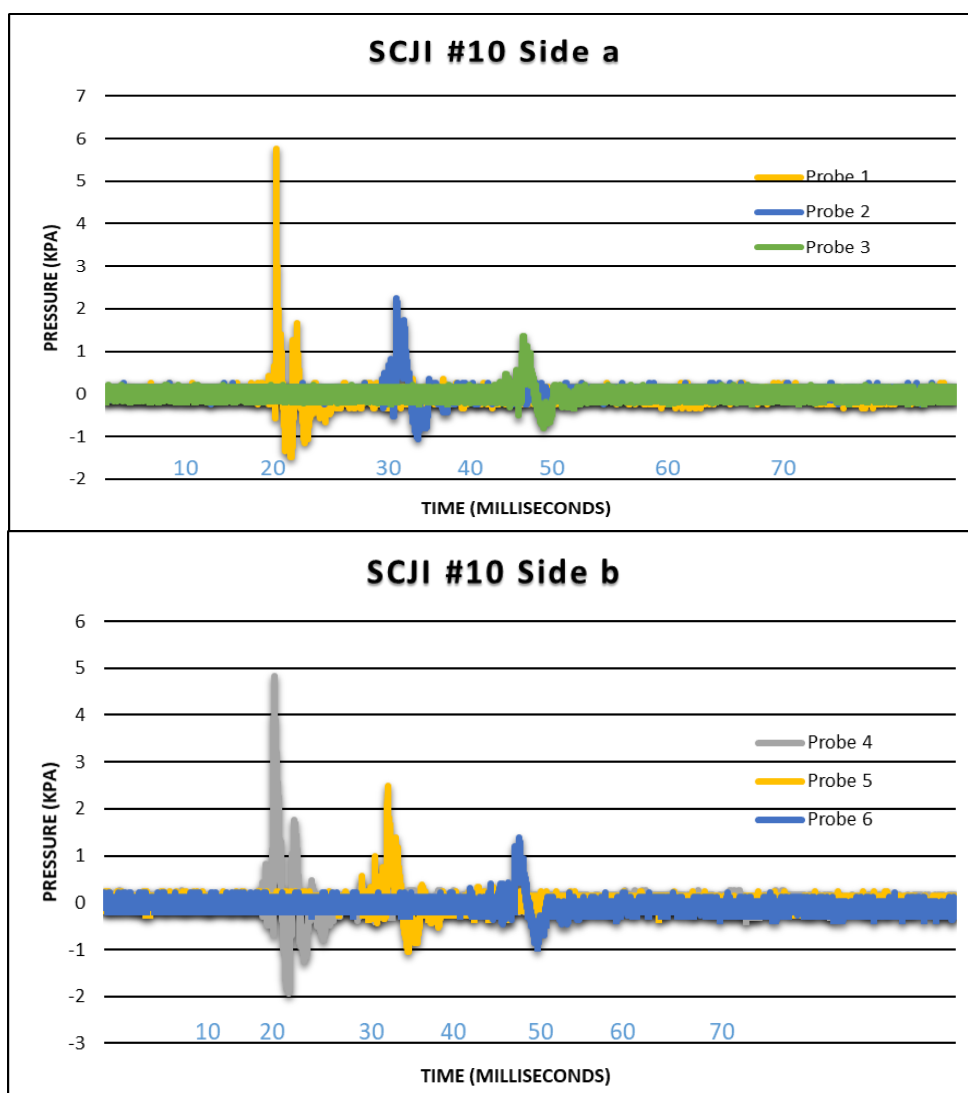
Explosive filling : 20/80 NTO/TNT

Barrier Thickness : 10 mm conditioning plate (steel)

SCJ Velocity : 6875 m/s

Screen1-Screen2 : 30 mm

**BOP:**



|                         | Probe 1 | Probe 2 | Probe 3 | Probe 4 | Probe 5 | Probe 6 |
|-------------------------|---------|---------|---------|---------|---------|---------|
| Measured Pressure (kPa) | 6.386   | 1.659   | 2.516   | 4.361   | 2.756   | 2.747   |
| True Pressure (kPa)     | 5.768   | 2.256   | 1.356   | 4.836   | 2.489   | 1.385   |
| Arrival Time (ms)       | 20.086  | 34.26   | 49.144  | 20.028  | 33.334  | 48.838  |

# Test: SCJI Test 11

Date & Time : 31/1/2018 @ 15h01

Item : 81mm mortar bomb

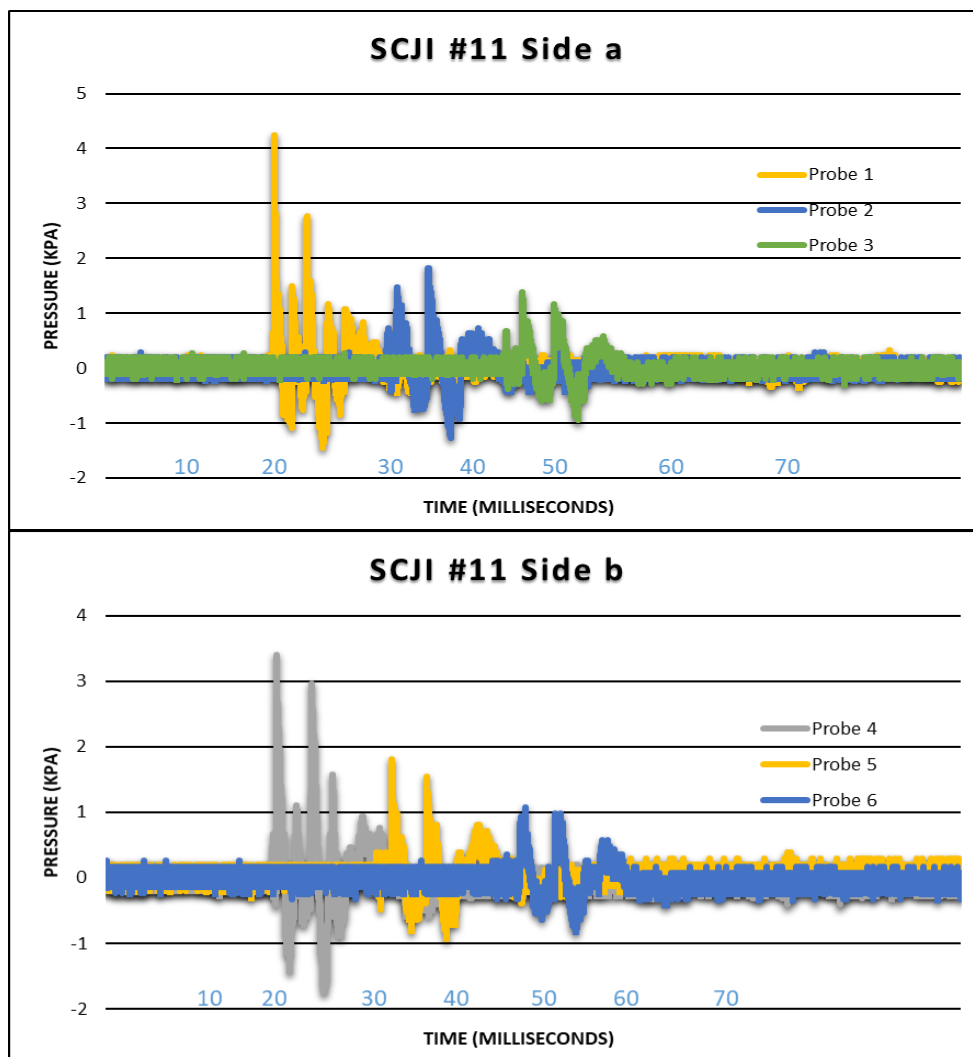
Explosive filling : 20/80 NTO/TNT

Barrier Thickness : No barrier

SCJ Velocity : 7484.69 m/s

Screen1-Screen2 : 30 mm

## **BOP:**



|                         | Probe 1 | Probe 2 | Probe 3 | Probe 4 | Probe 5 | Probe 6 |
|-------------------------|---------|---------|---------|---------|---------|---------|
| Measured Pressure (kPa) | 3.951   | 1.896   | 2.119   | 4.922   | 2.526   | 0.18    |
| True Pressure (kPa)     | 4.242   | 1.816   | 1.386   | 3.395   | 1.816   | 1.072   |
| Arrival Time (ms)       | 19.84   | 37.82   | 48.856  | 20.016  | 33.438  | 49.108  |

## Test: SCJI Test 12

Date & Time : 01/02/2018 @ 10h13

Item : 81mm mortar bomb

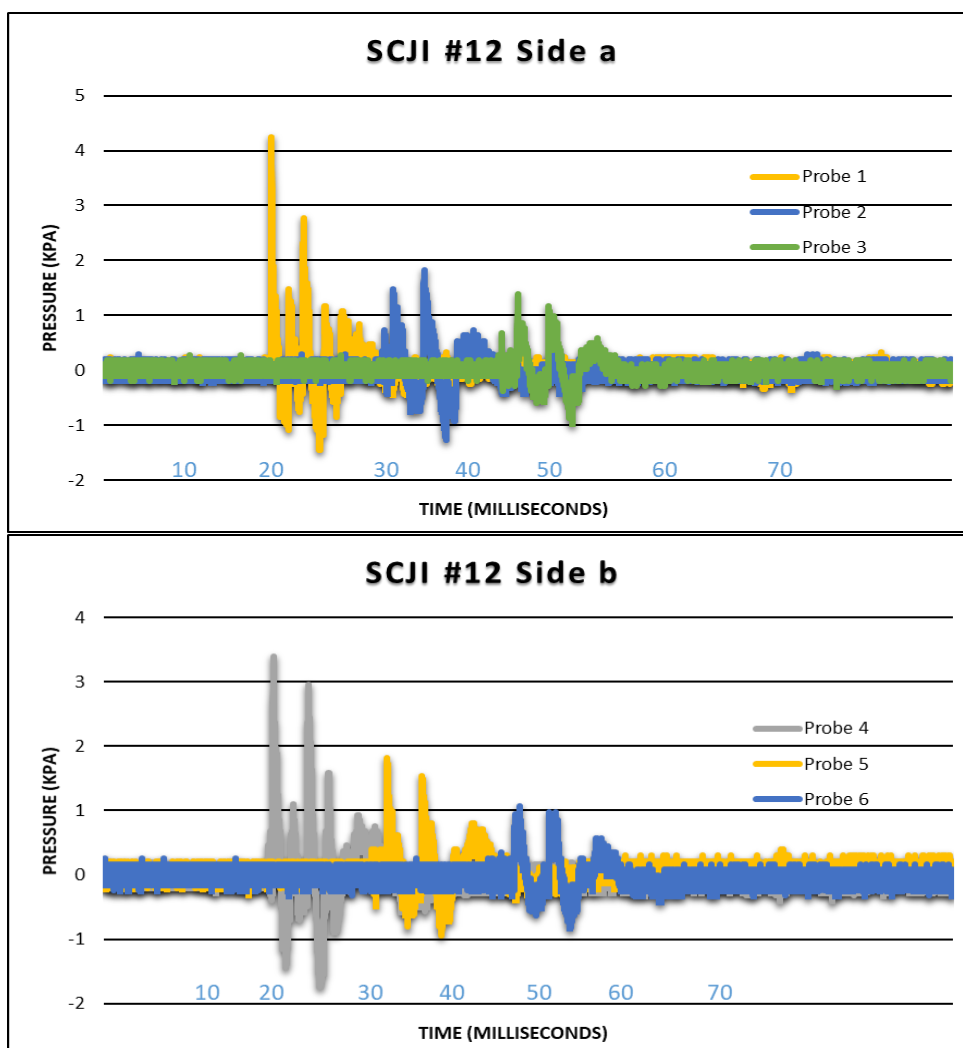
Explosive filling : 50/50 NTO/TNT

Barrier Thickness : 10 mm conditioning plate (steel)

SCJ Velocity : 5892.85 m/s

Screen1-Screen2 : 30 mm

**BOP:**



|                                | Probe 1 | Probe 2 | Probe 3 | Probe 4 | Probe 5 | Probe 6 |
|--------------------------------|---------|---------|---------|---------|---------|---------|
| <b>Measured Pressure (kPa)</b> | 3.951   | 1.896   | 2.119   | 4.922   | 2.526   | 0.18    |
| <b>True Pressure (kPa)</b>     | 4.424   | 1.816   | 1.386   | 3.456   | 1.816   | 1.072   |
| <b>Arrival Time (ms)</b>       | 19.821  | 36.823  | 48.856  | 20.01   | 33.435  | 49.108  |

### Test: SCJI Test 13

Date & Time : 01/02/2018 @ 10h43

Item : 81mm mortar bomb

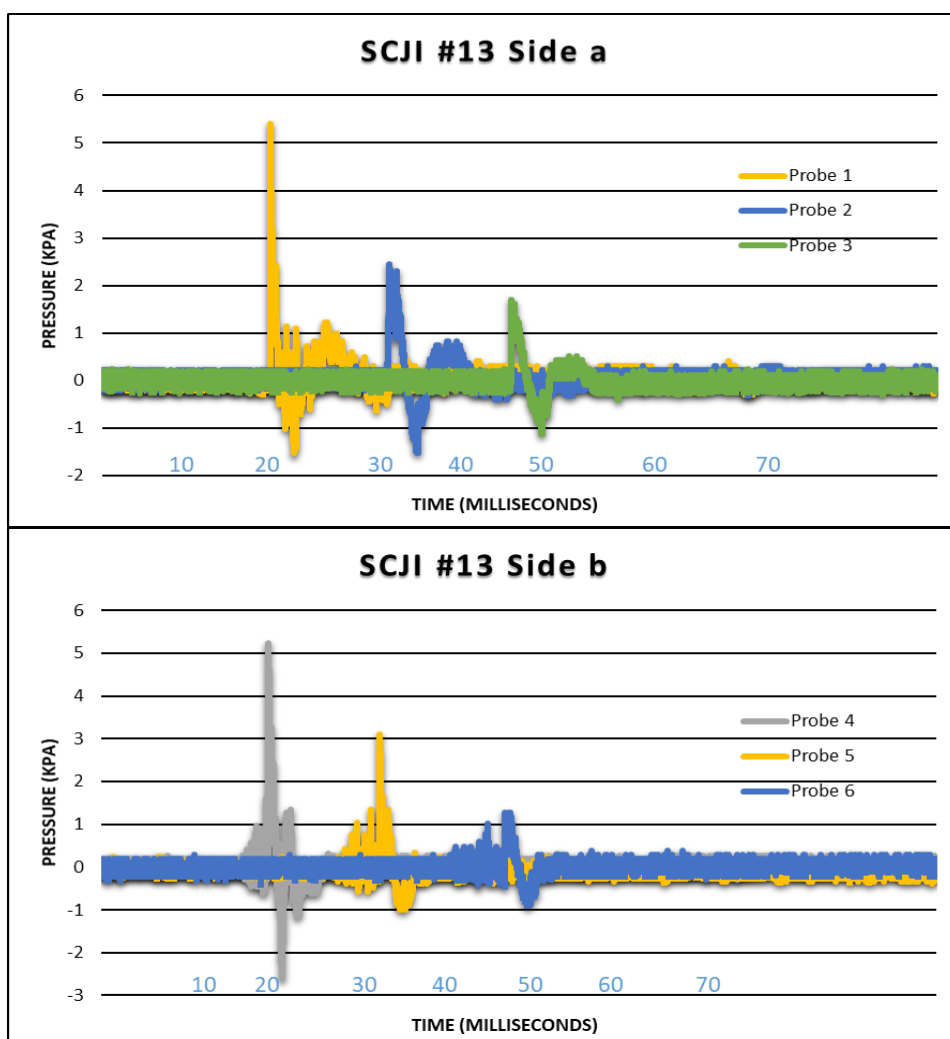
Explosive filling : TNT

Barrier Thickness : 10 mm conditioning plate (steel)

SCJ Velocity : 6273.76 m/s

Screen1-Screen2 : 30 mm

#### **BOP:**



|                         | Probe 1 | Probe 2 | Probe 3 | Probe 4 | Probe 5 | Probe 6 |
|-------------------------|---------|---------|---------|---------|---------|---------|
| Measured Pressure (kPa) | 5.946   | 3.726   | 1.842   | 4.404   | 2.803   | 2.883   |
| True Pressure (kPa)     | 5.351   | 2.339   | 1.653   | 4.416   | 2.479   | 1.756   |
| Arrival Time (ms)       | 20.166  | 34.388  | 49.08   | 20.008  | 33.572  | 47.95   |

Test: SCJI Test 14

Date & Time : 01/02/2018 @ 11h40  
Item : 81mm mortar bomb  
Explosive filling : TNT  
Barrier Thickness : 75 mm conditioning plate (steel)  
SCJ Velocity : 1245.28 m/s  
Screen1-Screen2 : 30 mm

**BOP:**

No Blast over Pressure Measured

# Test: SCJI Test 15

Date & Time : 01/02/2018 @ 13h51

Item : 81mm mortar bomb

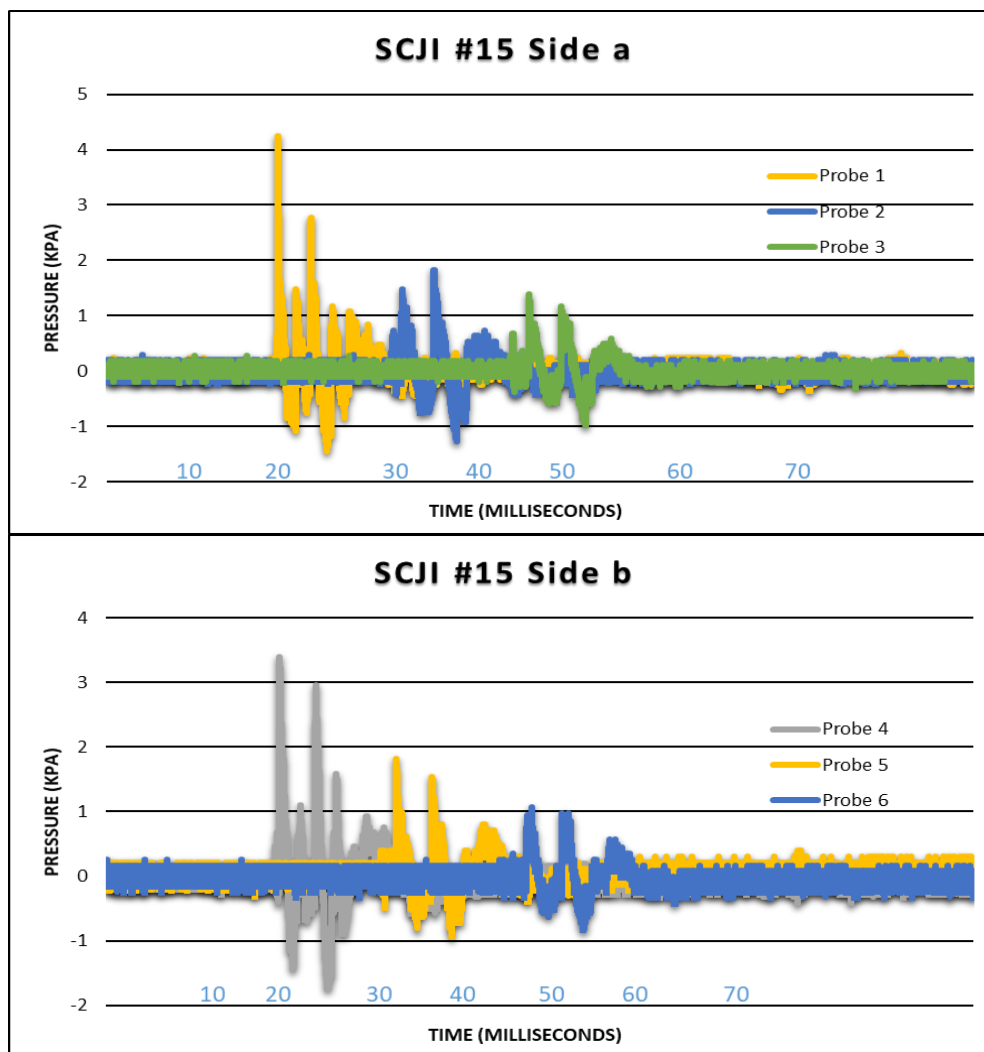
Explosive filling : 50/50 NTO/TNT

Barrier Thickness : **No barrier**

SCJ Velocity : 7032.35 m/s

Screen1-Screen2 : 30 mm

**BOP:**



|                         | Probe 1 | Probe 2 | Probe 3 | Probe 4 | Probe 5 | Probe 6 |
|-------------------------|---------|---------|---------|---------|---------|---------|
| Measured Pressure (kPa) | 3.950   | 1.889   | 2.119   | 4.931   | 2.520   | 0.187   |
| True Pressure (kPa)     | 4.424   | 1.811   | 1.345   | 3.389   | 1.816   | 1.073   |
| Arrival Time (ms)       | 19.84   | 37.82   | 48.80   | 20.16   | 33.438  | 49.100  |

Test: SCJI Test 16 (14 Retest)

Date & Time : 01/02/2018 @ 14h49

Item : 81mm mortar bomb

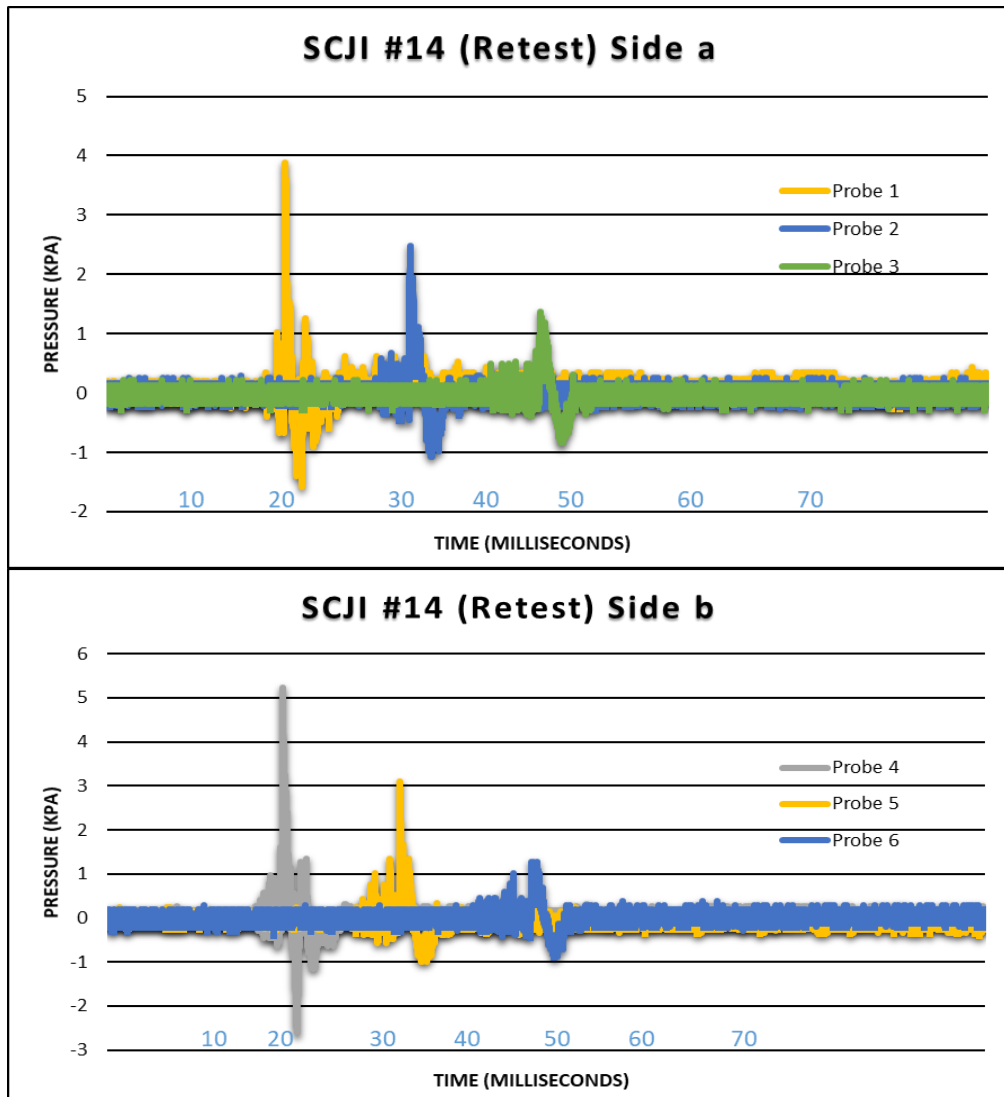
Explosive filling : TNT

Barrier Thickness : 60 mm conditioning plate (steel)

SCJ Velocity : Triggered one velocity screen

Screen1-Screen2 : 30 mm

**BOP:**



|                         | Probe 1 | Probe 2 | Probe 3 | Probe 4 | Probe 5 | Probe 6 |
|-------------------------|---------|---------|---------|---------|---------|---------|
| Measured Pressure (kPa) | 5.237   | 2.939   | 3.046   | 4.792   | 2.894   | 2.207   |
| True Pressure (kPa)     | 3.876   | 2.479   | 1.367   | 5.237   | 3.096   | 1.277   |
| Arrival Time (ms)       | 20.286  | 34.432  | 49.212  | 20.041  | 33.376  | 48.354  |



# Test 17: 81mm TNT **Reference Shot**

Date : 02/02/2018

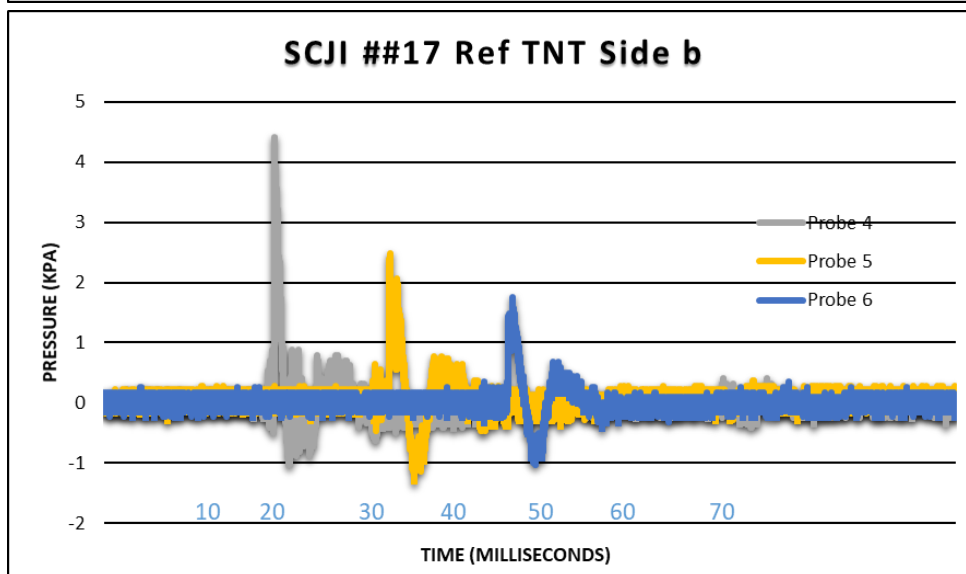
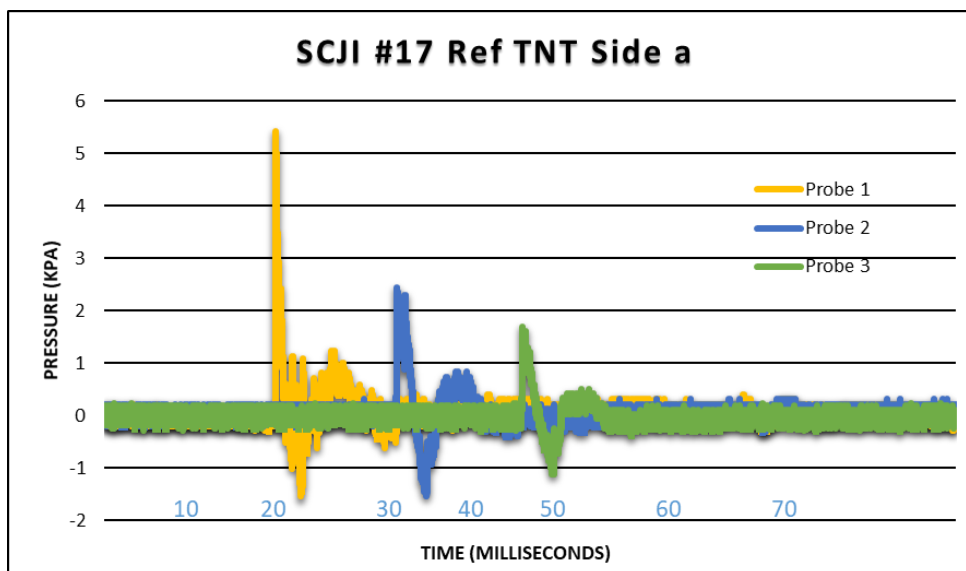
Item : 81mm mortar bomb

Explosive filling : TNT

Aim : Static Detonation

Initiation mechanism : M2A3 electric detonator+CH6 booster pellet

**BOP:**

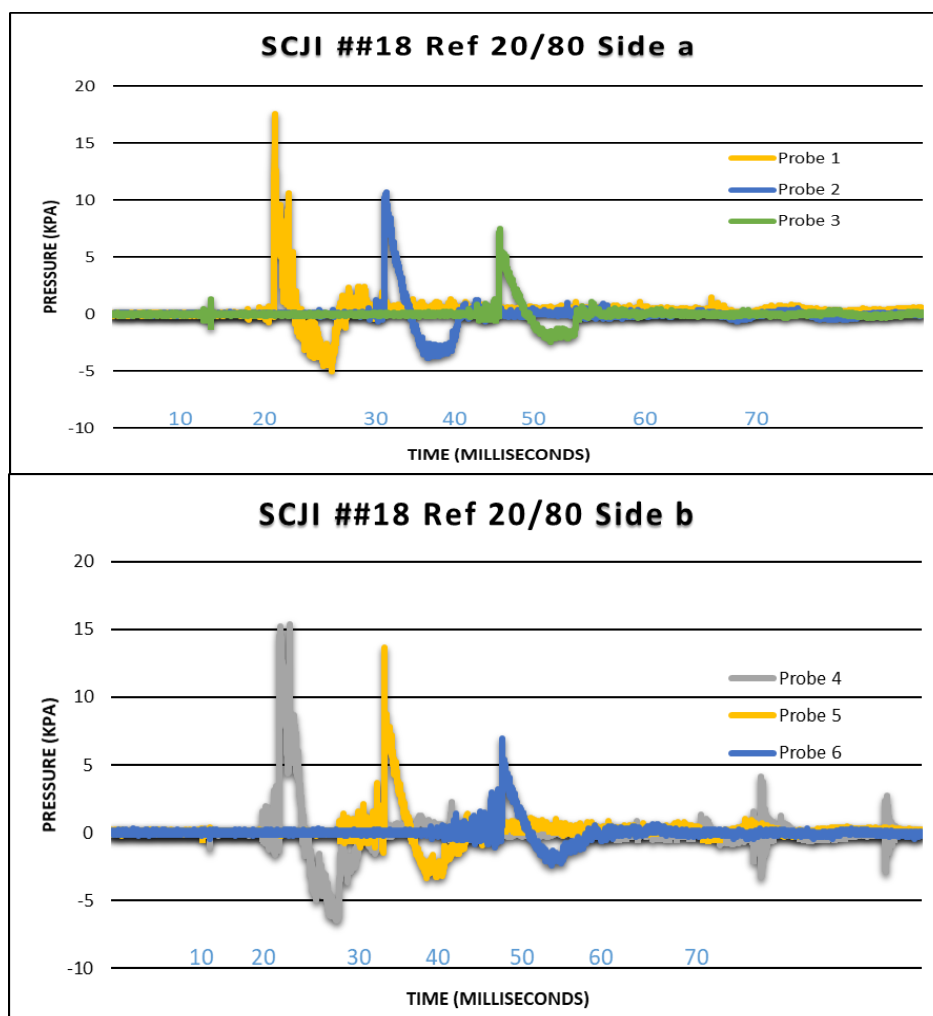


|                         | Probe 1 | Probe 2 | Probe 3 | Probe 4 | Probe 5 | Probe 6 |
|-------------------------|---------|---------|---------|---------|---------|---------|
| Measured Pressure (kPa) | 6.156   | 3.888   | 1.942   | 4.792   | 2.894   | 2.207   |
| True Pressure (kPa)     | 5.417   | 2.447   | 1.703   | 5.237   | 3.237   | 3.096   |
| Arrival Time (ms)       | 20.055  | 33.284  | 47.18   | 20.004  | 33.376  | 48.354  |

## Test 18: 81mm 20/80 NTO/TNT Reference Shot

Date : 02/02/2018  
 Item : 81mm mortar bomb  
 Explosive filling : 20/80 NTO/TNT  
 Aim : Static Detonation  
 Initiation mechanism : M2A3 electric detonator+CH6 booster pellet

**BOP:**



|                                | Probe 1 | Probe 2 | Probe 3 | Probe 4 | Probe 5 | Probe 6 |
|--------------------------------|---------|---------|---------|---------|---------|---------|
| <b>Measured Pressure (kPa)</b> | 16.953  | 10.478  | 8.167   | 15.009  | 13.416  | 6.667   |
| <b>True Pressure (kPa)</b>     | 17.59   | 10.681  | 7.491   | 15.412  | 13.627  | 6.912   |
| <b>Arrival Time (ms)</b>       | 20.033  | 33.83   | 47.856  | 22.01   | 33.734  | 48.27   |

# Test 19: 81mm 50/50 NTO/TNT Reference Shot

Date : 02/02/2018

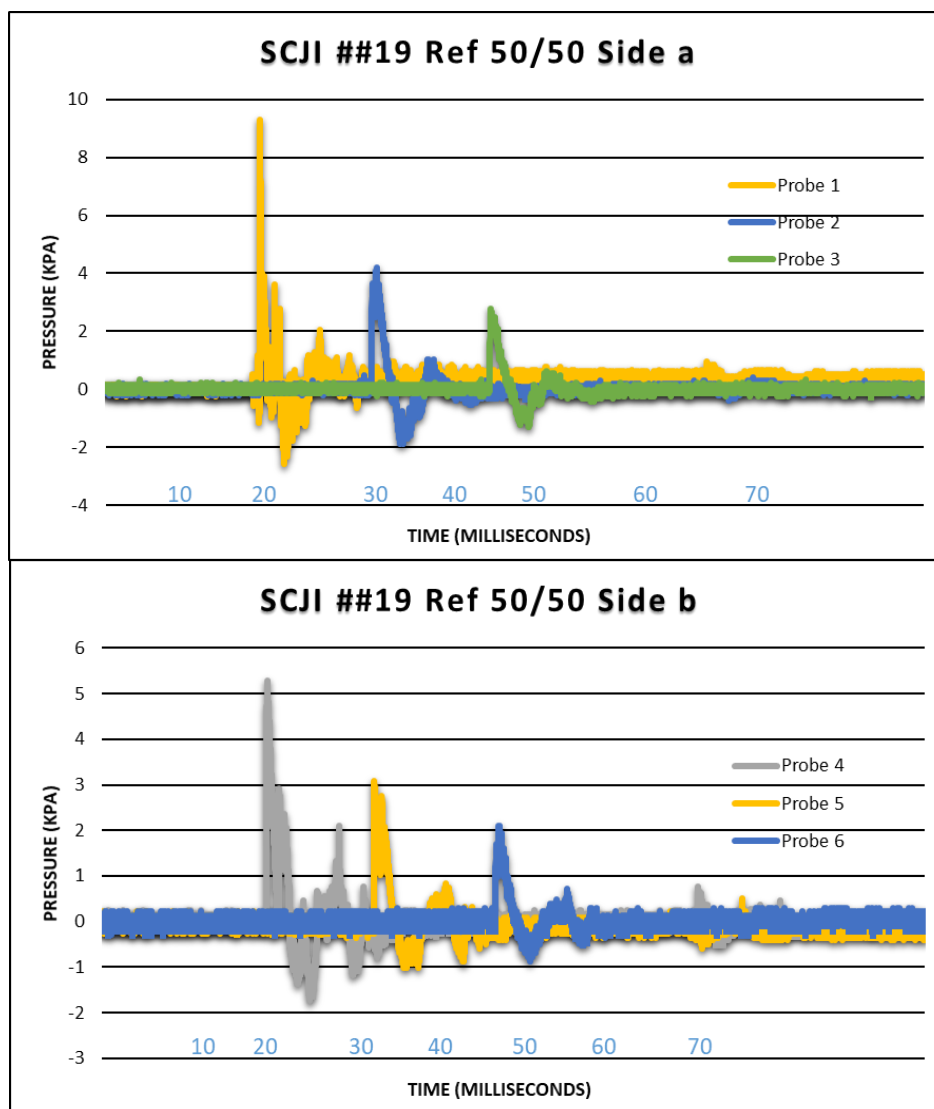
Item : 81mm mortar bomb

Explosive filling : 50/50 NTO/TNT

Aim : Static Detonation

Initiation mechanism : M2A3 electric detonator+CH6 booster pellet

**BOP:**



|                         | Probe 1 | Probe 2 | Probe 3 | Probe 4 | Probe 5 | Probe 6 |
|-------------------------|---------|---------|---------|---------|---------|---------|
| Measured Pressure (kPa) | 8.821   | 4.931   | 3.929   | 5.181   | 4.64    | 2.651   |
| True Pressure (kPa)     | 9.311   | 4.191   | 2.762   | 5.292   | 3.081   | 2.109   |
| Arrival Time (ms)       | 18.87   | 33.201  | 47.172  | 20.051  | 33.11   | 48.179  |